CDEC

LEVEL II

O. BOX

AD A076797

(6) THE EFFECT OF CERTAIN TARGET AND ENVIRONMENTAL VARIABLES ON THE DETECTION TIME OF OBJECTS IN A COMPLEX NATURAL VISUAL DISPLAY.

A Thesis

Presented in Partial Fulfillment of the Requirements
for the Degree Master of Science

(9) Master's thesis,

(15) DA-15-014-AII-2965

by

(10) JOHN JACOB RHEINFRANK III B.I.E.

The Ohio State University

(11) 1969

(12) 162

Systems Research Group
Ohio State University

Approved by

Albert B. Bishop
Adviser
Department of Industrial
Engineering

Sponsor: US Army Combat
Developments Command Armor Agency

79 10 22 161

267 355

JOB

DEPARTMENT OF THE ARMY
ARI FIELD UNIT, BENNING
U S ARMY RESEARCH INSTITUTE FOR THE BEHAVIORAL AND SOCIAL SCIENCES
P O BOX 2086 FORT BENNING, GEORGIA 31905

PERI-IJ 8 August 1979

SUBJECT: Shipment of Documents

Defense Documentation Center
Cameron Station
Alexandria, VA 22314
ATTN: Selection & Cataloging

The Documents in these shipments are approved for public release. The distribution is unlimited.

FOR THE CHIEF:

ALEXANDER NICOLINI
Major, Infantry
R&D Coordinator

ACKNOWLEDGMENTS

I hereby express my graditude to my advisor, Dr. A. B. Bishop, for his constructive criticism and guidance during the course of this research. Thanks are also due Mr. Stephen Stollmack, my immediate supervisor at Systems Research Group. Their insistance that my work, as an advisee and employee, meet their highest standards, is sincerely appreciated.

Thanks are due to all those members of the Systems Research Group who contributed to the completion of this study by creating an atmosphere condusive to the research task contained in this thesis. Frequent group discussions with the staff of Systems Research Group aided greatly in formulation and solution of the problem.

Special gratitude is due my future wife, Deby, without whose patience and understanding, completion of this thesis, which also serves as a wedding present, would have been possible.

Parts of this research were performed under Contract DA-15-014 AII-2965 O.I. No. K-11326-53 with the U.S. Army Combat Developments Command Armor Agency, Fort Knox, Kentucky.

A final acknowledgment is due to Mrs. Rosemarie Ashton for most effectively typing the final copy.

TABLE OF CONTENTS

LIST OF TABLES

LIST OF FIGURES

Figure		Page

Figure Page

CHAPTER I

INTRODUCTION

The visual aquisition of militarily significant objects in a natural terrain environment has, in the past two decades come to the forefront as a major consideration in the design of future military weapon systems. With the surge in sophistication of military hardware design, there is still a strong reliance on the capabilities of the human observer to successfully locate, identify, and bring fire upon enemy elements before he himself, is destroyed. This location of the enemy threat is most often accomplished without the assistance of any clues or devices other than the appearance of an object in the terrain.

Milita _ planners now rely heavily on computer-simulated war games to evaluate the desirability and investigate tactics and employment of proposed weapon systems in a combat environment. Other questions which might be asked are how certain changes in a system affect performance in combat. However, construction of sophisticated computer-simulation techniques has outpaced the development of models adequately describing the capabilities of the human visual system to locate and identify the enemy. In this thesis, models of the visual detection of stationary and moving targets in a natural terrain setting are developed, with emphasis toward their implementation in a combat simulation.

The Detection Phenomenon

The ability of the human visual system to successfully locate a threatening enemy plays an important role in the outcome of any battle. The detection of objects of military significance has been defined by Richardson (1968) as "...the act or process whereby an observer gains knowledge of the presence, the nature, and the location of an object of immediate or potential interest as a target. In applications related to military problems, it has been the usual practice to discuss target acquisition in terms of target detection, identification and location. It is by no means obvious that operationally significant distinctions can be made between the detection and identification parts of the acquisition process which hold true over the complete spectrum of tactical situations and conditions". Boynton and Bush (1955) discuss the phenomenon further: "The perception of a critical target can be complicated by the fact that the observer might think he sees something, but is uncertain as to its particular shape or configuration. This type of perception is compatible with the definition of detection in the practical...situation, in which the observer identifies some object of interest, although he may be unable to categorize it further. If, however, the observer is able to identify the object as belonging to a particular class of objects or as having particular attributes, we may safely surmize that he has not only detected an object but that he has also recognized it. Obviously, recognition implies prior experience, in so far as one cannot categorize a completely novel object."

From these statements, it is seen that detection, per se, is by no means an easily described process. A wealth of visual detection data has been collected in the past two decades. These data, taken under laboratory and field-based conditions, include both the detection of uniform-luminance diskes silhouetted against homogenous, uniformly illuminated backgrounds as well as the detection of complex three-dimensional objects in a natural setting. Data taken under these two diverse conditions have obvious advantages and disadvantages for application to a model of visual detection. Data taken in the laboratory under the careful control of the experimenter are lacking in realism since the conditions under which they are collected do not mimic natural conditions. Data taken in the field environment are most often of a specialized nature and the conditions under which they are collected are usually not sufficiently controlled. In this thesis, data of both kinds are used in the development of models of visual detection.

Probability Models

The ability of an observer to detect an object in a natural environment is dependent on the conditions of the target, its surroundings, and the observer. The time required to distinguish the target from other elements in the terrain has been used as a measure of detection performance (Stollmack, 1965). The occurrance of a detection within time t is a probabilistic event (Koopman, 1946). Stollmack (1965) has suggested that the negative exponential distribution describes the detection time of a human observer. The detection time model suggested by Stollmack is summarized below.

The probability, $P(\Delta t \mid t)$, that a detection occurs in a small time interval $(t, t + \Delta t)$ conditional on not detecting up to time t can be written (Stollmack, 1965) as:[1]

$$P(\Delta t \mid t) = \lambda(t)\,\Delta t + \tilde{o}(\Delta t) \tag{1.1}$$

where $\lambda(t)$ is the conditional detection rate at time t and it is assumed that $P(\Delta t \mid t)$ is proportional to the length of time, Δt.

Given the conditional probability, $P(\Delta t \mid t)$, the cumulative probabilities, $P(t + \Delta t)$, of detection in a time $(t + \Delta t)$ or less can be written as:

$$P(t + \Delta t) = P(t) + \left\{1 - P(t)\right\}\left[\lambda(t)\,\Delta t + \tilde{o}(\Delta t)\right], \tag{1.2}$$

where $P(t)$ is the cumulative probability of detecting in time t or less. Re-arranging terms in equation 1.2, we have:

$$\frac{P(t + \Delta t) - P(t)}{\Delta t} = \left\{1 - P(t)\right\}\left[\lambda(t) + \frac{\tilde{o}(\Delta t)}{\Delta t}\right] \tag{1.3}$$

If it is assumed $\frac{\tilde{o}(\Delta t)}{\Delta t}$ approaches zero as Δt approaches infinity, taking the limit of equation 1.3 as Δt approaches zero yields:

$$p(t) = Q(t)\,\lambda(t) \quad , \; Q(t) = \left\{1 - P(t)\right\}, \tag{1.4}$$

where $p(t)$ is the unconditional probability density function, the derivative of the

---

[1] $\tilde{o}(\Delta t) = \lambda(t)\,\Delta t^2 + \lambda(t)\,\Delta t^3 + \ldots$

cumulative density function P (t). Solving the differential equation given above, P (t) becomes:

$$P(t) = 1 - e^{-\int_0^t \lambda(\tau)\, d\tau} \qquad (1.5)$$

where τ is a dummy variable.

Several assumptions about the form of the conditional detection rate can be made. The simplest is that in which the rate is assumed constant during the entire appearance of the target as shown in Figure 1.

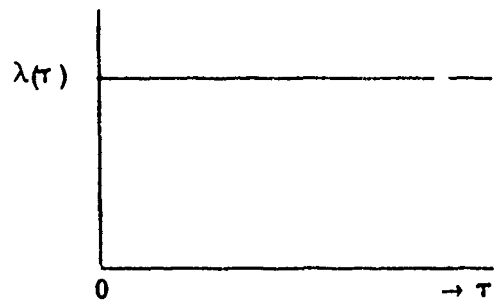

Fig. 1.--Constant Detection Rate

This case is most certainly true when the target is stationary and the environment in which it is located is fairly stable (no extraneous clues). However, for moving targets, detection clues are constantly changing, altering the form of the conditional detection rate. If these changes in the appearance of the target occur instantaneously during the course of the movement and are measurable, the detection rate will remain constant depending on the relative effect of the environmental change. If it is assumed that the effect of the change is constant until another change occurs, the detection rate will assume the form shown in Figure 2.

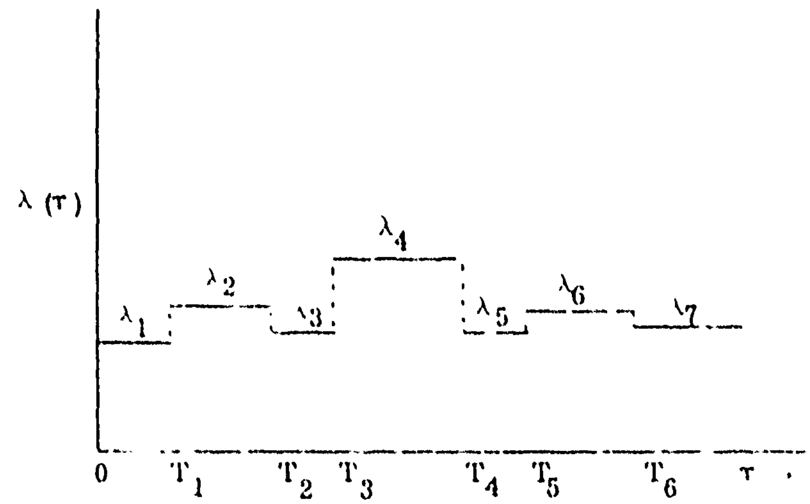

Fig. 2.--Detection Rate Changing Instantaneously With Time

In Figure 2, the target becomes intervisible to the observer at time 0 and has a conditional detection rate equal to λ_1. At time T_1, an abrupt change in the characteristics of the target apparent to the observer occurs, such as a change in apparent velocity, contrast of the target with its background, or a change in apparent size. This produces a change in the detection rate of the observer, raising it to a level λ_2 after time T_1. Similar changes occur throughout the course of the target's movement until it disappears from view. This case of abruptly changing detection rate is discussed further in Chapter 4, where data collected by Brown (1966) are used to estimate the detection rates, λ_i ($i = 1, 2, \ldots$). A description of the experiment conducted by Brown to measure the detection times of observers in the field is given in Appendix A.

In truth, the detection rate does not usually undergo the abrupt changes shown in Figure 2. The changes are much more subtle and occur more frequently,

so that the detection rate would more often appear as shown in Figure 3, where $\lambda(\tau)$ is a continuous function of time (depending on the movement trace of the target and/or the observer).

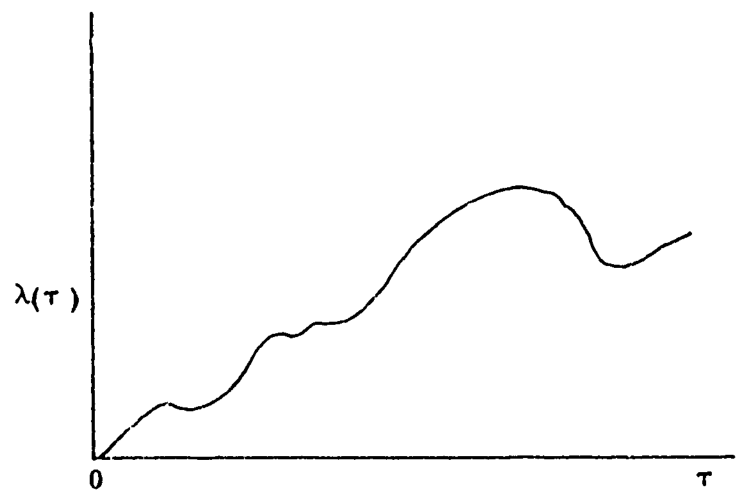

Fig. 3.--Hypothesized Form of the Conditional Detection Rate According to the Glimpse Model

It is obvious that any attempt to explain this phenomenon from observer detection-time data would be fruitless since an unwiedly sample size is necessary because of the high number of changes. For this reason a theoretical model of the conditional detection rate which is compatible with computer simulation requirements is developed which draws on an extensive review of the literature pertinent to visual detection. This model which combines elements of search and psychophysical data is of the form:

$$\lambda(\tau) = \mu \; p \; g(\bar{S}, \tau) \qquad (1.6)$$

where μ is the rate at which fixations (glimpses) are made by the observer, p is a constant which corrects for the number of forms in the scene which resemble the target (confusing forms), and g (S, τ) is the probability that the target is detected on a single glimpse, a function of a set environmental variables, S, and the time τ.

A model which predicts the single-glimpse detection probability, $g(S, \tau)$, developed in Chapter 3, draws heavily on the discussion of the pertinent literature on the detection phenomenon, discussed in Chapter 2. The model discussed in Chapter 3 predicts the single-glimpse detection probability based on the best evidence available to the writer.

In Chapter 3, environmental variables such as target and terrain reflectance and the position of the source illuminating the target and terrain are used to predict the luminance of the target and its surrounding. Contrast of the highlighted and shaded areas of the target with the background and foreground, respectively, are used in an expression for the single-glimpse detection probability of the target. To derive this expression several simplifying assumptions are necessary. These assumptions are made according to the evidence presented in the literature review (Chapter 2) and the judgment of the writer. With these assumptions data is available to permit derivation of the model. During the course of this thesis, it will become evident to the reader that additional basic data concerning the detection phenomenon are quite necessary. However, since only a limited amount of very basic data is available it must suffice for the development contained in Chapter 3. The development of a detection-time

model with continuous-time detection rate, hereafter called the "glimpse model" is presented in Chapter 4. The validity of the "glimpse model" is rather difficult to test because of the limitied capability to obtain dependable continuous physical measures of the quantities used in its development and an inability to approximate its time dependency with any great accuracy. For these reasons, the reader must digress a step and consider a model developed and tested for abrupt changes in the detection rate based on actual field data. The form of the detection rate from the glimpse model should be close to that of the abrupt-change model with minor fluctuations as shown in Figure 4.

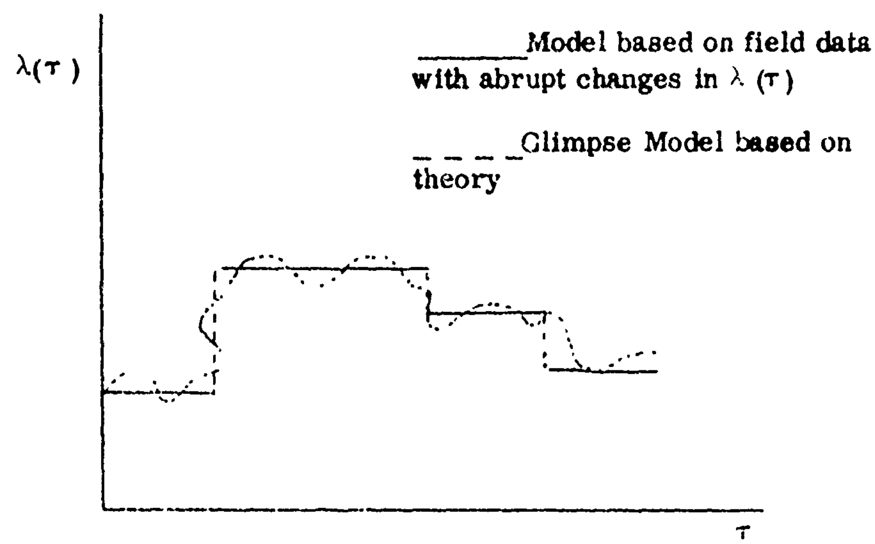

Fig. 4.--Comparison of the Conditional Detection Rate for the Model Based on Field Data with that of the Glimpse Model.

Detection-time data are available from an experiment conducted by Brown (1966). From these data, it is possible to estimate the conditional detection rate in

each of the time intervals used in the simplified probabilistic model. Moving pictures of the scenes used by Brown were available, so an attempt was made to investigate the correspondence between the glimpse model and the simplified model. However, it was impossible to measure all of the target scene variables necessary for complete validation. The method of validation and unsuccessful attempts to collect data from films are discussed at the end of Chapter 4.

Chapter 5 contains a discussion of the area of target detection research, with emphasis on the implications of the models contained in this thesis. As will be noticed from time to time, an extensive amount of additional data are needed to improve the resolution of the model. Some of these data needs are discussed in the final chapter.

CHAPTER 2

FACTORS AFFECTING TARGET DETECTION

Light contains information of the nature of objects in the environment. Structures or patterns of different intensities and compositions (such as margins, texture, pattern, contour or form) evolute responses in the individual. The geometric perspective of these clues are used to analyze information about the environment.

The eye is an instrument exploring the environment employing pursuit, compensatory and saccadic movements which produce a response to the environment. Vernon (1957) suggests that:

> "Perception is selective and is determined in accordance with the classification of incoming sensory data into organized categories of schemata, in which the sensory data are selected and combined systematically with the relevant cognitive data and tendencies to appropriate action." Furthermore, "Schemata are utilized to form hypotheses about the nature of the immediate situation. These hypotheses are tested by attempting to select from the incoming sensory data those which fit them. Data that do not fit may be ignored or rejected. If they are unusually vivid or persistant, the observer may take some active measures to check them and if necessary, to modify the hypotheses to accomodate them. If data are inadequate or ambiguous, the observer will perceive what his schemata lead him to expect. Where schemata are too broad or insensitive to afford perceptions that are accurate in every detail, they may be refined by perceptual learning."

Detection as discussed in Chapter 1 is a subclass of the phenomenon of perception discussed by Vernon. The task of the observer is to classify the object into a recognizable subset based on a known set of attributes. This classification

system, inborn in the observer, is affected only by the physical appearance of the object. This chapter is denoted to a discussion of several recent experimental works, conducted both in the laboratory and the field, to identify some of these factors and quantify their influence on detection and identification performance. The following factors are explored in some detail:

1. Target Size
2. Target Shape
3. Confusing Forms
4. Eye Movements
5. Target-to-Background Contrast
6. Target Form
7. Target Motion

The effects of these factors are then used in Chapter 3 to predict the probability that a target in a natural terrain setting is detected on a single glimpse. Information in this chapter is again used in Chapter 4 to predict the conditional detection rate, $\lambda(\tau)$, discussed in Chapter 1.

Target Size

The effect of target size on detection has been investigated by several experimenters. It has been shown (Kincaid, et al., 1960) that the probability of detecting a target increases as its apparent size to the observer increases. Target detection is discussed in terms of an "element contribution" theory of spatial summation which predicts that the threshold decreases as the target size increases. Steedman and Baker (1960) conducted an experiment to

to determine how the ability of an observer to identify an object is affected by the size of the object in a complex abstract display. Targets were generated on a 90,000-cell matrix of confusing forms. After being shown a reproduction the target in the same orientation as it was to be seen, the subject was told to locate the target in the display containing the confusing forms. The major finding was that identification time was constant for targets above 12 minutes of arc, while performance deteriorated for targets below 12 minutes. Richardson (1962) measured the maximum sighting range for ships of various lengths at sea. Figure 5 shows the relationships between the range at which 50 percent of the observers detected the ship and the length of the ship. From this figure, it can be seen that larger targets (ships having greater length) are detected before the smaller targets (that is, at high target-to-observer ranges, large targets are naturally more detectable than small targets). In a study by Boynton and Bush (1955) it was shown that the probability of recognizing (identifying)a target form increases as the target-to-observer size increases regardless of the nature (shape) of the form. Fox (1956) investigated the effect of object size on both detection and recognition. Circles, irregular shapes, squares, triangles, crosses, and stars of three different sizes were presented to observers. It was shown that an increase in object size decreased the detection and recognition threshold and increased the frequency of correct identification.

The results of these few experiments illustrate a rather intuitive notion about target detection ability. That is, the larger a target appears to the observer, the easier it is to detect and identify. However, a measure of this

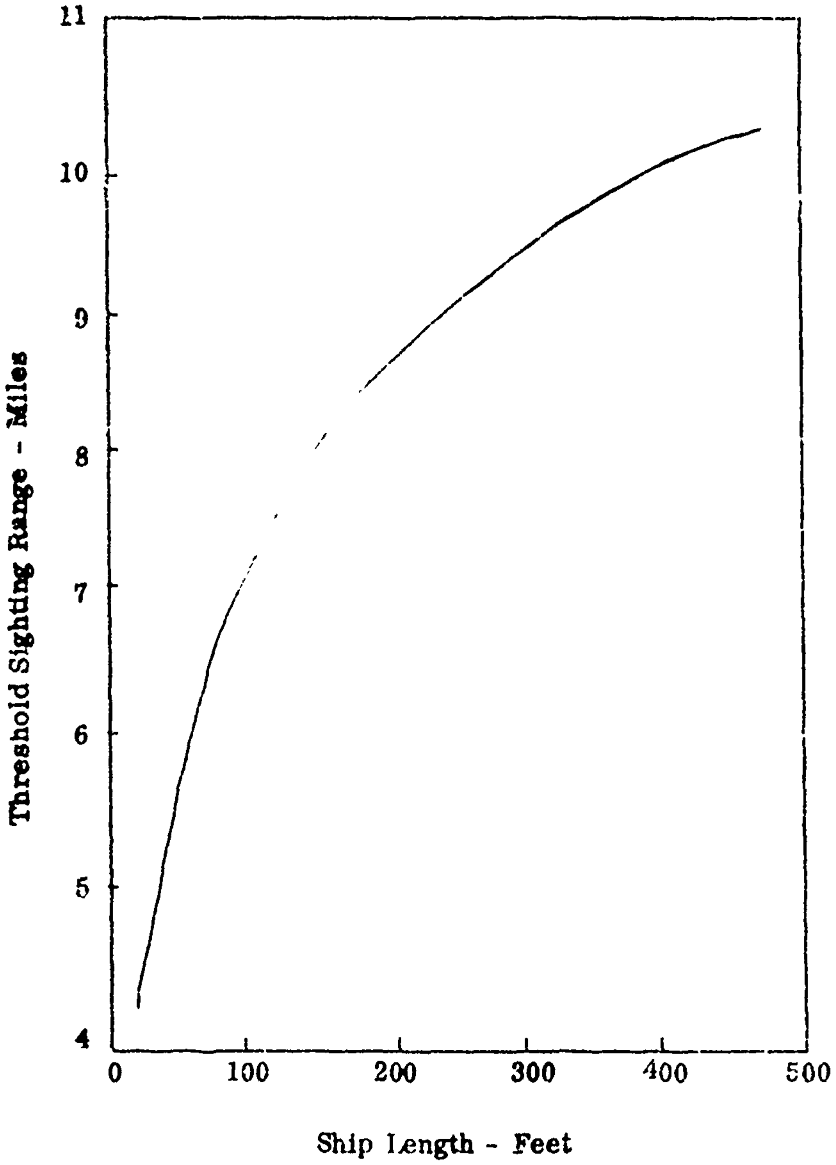

Fig. 5.--Fifty Percent Sighting Range of a Ship At Sea Versus Length of Ship.

target size is not so intuitive, since the shape of a target commonly encountered in a natural environment is very complex, presenting an infinite number of linear dimensions which might qualify as that measure which ~~dictates~~ detectability. That measure of size most often used is the angular subtense of the target,[2] defined as (Wulfeck, et al., 1958):

> "The angle subtended by an object of vision at the nodal point of the eye. The magnitude of this angle determines the size of the corresponding retinal image, irrespective of the size or distance of the object."

This definition can apply to any linear dimension of the target, be it the diameter of a circular target, the greatest linear dimension of a rectangular or complex target, or the perimeters of any shaped target (Harris, 1964). Most of the psychophysical data available on object detectability use the angle subtended by the diameter of a circular target as the measure of target size (Blackwell, 1946; Taylor, 1964). The use of these basic psychophysical data to predict the detectability of a complex target in a complex natural environment is discussed in Chapter 3.

Target Shape

Closely related to the size of the target is its shape or "form" apparent to the observer. Targets typically encountered in the field are complex three-dimensional objects which, due to changes in surface orientation relative to the observer and the illuminating source (the sun, etc.), appear as a pattern of

---

[2]Boynton and Bush (1957) investigated the differential effect of target size as opposed to observer to target distance on the probability of correct identification. For targets subtending the same visual angle, the percent correct recognition for the physically smaller targets was 32.1 percent, while the physically larger targets used to imulate the same distance were correctly identified only 27.0 percent of the time.

brightnesses which must be discerned by the observer as the object of interest. Most studies investigating target shpae have been performed with rather simple two-dimensional objects (circles, squares, rectangles, triangles, etc.) Smith (1961) measured the mean time required to identify variously shaped targets (triangles, squares, pentagons, and hexagons) from similar confusing forms (circles of the same area and contrast) in a circular display. Figure 6 shows the effect of target shape on the mean search time for four observers. From Figure 6 it is noted that as the number of sides the form has increases, so does the mean search time. This suggests that as the shape of the target approaches that of the other forms in the display, it is more difficult to identify or discriminate from these other forms. In the field situation, this would correspond to a target whose shape or form is altered by the use of camoflage to resemble elements of the terrain. The results of a study by Lamar, Hecht, Shlaer, and Hendley (1947) indicate that the ratio of the length of a rectangular target to its width significantly affects the ability of an observer to detect the object. As shown in Table 1, the contrast threshold[3] of the target increases with this ratio at two of the different levels of background luminance studied. In Table 1, it appears for targets of the same area threshold contrast is essentially constant when the ratio of length to width of the target is below seven. However, for targets of equal area having ratios of length to width above seven, the threshold contrast appears to increase.

---

[3]Contrast threshold will be discussed later in this chapter.

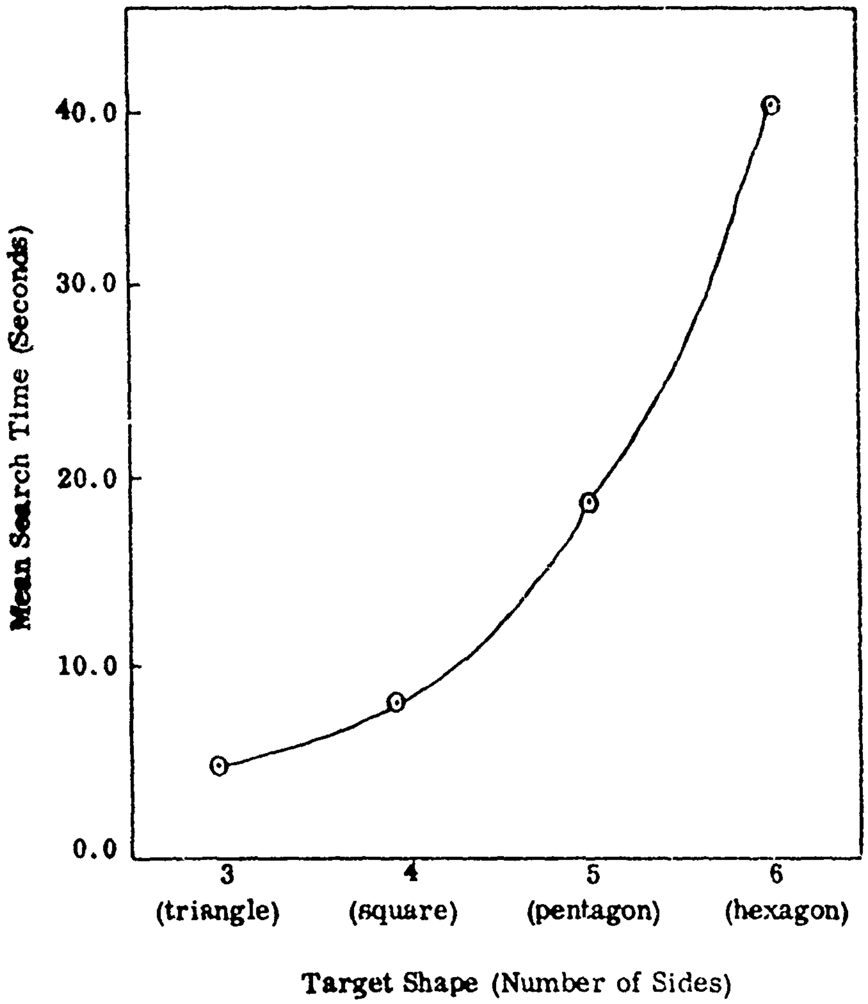

Fig. 6.--Mean Search Time as a Function of Target Shape (from Smith (1961)).

TABLE 1

RELATIONSHIP BETWEEN THRESHOLD CONTRAST AND TARGET AREA FOR RATIO, (L/W) OF LENGTH TO WIDTH OF A RECTANGULAR TARGET TAKEN FROM LAMAR, et al., 1947

Background Luminance (ft. lamberts)	Target Area (min^2)	$\frac{L}{W} = 2$	$\frac{L}{W} = 7$	$\frac{L}{W} = 20$	$\frac{L}{W} = 70$
2950	0.50	0.331	0.288	0.402	0.631
	0.75	0.205	0.207	0.252	0.470
	1.00	0.138	0.154	0.187	0.372
	1.50	0.102	0.118	0.172	0.278
	3.00	0.0582	0.0662	0.108	0.166
	10.00	0.0321	0.0330	0.0445	0.0506
	50.00	0.0167	0.0167	0.0182	0.0226
	100.00	0.0196	0.0132	0.0141	0.0189
	300.00	0.0166	0.0132	0.0117	-
	800.00	0.0200	0.0158	0.0109	-
17.5	0.50	0.715	0.850	1.020	1.540
	0 0.75	0.450	0 576	0.750	1.240
	1.00	0.373	0.434	0.553	0.911
	1.50	0.282	0.330	0.466	0.702
	3.00	0.141	0.177	0.228	0.382
	10.00	0.0594	0.0716	0.115	0.161
	50.00	0.0306	0.0312	0.0394	0.0572
	100.00	0.0244	0.0237	0.0266	0.0408
	300.00	0.0197	0.0165	0.0154	-
	800.00	0.0195	0.0162	0.0141	-

Based on these results, the authors suggest that luminance around the edge of the target, not its area, dictates detectability. In a derivative study by Nachman (1953), verifying the results of Lamar, et al., it was found that targets which varied in area but were equal in the amount of useful edge had equal contrast thresholds, as hypothesized by Lamar and his colleagues.

In the experiment conducted by Fox (1956), discussed earlier, the shape (circle, irregular figure, square, triangle, cross and star) of the object did not affect the detection threshold for small targets. However, for larger size targets, shape did have a pronounced influence on the detection threshold. However, according to the results of Fox, shape did have significant effect on the identification threshold. The irregular figure and the cross had higher recognition thresholds than the circle, star, square and triangle. Based on his results, Fox suggests that complex, more unfamiliar forms are more difficult to identify than the simple, more familiar forms.

Zusne and Michels (1962a, 1962b) in an attempt to quantify target shape, asked subjects to rate several target shapes, on a point scale according to their regularity or familiarity. Bilaterally symmetrical shapes (squares, rectangles, diamonds, and parallelograms) were judged more familiar than asymmetrical shapes. It was also suggested that compactness as indicated by the ratio of perimeter to area and elongation (ratio of length to width) contributed significantly to familiarity of a shape, and consequently the ease with which it is identified by an observer.

Kristofferson (1957) and Kincaid, et al., (1960) discuss detection in terms of an "element contribution" theory which predicts that for equal area, all non-circular targets should have higher contrast thresholds 50 percent level than circular ones. Data are presented which indicate that circles have the lowest contrast threshold followed by simple geometric forms (squares, triangles, stars, etc.), and long thin rectangles.

Kristofferson and Blackwell (1957) measured the contrast threshold for circles, squares, rectangles, crosses, and several other regular target shapes in a uniform background. Circular targets were found to have the lowest contrast threshold, while the contrast threshold of rectangles increases as the ratio of length to width increased. This result agrees fairly with the results of Lamar, Hecht, Shlaer, and Hendley (1947) discussed earlier in this chapter. Based on their results, Kristofferson and Blackwell (1957) conclude that geometrical forms (squares, crosses, stars, etc.), which were equal in area to a 32 minute diameter circle, had approximately the same contrast threshold as the circle. Thus, for targets of this size, target shape has very little effect on detectability, and can be neglected. Duntley (1964) generalizes the relative importance of size to shape by stating that the "...shape of an object is of minor consequence compared with the effect of angular size". The effect of having forms in the display which resemble the target both in size and shape is discussed in the following section.

Confusing Forms

Objects other than the target in the area in which an observer is searching can compete for his attention because they closely resemble the target. In a natural scene these similar forms are almost impossible to isolate and enumerate since it is not known how the eye processes information contained in a visual stimulus. Any number of light and dark spots in the scene, while not really resembling the target, attract the observers attention and affect his ability to successfully detect and identify the object of interest. In an attempt to quantify the effect of conflicting search cues on search behavior, experimenters (Smith, 1961; Boynton and Bush, 1957) have placed a target whose configuration is known to the observer in a field of similar geometric forms, and required to subject to correctly discriminate the true target form from the confusing forms.

Boynton and Bush (1957) investigated the ability of observers to correctly identify a known geometric form presented in a display containing similar struniforms (confusing forms) having curved edges. The contrast of the forms with the background, the number and size of the confusing forms, and the time that the display was exposed to the subject were varied. Exposure times of 3, 6, 12 and 24 seconds were used and the number of confusing forms was either 8, 16, 32, 64, 128, 256, 512 or 1024. Target to background contrasts of -1.00, -.85, -.67, -.44, and -.18 were used. To reduce false detections, a reward was given the subject for a correct response to a target presentation. A reward (motivating) level was discovered which resulted in approximately 5 percent of the detections being false.

Figure 7 shows the probability that the target was correctly identified from the confusing forms as a function of the exposure time and the total number of forms in the display, averaged over all target-to-background contrasts.

Smith (1961) also suggests that search time depends on the number of objects in the display and the similarity between the object of interest and the false targets. Smith used a regular polygon (triangle, square, pentagon, and hexagon) as the target and circles of equal area and contrast as the confusing forms. To minimize false detections, after each trial, the sheet upon which responseswere scoredwas marked incorrect or correct. On this score sheet was a circular display upon which the approximate location of the target was marked. Pay was contingent on speed and accuracy of response. A report of performance was given after each display presentation. Errors or false detections were penalized whenever they occurred-most severely during early sessions, less severely during later ones.

The time required for an observer to successfully locate the target was measured as a function of the number of forms in the display. Figure 8 shows the results obtained by Smith for square targets contained in a display of circular false targets. He suggests that the equation,

$$\log t = m \log N + n \qquad (2.1)$$

where m is the slope, n is the intercept N is the number of confusing forms, and t is the time required to correctly identify the target, explains observer performance. In the same experiment, Smith varied the difference between the

size of target and false target and the contrast of the target and false target with the background. Figure 9 shows the time required to locate a square target in a display containing 256 false (circular) targets as a function of target-false target percent size and contrast difference. Percent contrast difference is defined as the ratio of the target to pseudotarget contrast multiplied by 100. If C_T is the contrast of the target with the background and C_{PT} is the contrast of the pseudotarget with the background the percent contrast difference, $\overline{C}$ is:

$$\overline{C} = \frac{C_T}{C_{PT}} (100) \quad . \tag{2.2}$$

Percent size difference is defined as the ratio of the area of the target to the area of the pseudotarget multiplied by 100. If A_T is the area of the target and A_{PT} is the area of the pseudotarget, the percent size difference, $\overline{A}$, is

$$\overline{A} = \frac{A_T}{A_{PT}} (100) \quad . \tag{2.3}$$

From Figure 9, it can be seen that search time increases as the size and contrast of the false targets approaches the size and contrast of the true target.

These studies indicate that increasing the number of competing stimuli in a display degrades the ability of an observer to successfully locate a target. While the forms used by Smith and Boynton and Bush were easily countable due to the carefully controlled nature of the laboratory experiments, there is no existing methodology for locating such forms in a natural scene. Since, confusing forms in a natural scene will undoubtedly vary within each scene

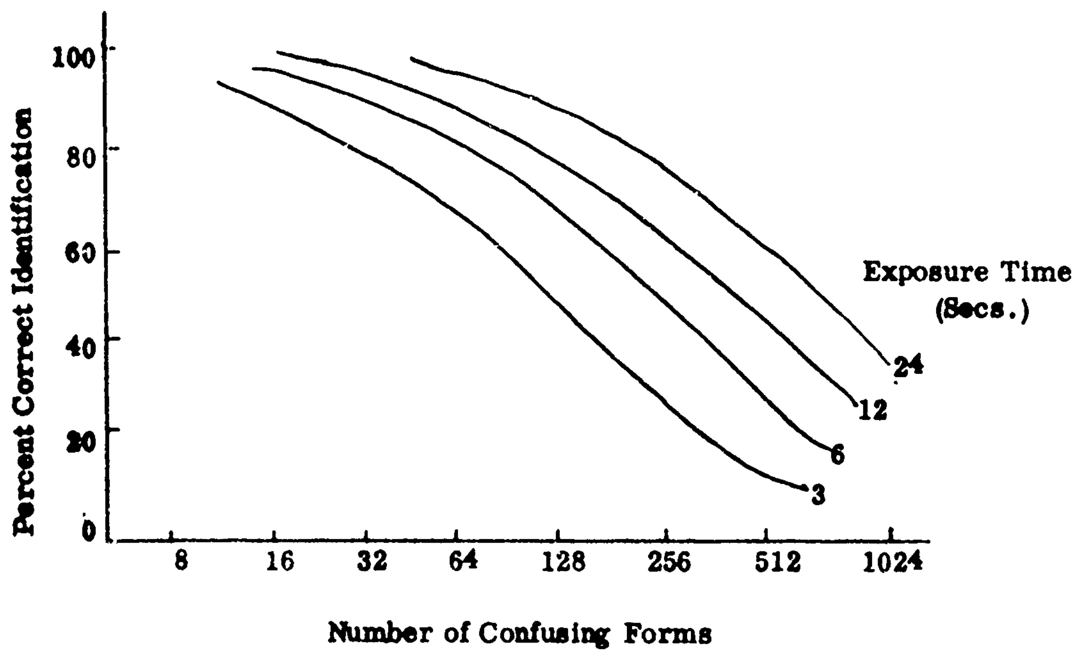

Fig. 7.--Percent Correct Recognition as a Function of the Number of Confusing Forms and Exposure Time According to Boynton and Bush (1957). Target to Background Contrast of -1.00, -.85, -.67, -.44, and -.18 are Randomized Over All Exposure Times.

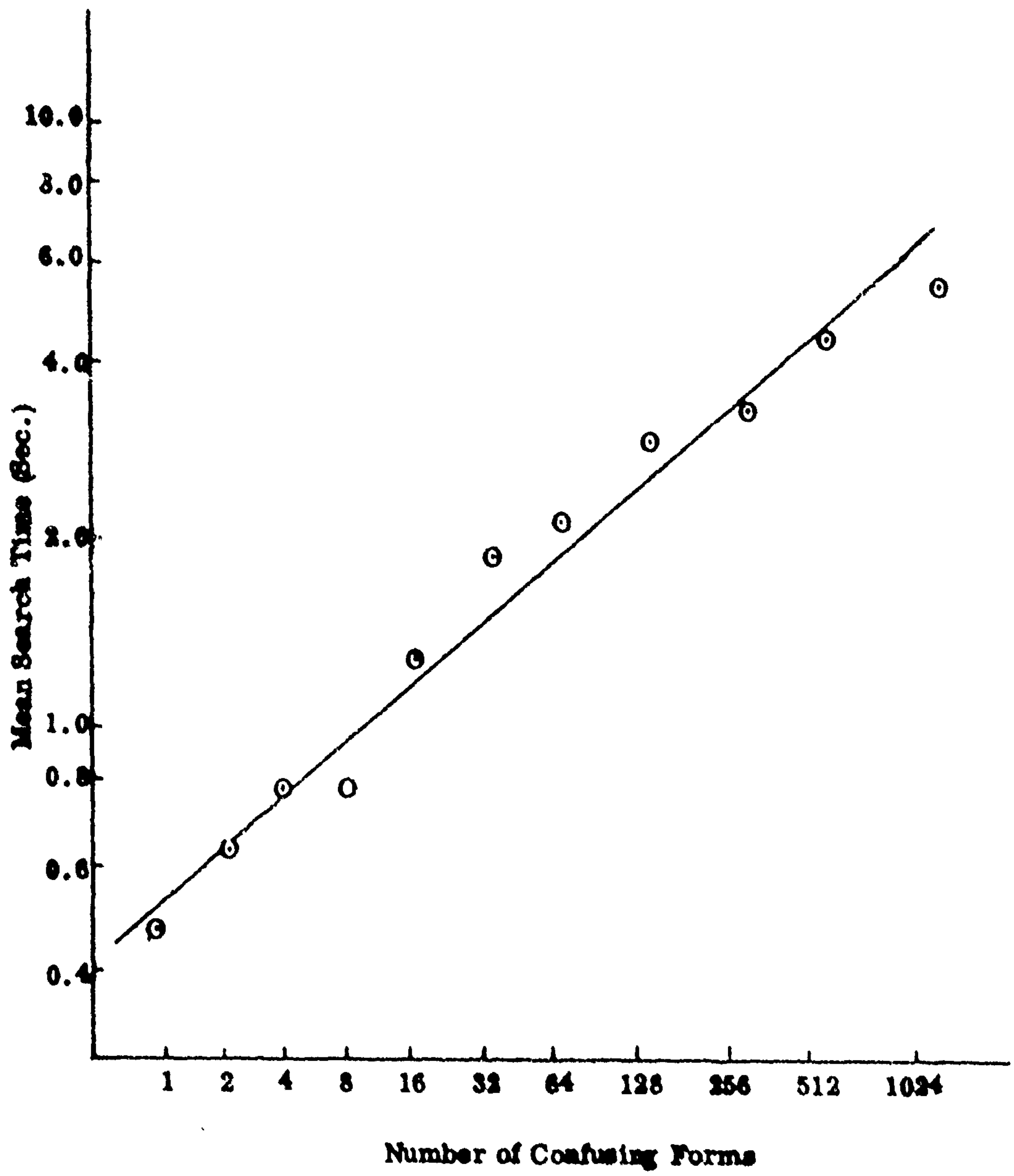

Fig. 8.--Time Required to Identify a Square Target as a Function of the Number of Circular Confusing Forms of the Same Area and Contrast as the True Target Taken from Smith (1961).

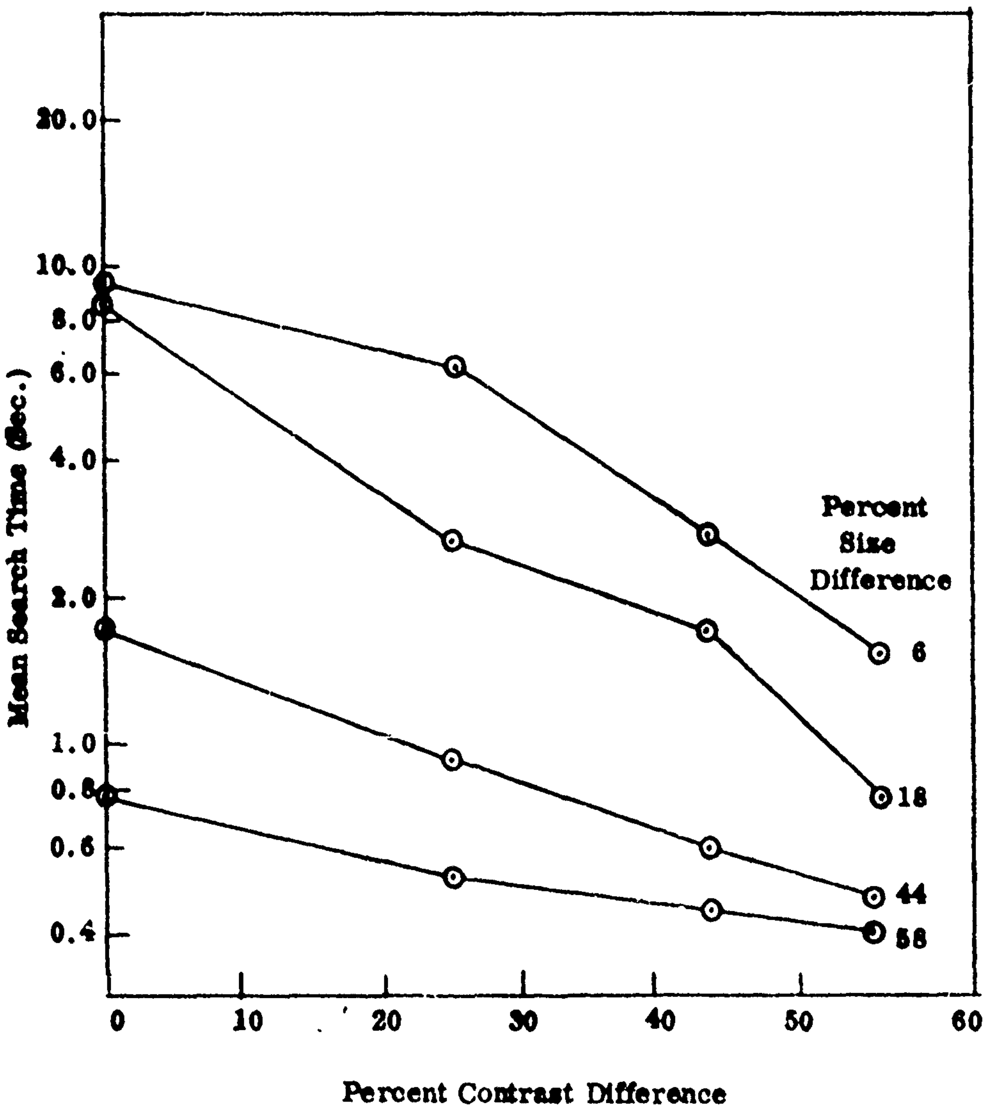

Fig. 9.--Mean Search Time as a Function of Target-Confusing Form Size and Contrast Difference Taken from Smith (1961).

from the target in size, contrast, and shape, making them impossible to isolate, some other interpretation of competing stimuli must be made. A measure of competing stimuli, which is still measured subjectively but is somewhat easier to verify, is discussed in Chapter 4.

Eye Movements

The way the observer looks for a target affects his ability to successfully locate the target. Many techniques have been devised for recording the movement of the eye as it searches a display. These methods are described in Alpern (1962).

When an observer is performing a search task, the eyes do not scan smoothly over the area of search responsibility, but sporadically in a series of jumps called "saccadic" movements (Smith and Semmelroth), 1961), separated by brief pauses called "fixations" (Ford, et al., 1959). For all practical purposes, these fixational pauses are the only periods during which detection can occur (White, 1964), and consequently are of most importance. These fixational pauses are often referred to as "glimpses" at the object of interest. Smith and Semmelroth (1961) suggest that peripheral vision plays a major role in visual search:

> "...the eyes usually move ballistically from one quite clearly defined object or element in the display to another such element, i.e., the path of the movement and the stopping point are determined before movement begins. For this to occur, the object of each succeeding fixation must be perceived peripherally before it is perceived fovially."

The duration of the fixational pause and ballistic movement, measured under several different conditions, is discussed below.

Ford, White and Lichtenstein (1959) suggest that when the observer is looking for an object in a relatively homogeneous field, the average duration of the fixation is about 0.27 second, with none less than 0.10 second. Due to the time taken by the saccadic movements, several investigators (e.g., White, 1964; Ryll, 1962) suggest that 3 fixations can be expected each second under free search situations. However, as the scene becomes more complex (as more forms compete for attention), the average duration of the fixation decreases. Townsend, Enoch and Fry (1958) measured the fixation duration of an observer searching a display with varying complexity. Complexity was reduced by passing opaque filters of several densities between the display and the observer. Their results suggest that a smaller area per unit of search time is covered for the complex scenes (those scenes unblurred). It is also suggested that the average duration of the eye fixation increases as the overall contrast of the scene is reduced and the average extent of individual eye movements decreases as the overall contrast is reduced as a result of blurring[4] by the opaque filter. The effect of scene complexity defined as the relative amount of blur present in the scene, on fixation duration, as suggested by Townsend, Enoch, and Fry is given

[4]Blur is a measure of edge definition and distortion and is not necessarily completely described by a contrast measurement. Targets of equal contrast in displays with different degrees of blur are not equally detectable.

in Figure 10. From Figure 10, it appears that the duration of the fixation is fairly constant at 0.25 for the unblurred and slightly blurred displays and increases rapidly as the complexity of the scene decreases. These results would suggest that fog, haze, and smoke would not only affect single-glimpse detection probability (the probability of detection on a single fixation pause) in the field by degrading target contrast, but will increase search time by increasing the average duration of a fixation.

The effect of display size on the fixation duration has been investigated by Enoch and Fry (1958). The results of this study given in Figure 11, indicate that the fixation duration is fairly constant (0.35 second) for display subtending a visual angle greater than 10 degrees. However, as the size of the display decreases (below 10°), the duration of the fixation increases at an increasing rate. The results discussed in this section indicate that a glimpse duration of approximately 1/3 second is appropriate for essentially all search conditions in the field except extreme conditions of fog, haze, or smoke. In the following section the probability of detecting a simple cir- -lar target as a function of its contrast with its surroundings during one fixation (glimpse) is discussed.

Target-to-Background Contrast

The apparent contrast, C, of a target is defined in psychophysical terms as the ratio of the difference between the brightness of the target, B_t, and its surroundings, B_s, to the brightness of the surroundings (Blackwell, 1946); i.e.,

$$C = \frac{B_t - B_s}{B_s}, \qquad (2.4)$$

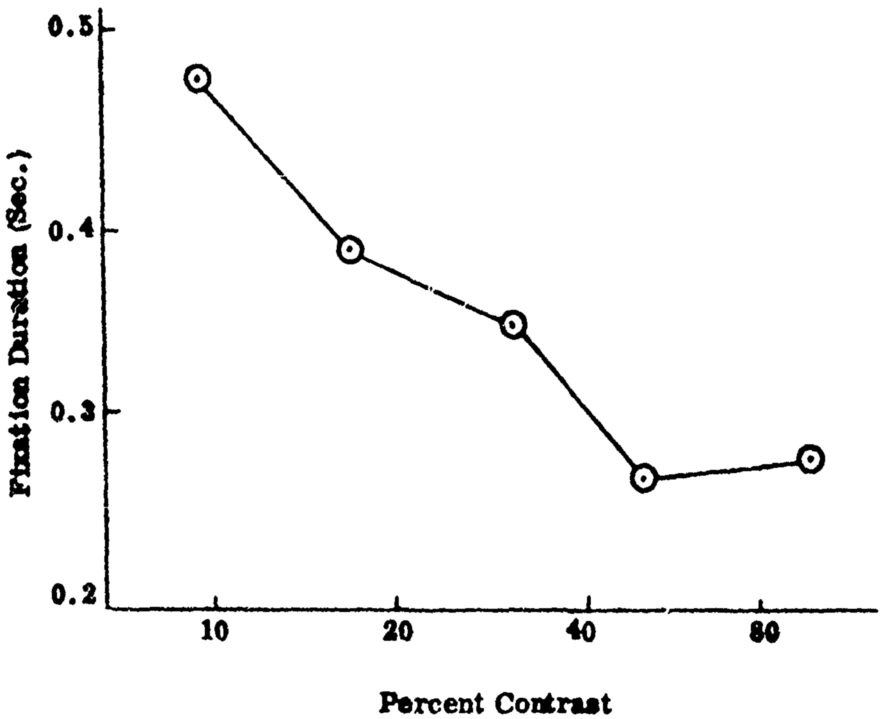

Fig. 10.--Fixation Duration as a Funcation of Over All Target-Scene Contrast (Display Blue) Taken from Townsend, Enoch, and Fry (1958).

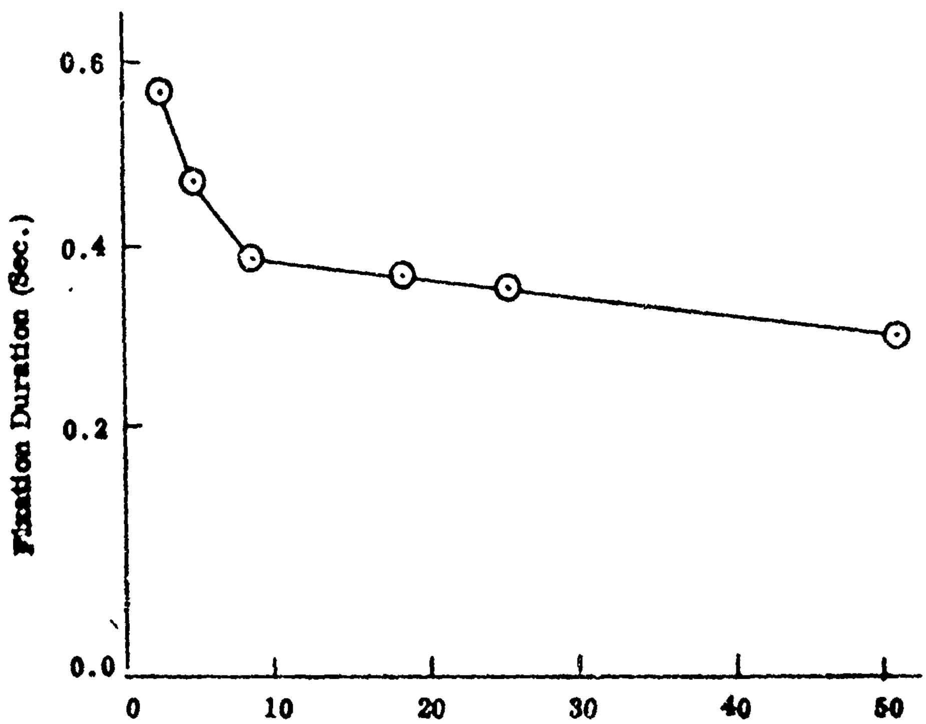

Fig. 11.--Fixation Duration as a Function of the Size of the Display Taken from Enoch and Fry (1958).

where B_t and B_s are brightnesses as seen at the observer's position. Being the result of a sensation, brightness is not measurable. However, the luminance of the background and foreground, the physical counterparts of brightness, are used to calculate inherent brightness contrast. The inherent contrast of the target C_o, is defined as:

$$C_o = \frac{L_o - L_s}{L_s} \quad , \tag{2.5}$$

where L_o is the luminance at a point on the object and L_s is the luminance at a point on the surface surrounding the object, both measured at the target. The apparent contrast C, is that contrast actually seen by the observer. It is usually less than C_o because the particles in the atmosphere between the observer and target attenuate some of the contrast by scattering and absorbtion. This degradation in contrast, which is a function of the atmospheric conditions (fog, smoke, haze, etc.) and the target-to-observer range, is discussed in Chapter 3.

In the detection literature, the contrast that is usually mentioned is that apparent contrast which results in a 50 percent probability of detection. This is known as the threshold contrast, C_t. Blackwell (1946) conducted an extensive study to determine the effect of target size and background brightness on the contrast threshold of targets exposed to the observer for 1/3 second. Taylor, (1960a, 1960b) extended Blackwell's work to larger targets. Their data, shown in Figure 12 apply only to circular targets viewed against a background of uniform luminance.

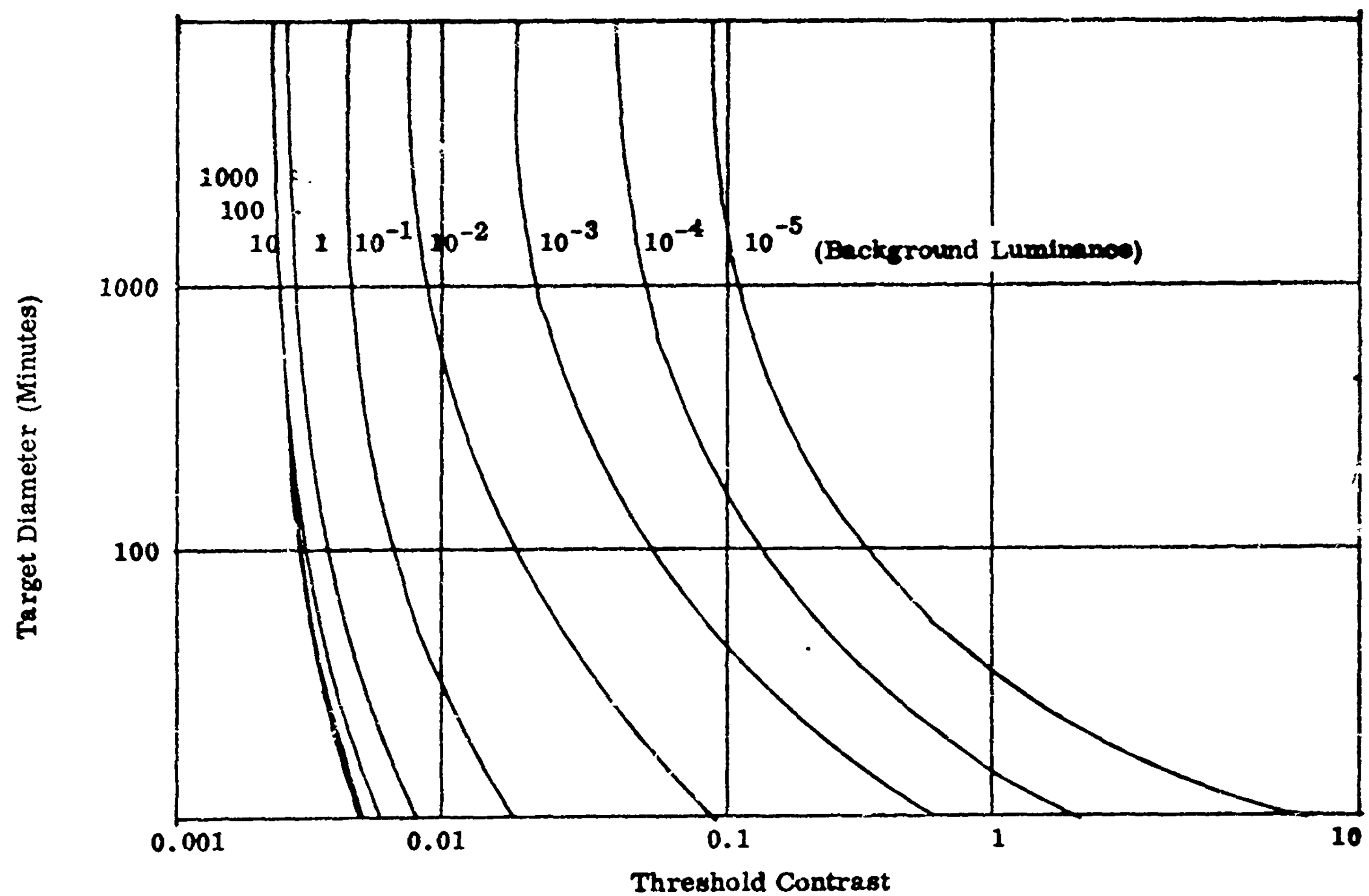

Fig. 12.--Contrast Threshold as a Function of Target Size and Background Luminance According to Blackwell, (1946) and Taylor, (1960a, 1960b).

TABLE 2

CONTRAST THRESHOLD FOR DIFFERENT SIZE TARGETS AS A FUNCTION OF THE ANGULAR DISTANCE OF THE TARGET FROM THE FIXATION DIRECTION ACCORDING TO TAYLOR (1961)

Degrees from fixation direction	Target Size (minutes of arc)				
	100	1.74	3.60	15.0	120.0
0	0.539	0.196	0.0488	0.0162	0.0078
1.25	0.772	-	0.0793	0.0214	0.00921
2.50	1.39	0.386	0.0960	0.0240	-
5.00	2.75	0.786	0.218	0.0356	0.0121
7.50	3.72	1.03	0.278	0.0465	0.0127
10.00	4.55	1.48	0.333	0.0557	0.0135
12.00	5.73	1.69	0.545	0.0725	0.0154

where σ is the standard deviation of the normal ogive. Dividing the numerator and denominator of the argument of Φ in equation 2.7 by the contrast threshold, the single-glimpse detection probability, g, becomes:

$$g = \Phi \left\{ \frac{C/C_t{}^{-1}}{\sigma/C_t} \right\} \qquad (2.8)$$

Blackwell (1963) suggests that the ratio σ/C_t in equation 2.8, remains constant regardless of the time the target is exposed, the size of the target, and the background luminance. Data presented in Blackwell (1963) are discussed below to illustrate the effect of target-scene variables (stimulus conditions) on the ratio σ/C_t.

Effect of Target-Scene Variables on the Ratio σ/C_t

The effect of target size, target shape, and background luminance (adaption brightness) on the ratio σ/C_t has been studied by several experimenters (Blackwell, 1963). Results from experiments discussed in Blackwell (1963) illustrating the effect of target-scene variables on σ/C_t are discussed in the following three sections.

Background Luminance

Data given in Blackwell (1963), taken from a study by Blackwell and Law (1958) indicate that the ratio σ/C_t increases as the background luminance decreases. For a constant exposure time of 0.01 second and target diameters of one to 45 minutes of arc, the ratio σ/C_t varied as shown in Figure 13.

Taylor (1961) suggests that the contrast threshold changes with the retinal position of the object in the field of view. The results of this study, given in Table 2, indicate that the threshold contrast increases as the location of the target from the point of fixation increases. This implies that the probability of detecting a target in the periphery is less than the probability of detecting the same target when the fixation is located directly on the target.

Blackwell (1946) and Duntley (1964) demonstrate that for these simple (circular) targets of uniform luminance viewed against backgrounds of uniform luminance, targets of equal contrast brighter and darker than their background are equal in detectability. It is customary to refer to targets brighter than their background as having positive contrast, and targets darker than their background as having a negative contrast. Most often the sign of the apparent contrast is ignored (Duntley, 1964), so that equation 2.4 becomes

$$C_o = \left| \frac{B_t - B_s}{B_s} \right| , \tag{2.6}$$

where $\left| \frac{B_t - B_s}{B_s} \right|$ is the absolute value of the quantity $\frac{B_t - B_s}{B_s}$.

Blackwell (1963) suggests that the detection probability of a circular object with apparent contrast, C, is given by

$$g = \Phi\left(\frac{C - C_t}{\sigma}\right) \tag{2.7}$$

From Figure 13, it appears that the ratio σ/C_t is a constant 0.44 at low background luminance and decreases as background luminances increases (above 1 foot candle).

Target Size

Blackwell (1963) also demonstrates the effect of target size on the ratio. Data taken from experiments by Blackwell and Austin (1952) and Kristofferson and Blackwell (1958) is given in Table 3. From Table 3, it can be seen that the ratio σ/C_t for targets of varying size viewed for 0.001 second at zero background intensity varies without pattern between 0.308 and 0.402. These data, taken from Blackwell and Austin (1952), indicate that target size has a random effect on the ratio at this background luminance and exposure time. The data given in the second column of Table 3 also illustrate this random effect. These data, taken from Kristofferson and Blackwell (1958), are for a background luminance of 10 foot-lamberts and exposure duration of 0.01 second.

Target Shape

Data given in Blackwell (1963) indicate that the ratio σ/C_t remains essentially constant for different target shapes. Ratios of σ/C_t are given for circles, rectangles, and complex forms. These data, reproduced in Table 4, are taken from studies by Kristofferson and Blackwell (1958) and Blackwell and Smith (1959). Target sizes, exposure times, and background luminance were different for the two studies. From Table 4, it can be seen that target shape (for those shapes studied) has little effect on the ratio. The data also indicate, as did the data of Figure 13, that the ratio σ/C_t increases as background

TABLE 3

EFFECT OF TARGET SIZE ON THE RATIO σ/C_t
AS GIVEN IN BLACKWELL (1963)

Target Diameter (min.)	From Blackwell and Austin (1952) σ/C_t σ/C_t	From Kristofferson and Blackwell (1958) σ/C_t
64	0.367	0.285
32	0.402	0.338
16	0.308	0.308
8	0.372	0.330
4	0.372	0.340
2	0.311	0.308
1	0.345	0.345
	MEAN = 0.354	MEAN = 0.322
Exposure time	0.001 second	0.01 second
Background Luminance	zero	10 foot-lamberts

TABLE 4

EFFECT OF TARGET SHAPE ON THE RATIO σ/C_t
AS GIVEN IN BLACKWELL (1963)

Shape	From Kristofferson and Blackwell (1958) σ/C_t	From Kristofferson and Smith (1959) σ/C_t
Circles	.322	.527
Rectangles	.303	.547
Complex Forms	.289	.484
	MEAN = 0.305	MEAN = 0.519

Exposure Time	0.01 second	0.01 second
Background Luminance	10 foot-lamberts	zero

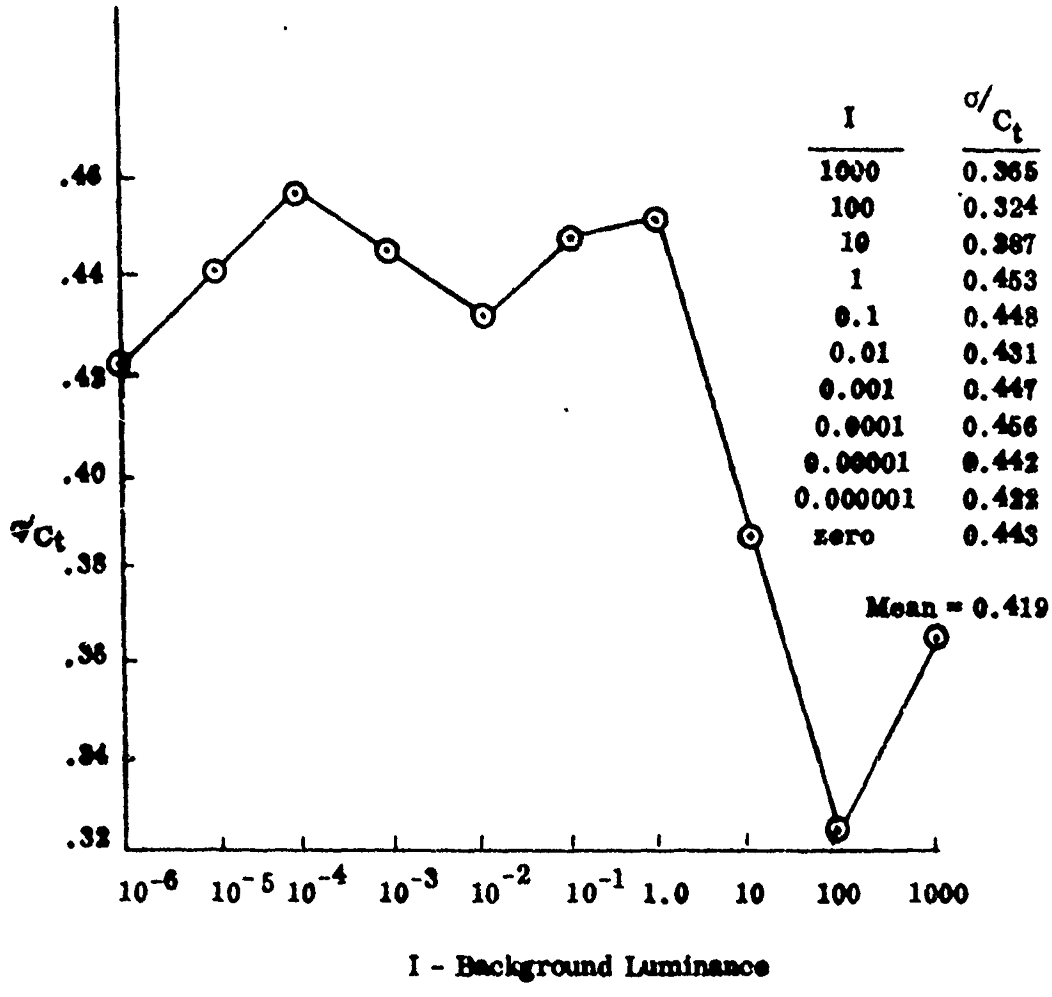

I	σ/C_t
1000	0.365
100	0.324
10	0.387
1	0.453
0.1	0.448
0.01	0.431
0.001	0.447
0.0001	0.456
0.00001	0.442
0.000001	0.422
zero	0.443

Fig. 13.--Effect of Background Luminance on the Ratio σ/C_t For a Constant Exposure Time of .01 Second.

luminance decreases for constant exposure time for targets having shapes other than circular.

The effect of randomized target sizes, exposure times, and background luminance on the ratio σ/C_t was investigated by Blackwell and McCready (1958). Data given by Blackwell and McCready, reproduced in Table 5, indicate that a typical value of σ/C_t of 0.390 can be used for most stimulus conditions of interest. These data are based on 80,000 observations obtained from four observers.

Examination of the data presented in Blackwell (1963) suggests that the ratio σ/C_t varies very little over all the stimulus conditions investigated. Blackwell calculated the ratio of σ/C_t for 36 observers, representing over one million data points. The values of σ/C_t for these 36 observers are given in Table 6, taken from Blackwell (1963). These observations taken from numerous authors represent the measurements of σ/C_t for almost any conceivable combination of stimulus conditions. From Table 6, it appears that σ/C_t varies randomly between 0.314 and 0.584. A X^2 - goodness of fit test performed on the data given in Table 6 showed that the hypothesis that the data comes from a uniform distribution of the form:

$$f\left(\frac{\sigma}{C_t}\right) = \frac{1}{b-a} \tag{2.9}$$

where,

$a = .314$, and
$b = .584$

could not be rejected at the .05 level.

TABLE 5

VALUES OF σ/C_t DETERMINED BY BLACKWELL AND MCCREADY (1958) FOR SEVERAL TARGET SIZES, BACKGROUND LUMINANCES, AND EXPOSURE TIMES. WITHIN EACH CATEGORY, THE OTHER TWO VARIABLES ARE CONFOUNDED WITHIN THE VARIABLE OF INTEREST

Diamter of Target (min)	σ σ/C_t	Background Luminance (foot-lamberts)	σ/C_t	Exposure Time (sec)	σ/C_t
51.4	0.384	100	0.357	1.0	0.467
12.8	0.397	10	0.382	0.1	0.370
3.21	0.418	1	0.398	0.01	0.358
0.802	0.367	0.1	0.420	0.001	0.333
			0.420		
		0	0.419		

GRAND MEAN=0.390

TABLE 6

VALUES OF σ/C_t FOR 36 OBSERVERS AS GIVEN BY BLACKWELL (1963) SUMMARIZED OVER SEVERAL ENVIRONMENTAL CONDITION

Observer Number	σ/C_t	Observer Number	σ/C_t
1	0.420	19	0.320
2	0.479	20	0.470
3	0.418	21	0.556
4	0.446	22	0.550
5	0.467	23	0.392
6	0.491	24	0.491
7	0.467	25	0.456
8	0.463	26	0.584
9	0.546	27	0.519
10	0.370	28	0.400
11	0.434	29	0.409
12	0.411	30	0.467
13	0.430	31	0.429
14	0.424	32	0.480
15	0.368	33	0.390
16	0.396	34	0.347
17	0.360	35	0.314
18	0.352	36	0.396

Maximum-likelihood estimates of the mean and variance of the distribution of σ/C_t were calculated. It was found that the mean of the sample shown in Table 6 is 0.434 and the variance is 0.0061. Using a value, $(\sigma/C_t)^*$, of σ/C_t sampled from the uniform distribution given in equation 6, the probability, g, of detecting the target on a single glimpse becomes:

$$g = \Phi \left\{ \frac{C/C_t - 1}{(\sigma/C_t)^*} \right\} \tag{2.10}$$

Equation 2.10 now represents the single-glimpse detection probability for any observer, based on a sample of 36 observers, supposedly chosen at random from the universe of observers and stimulus conditions. For the average observer, under randomized stimulus conditions, equation 2.10 reduces to:

$$g = \Phi \left\{ \frac{C/C_t - 1}{.434} \right\} \tag{2.11}$$

In equation 2.11, the contrast threshold, C_t, was taken under the most ideal laboratory conditions, that is, i.e., all stimulus conditions were carefully controlled. Subjects in the laboratory were told precisely where and when the stimulus was to appear, and were well practiced in the detection task (each observer had detected several thousand such targets). Several investigators (Taylor, 1964; Blackwell, 1958; Blackwell, 1967) have suggested that C_t be multiplied by a constant, K, so that it applies to field conditions. This multiplicative constant, often referred to as the field factor, is given by Taylor (1964) as.

$$K = \prod_{i=1}^{n} k_i , \tag{2.12}$$

where the k_i ($i = 1, \ldots, n$) are the multiplicative constants causing the respective difference i ($i = 1, \ldots, n$) between laboratory and field conditions. Blackwell (1958) suggests the use of three such k_i as follows:

k_1 = 1.09, to correct for lack of knowledge of target size and duration of appearance,

k_2 = 1.31, to correct for observer uncertainty about where the target is to appear, and

k_3 = 2.40, correction made when necessary to adjust forced-choice data to yes-no detection data.[5]

Taylor (1964) suggests an additional factor, $k_4 = 1.90$, which corrects the contrast threshold for the difference between trained and naive observers. When all four of these conditions apply, equation 2.12 becomes:

$$K = \prod_{i=1}^{4} k_i , \tag{2.13}$$

which reduces to

$$K = 6.5.$$

With a total field factor $K = 6.5$, equation 2.10 corrected for four differences between laboratory and field conditions becomes:[6]

$$g = \Phi \left\{ \frac{C/6.5(C_t) - 1}{.434} \right\} \tag{2.14}$$

[5]A comparison of these types of data collection is given in Lawson(1968).

[6]In this expression, it is assumed that the ratio, σ/C_t', where C_t' is the contrast threshold under field conditions, and σ' is the standard deviation of the normal 0 give in the field, remains constant at 0.434.

No additional field factors, k_i ($i = 5, \ldots, n$), have been discovered after an extensive review of the current literature. However, it is conceivable that some or all of the following factors might contribute to a degradation in field performance which would be reflected through the inclusion of additional field factors in equation 2.14:

1. Presence of similar forms in the background(confusing forms),
2. Other sensory clues present in the natural environment,
3. Geometric form of the target (complex as opposed to simple circular targets),
4. Light scattering causing the image to blur, and
5. Spectral and spacial distribution of light on the target's surface (highlights and shadows).

Blackwell and Bixel (1963) investigated the effect of a complex non-uniform background on the contrast threshold of a circular target. Three non-uniform backgrounds were used with targets of various size, luminance and location in the background. Two of the backgrounds were formed from ball bearings while the third was a terrain photograph. In general, it was found that:

> "...when the background luminance varied within the area occupied by the target, it was the target contrast with the luminance at its border which determined target visibility."

This implies that the detectability of an object located anywhere in a complex display having non-uniform luminance is governed at least in part by its contrast with its immediate surroundings, not its average contrast with points over the entire display.

The use of contrast threshold, discussed in this section, to predict object detectability is discussed in Chapter 3. In Chapter 3 the object is represented as a simple variously oriented three-dimensional object (sphere) so that the image formed by contrasting the object with its surroundings can be described without great difficulty.

Target Form

As evidenced in the preceding discussions, the vast majority of basic detection and recognition data has been obtained using simple (most often circular) targets of uniform luminance. This type of target is adequately described by specifying the contrast of the target with its background and its angular size (Blackwell, 1946). However, under most field conditions, the target is not simple in shape nor does it have uniform luminance. In such cases, shadows and highlights within an object are strong clues for detection and recognition. Therefore, with the large number of ways in which the rays from the illuminating source strike the variously oriented surfaces of the target, there are a correspondingly infinite number of sizes, shapes, and patterns an object can present to an observer.

Kaure (1965) expanded on the difficulty of describing this image when he stated that,

> "Complex photographic, high-resolution radar, infrared, or electro-optical images have been the stimuli in many psychological studies of target recognition and photo-interpretation. The comparison or generalization of the results of these studies has been almost impossible because no adequate, objective definition or description of these stimuli has been possible. An

> objective and quantitative measure of the structure of an image would make this comparison and generalization possible and would allow the determination of the relative importance of image complexity in target identification."

For the purpose of this study, no attempt will be made to accurately describe the form of the target which acts as a stimulus for detection, but several of the important characteristics of a patterned target-background complex are discussed below.

The ability of an observer to discriminate this patterned target from elements of the terrain in a natural scene has been the subject of considerable research in recent years (Wulfeck and Taylor, 1961). The pattern of luminances which the target presents to the observer must be recognized as the object of interest or detection and subsequent recognition by the observer will not occur. The difficulty with predicting the ability of an observer to successfully discriminate the target is to isolate the stimuli which initiate the detection and identification response. Morris (1959) studied the effect of this "target pattern" on detection and identification. Morris states that a target is patterned:

> "...If it has distinguishable areas of various size and reflectance, such that, as a whole, the target cannot be brought to zero contrast within a uniform background through adjustment of target illumination."

This definition fits targets commonly encountered in a natural terrain scene, in that the pattern of luminances created on the surface of the target and its surroundings presents an infinite number of contrasts to the observer. Morris also states that "the discernable elements in the patterned target may be considered as several independent targets simultaneously viewed, each with its own detection

range." This fact is used in Chapter 3 to estimate the single-glimpse probability of the target, where areas of different luminance formed on a simplified representation of the target are treated as independent objects when contrasted with elements of the terrain and the target itself.

The relationship between complexity, recognition, and the number of forms competing for the subject's attention was investigated by Deese (1956). Simple several-sided two-dimensional targets were constructed using:

1. Right angles (regular forms), and

2. Obtuse and acute angles (irregular forms).

The measure of complexity was the number of angles present in the form (target). That is, a simple form had fewer angles present. The background against which the targets were silouetted were of uniform luminance. The study was conducted with three levels of background luminance. A pay scheme was used to motivate the subject to avoid false detections. The subject was severely penalized each time an incorrect response was made. This minimized the number of false detections which had to be eliminated from the data analysis. The results of the experiment showed that:

1. For the regular forms, there were more recognition errors with the simple forms than with the complex ones, but the time required to recognize the target was slightly longer for the complex figures.

2. For the irregular forms, there was no difference in frequency of error between the simple and complex targets, but the time required to recognize the target was longer for the complex figures.

These results indicate that as the number of abrupt changes in the outside surfaces of a target form increases, the time required to correctly identify the form increases, regardless of the nature of these changes. Under field conditions, this suggests that a target having subtle changes in contour (such as camoflage or shading) would be more difficult to identify than a simple uniform-luminance target.

Image Characteristics

The quality and content of the image seen by the observer greatly effect his ability to successfully detect or identify objects of interest on an artifical laboratory display or in a natural environment. Rhodes (1964) attempted to relate selected psychologically meaningful variables taken from aerial reconnaissance photographs to the difficulty observers had identifying targets in the photographs. In this study, 200 photographs were first rated by 35 photo-interpreters on an arbitrary scale between one and ten according to their "difficulty". These 200 photographs were then divided into two groups of 100 each having equal difficulty as measured by the arbitrary scale of the raters who screened them. Typical target types contained in the photos were:

1. Bridge,
2. Storage tank(s),
3. Plane(s),
4. Dam,
5. Roundhouse,

6. Ship(s),

7. Building(s), and

8. Others

The experiment was divided into two phases. In phase one, 20 subjects were required to detect and identify targets of various shapes and sizes from each of 100 photographs after they had examined a 7/16" reproduction[7] of it. In the other phase, 20 other subjects were asked to rate the same 100 images on a scale from one to seven according to how strongly they felt the image had the following subjective characteristics:

a. Frequency of occurrence in the picture of objects that could be confused with the target.

b. Distinctiveness of the target shape, that is, how much the target stands out because of its shape.

c. Amount and variety of picture detail.

d. Distinctiveness of the target contrasts, i.e., how much the target stands out because of its lightness or darkness.

e. Size of target relative to size of other objects in the picture.

f. Freedom of target location, that is, the extent to which the nature of the target allows it to be located anywhere in picture (e.g., building has more freedom than bridge).

g. Homogeneity of picture content (excluding target).

h. Overall picture contrast, that is, the range of black-white gradation.

---

[7]The 7/16" size was used since it was approximately the average size of all objects viewed by the subject. This size reproduction was shown to all subjects. It was felt that a reproduction of exactly the same size would aid the subjects too much.

i. Isolation of the target from background.

j. Distinctiveness of the target pattern, that is, how much the target stands out because of arrangement, detail and texture of its elements.

k. Sharpness or clarity of picture detail.

l. Distinctiveness of target size, that is, how much the target stands out because of its size.

In addition to these twelve subjective measures of the difficulty of the image the physical size in centimeters (m) and distance of the target from the display center (in centimeters) (n) were measured.

Following the collection of phase-one and two data for the first set of 100 photographs, the roles of the two sets of subjects were reversed, that is, the 20 subjects who subjectively rated the first group of 100 photos, participated in the detection phase for the second group of 100 photographs and those 20 subjects who detected from the first group rated for the second group. Subjects consisted of 20 trained photo-interpreters and untrained 20 college students.[8]

Rhodes then attempted to relate the 14 measures (a, ..., n) of the images content and quality mentioned previously to:

1. The time required to detect and identify the target (T), and

2. The difficulty scale of the photograph obtained while the photos were being screened (D).

---

[8]Ten each of the photo-interpreters and college students were assigned to each group.

Linear multiple regressions (Hogg and Craig, 1960) of the form

$$T = \alpha_o + \alpha_a (a) + \alpha_b (b) + \ldots + \alpha_n (n) , \qquad (2.15)$$

and

$$D = \alpha'_o + \alpha'_a (a) + \alpha'_b (b) + \ldots + \alpha'_n (n) , \qquad (2.16)$$

where $\alpha_o, \ldots, \alpha_n$ and $\alpha'_o, \ldots, \alpha'_n$ are constants determined from the values of the variables T, D, a, b, c, d, e, f, g, h, i, j, k, l, m, and n , were performed on the data for the different sets of subjects. The regressions shown in equations 2.15 and 2.16 given by Rhodes did not necessarily include the effects of all of the 14 variables a, ..., n, since some of the constants $\alpha_a, \ldots, \alpha_n$ were forced to be zero to see whether they were significant in predicting either T or D. Multiple correlation coefficients for 16 such relationships given by Rhodes ranged from 0.73 to 0.90, meaning that up to 81 percent of the variability in the data was explained by these 14 variables.

The results of this experiment indicate that any or all of the measures incorporated by Rhodes affect the detection time of targets in a photographic display. It is quite clear that the targets contained in these photographs are not physically similar to those contained in the films of Brown (See Appendix A), not only because of differences in viewing angle and target type, but because of target motion in the films of Brown. However, it is felt that the characteristics presented here as quantified by Rhodes represent a good summary of the factors in any natural target scene which dictate detectability of any object.

Target Motion

Movement of the target across the field of view was shown by Brown (1966) to be a significant variable affecting detection time. Due to the great changes in the scene carried by motion of the target, it is an obvious clue. It would be hypothesized that these same differences are caused by changes in the terrain against which the target is silouetted, changing the apparent contrast discussed earlier in this chapter. This hypothesis is discussed in Chapter 4. Because this contrast changes continually for a moving target in a natural scene, target motion is readily discernable to the observer. The effect of the target crossing velocity on detectability is considered as a variable affecting detection performance in Chapter 4.

Conclusions

In this chapter, basic laboratory and field experiments conducted over the past four decades have been discussed. Data from these experiments, when examined as a whole, give clues to the detection of objects in a complex environment, although each individual piece may apply to only one specialized segment of the entire problem. Using the experience and intuition of the author, these data are incorporated in a model in Chapter 4 to predict the probability that a complex target is detected in a natural environment. However, it must be remembered that even with the complex development which is to follow, the phenomenon of field detection has been simplified to the point that it may no longer be valid. Since other attempts to do the same have resulted in conflicting results, this must be regarded as simple another attempt. This philosophical problem will be discussed in detail in Chapter 5 of this thesis.

CHAPTER 3

TARGET CONTRAST

Introduction

A combat vehicle in a natural terrain setting will present a complex luminance pattern to an observer. Contrast varies continuously along the edge and across the face (internal surface) of such targets. That is, military targets are not usually characterized by a single value of contrast as are the simple forms used in laboratory experiments to generate relationships, such as those in Figure 12 of Chapter 2, for predicting the single-glimpse detection probability. Data on the single-glimpse detection probability for complex contrast patterns are not available. Certain assumptions can be made, however, so that the relationships of Chapter 2 can be applied to estimate the single-glimpse detection probability for military vehicles in natural terrain settings. These assumptions are based on the best evidence available to the author on the detection of objects under natural (field) conditions as opposed to artifical (laboratory) conditions. Since no significant work on the detection of natural objects in complex surroundings is in evidence, the authors intuition has played a major role in the development of this chapter. The simplifications and assumptions which have been imposed were necessary to prevent the problem from growing without bound. Since the mechanisms by which visual information is integrated

into perception are not completely understood , the major results from Chapter 2 serve as a framework for a model of glimpse probability to be developed in this chapter. Following the development of the glimpse model, Chapter 4 will be devoted to a discussion of a model of detection probability based on this glimpse model. In addition, a means of testing the validity of the model based on detection-time data will be discussed.

In this chapter, the target is represented as a simplified three-dimensional form. The sizes of the highlighted and shaded areas of this target representation are related to the position of the illuminating source and the observer. Then, a method is presented for predicting the contrasts that the highlighted and shaded areas have with each other and with the background and foreground, respectively. This method is based on reflectance data collected for common background features (trees, grass, etc.) and for materials similar to tank armor. Each highlighted and shaded area is regarded as a separate visual stimulus. Methods for determining contrast thresholds and glimpse probabilities for each area are proposed. Next, a theoretical relationship is presented relating the different glimpse probabilities to one representative glimpse probability for the target.

Determination of Apparent Contrast

The inherent contrast, C_o, of a point source, P, is defined as

$$C_o = \frac{L_P - L_B}{L_B} , \qquad (3.1)$$

where L_P is the luminance of the point and L_B is the luminance of the area surrounding that point, i.e., its background. Both luminances are measured at zero distance from the point. If the point and its background are on the same surface, C_o, as given by 3.1, would be referred to as inherent internal contrast. That is, the inherent internal contrast, C_o, between any two points within the target with luminance L_1 and L_2, respectively, is defined as:

$$C_o = \begin{cases} \dfrac{L_1 - L_2}{L_2} & L_1 > L_2 \\ 0 & L_1 = L_2 \\ \dfrac{L_2 - L_1}{L_1} & L_2 < L_1 . \end{cases} \qquad (3.2)$$

The inherent contrast of a point within a homogeneously illuminated flat-surface target would usually be zero since its background would be part of the same target. Thus, it is common to speak of inherent edge contrast, C_{E_o}, as (Duntley, 1964)

$$C_{E_O} = \frac{L_E - L_B}{L_B} \quad , \tag{3.3}$$

where L_E is the luminance of a point on the edge of the target and L_B is the luminance of the background directly behind this point (along the observer's line of sight) both measured at the target. When the target and its background both have uniform luminances, edge contrast is identical to the contrast of an internal point with the background. Thus, the distinction between edge contrast and internal contrast is usually not made for such situations.

The apparent contrast, C, of an object is related to its inherent contrast, C_o, by (Middleton, 1968),

$$C = C_o e^{-\sigma R} \quad , \tag{3.4}$$

where R is the target-to-observer range in meters, $\sigma = \frac{3.912}{R^*}$ is the attenuation coefficient of the intervening media, and R^* is the meteorological range in meters. Meteorological Range (Also called the standard visibility or standard visual range) is defined by Dudel (1967) as

> "...an empirically consistant measure of the visual range of a target; a concept developed to eliminate from consideration the threshold contrast and adaption luminance, both of which vary from observer to observer. The meteorological range is the distance V in the block target form of the visual range formula,
>
> $$V = \frac{1}{\sigma} \ln \frac{1}{\epsilon} \quad .$$

> Since the threshold contrast, ϵ, is set equal to 0.02, V is only a function of σ, the extinction coefficient of the atmosphere at the time and place in question."

Records of the variation in meteorological range, R^*, by hour of the day and month of the year for a given area can usually be obtained from local weather stations. A sample of such records for a German weather station is given in Appendix A.

Irregularities in the surface of military vehicles cause the target to have a multitude of inherent contrasts for any particular level of illumination. In the following section, the target is represented as a simple three dimensional form so that variations in inherent contrast across its surface can be predicted.

Simplified Vehicle Representation

Both combat vehicles and their backgrounds are far from being of uniform luminance. The pattern of luminances presented to an observer is complex and, for practical purposes, unpredictable. Duntley, (1964), states that:

> "The shape of an object is ordinarily of minor consequence composed with the effect of its angular size."

Based on this fact, in this section the shape of the target is simplified by reducing the target area to a sphere so that the analytic geometry involved in calculating highlighted and shaded areas is uncomplicated. If this approximation to the target shape were not made, the analysis necessary to calculate apparent sizes of the target areas would be extremely difficult. Precedent for this simplification is discussed by Ryll (1962). In addition to the geometry problem, as is discussed in Chapter 2, the majority of detection data available is for circular targets.

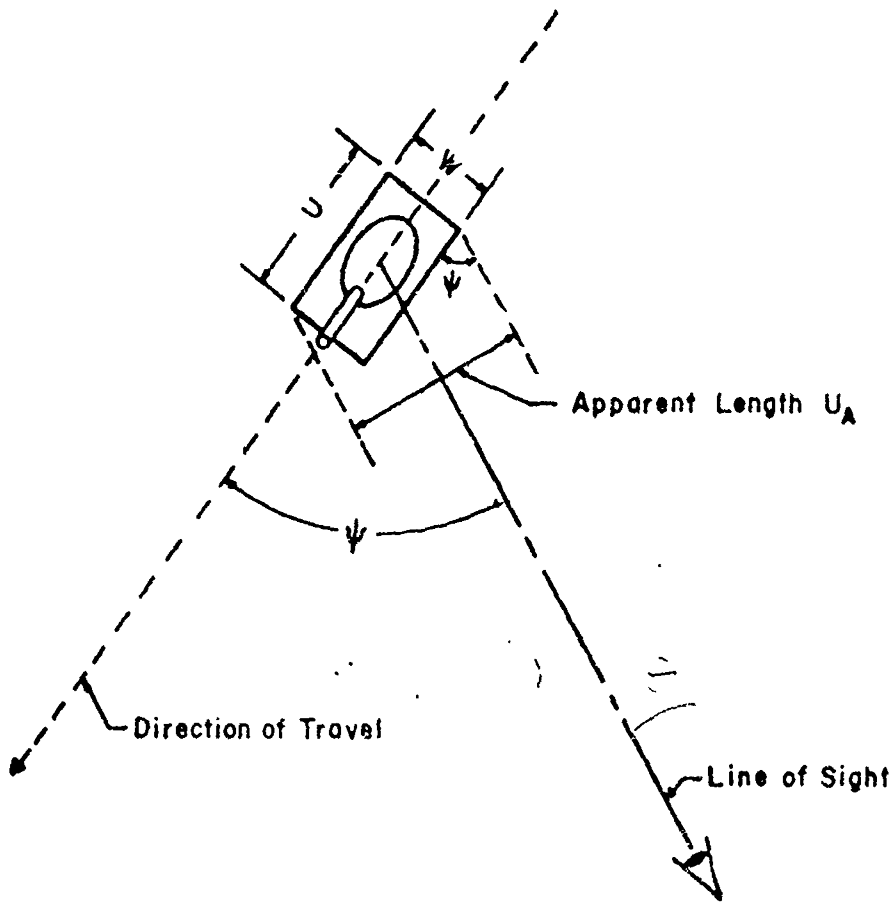

Fig. 14.--Apparent Size of a Tank-Type Target

The variations in contrast across this sphere's surface can readily be described in terms of its orientation with respect to the observer, the illuminating source, and features of the background; and the reflectance properties of the target's s surface and of the background. The characteristics of the sphere most closely approximating the observer's image of a tank in the field are developed below.

The top view of a rectangular tank-type target of length U height V, and width W, is shown in Figure 14 moving at an angle Υ with the observer's line of sight. Such a target, when on level ground, will appear as a rectangle having a height V and length U_a given by

$$U_a = U \sin \Upsilon + W \cos \Upsilon \qquad (3.5)$$

when viewed from ground level. The sphere approximating the rectangular target will appear as a circle to the observer.

The angular size, Ω in minutes of arc, subtended by the diameter of a circle having an area A equivalent to the area of this rectangle is

$$\Omega = \frac{6875.6}{R} \left(\frac{A}{\pi}\right)^{\frac{1}{2}} , \qquad (3.6)$$

where R is the distance to the target, $A = VU_a$ and U_a is given by equation 3.5 Since the probability of detecting a rectangular target of area A is essentially equal to the probability of detecting a circular target of the same area. (See

Chapter 2), the visual angle Ω, given by equation 3.6 can be used[7] in Figure 12 of Chapter 2 to determine the threshold contrast of the rectangular target. Thus, the rectangular tank-type target is conceptualized as a circle whose diameter subtends an angle Ω at the observer's eye when viewed from a distance R as given by equation 36. The predominant contrasts of this spherical target representation with its background and foreground are discussed below.

Under natural lighting the lower surface of a tank-type target and also the spherical target would almost always be shaded and some part of the top surface would be highlighted. Let these surface areas be referred to as:

A_H = the highlighted part of the sphere's surface exposed to the observer, and

A_S = the shaded part of the sphere's surface exposed to the observer.

Five distinct contrast values can be obtained: the contrast of each area with the target's background and foreground and the internal contrast existing between the areas. According to arguments presented below, only three of these contrasts:

---

[7]As was mentioned earlier, detection data is best tabulated for circular targets of uniform luminance silhouetted against a uniform luminance background.

C_{HB} = the apparent contrast of the highlighted part of the object with the background,

C_{SF} = the apparent contrast of the shadowed part of the object with the foreground, and

C_I = the apparent internal contrast,

are considered as being important to the detectability of the target.

There are two reasons for not considering either the contrast of the highlighted area, A_H, with the foreground or the contrast of the shaded area, A_S, with the background. First, the foreground will not appear adjacent to A_H unless the target is completely backlighted or in the shadows cast by terrain features[8] which block the sun's rays. Similarly, background features will rarely appear adjacent to A_S unless the target is completely frontlighted. Second, when an area is silhouetted against a background of nonuniform luminance, that part of its area which has the highest contrast would be most important in determining its detectability. The question considered next is how these three contrasts can be combined to give one value of contrast which can be used to obtain a single glimpse detection probability for the target.

---

[8]A procedure to determine whether or not the target is in the shadows cast by features in the background is presented later in this chapter.

According to our assumptions, the spherical target will appear similar to the circular targets shown in Figure 15. From inspection of Figure 15, it can be seen that as the relative size of a high-contrast area decreases its

Fig. 15.--Example Illustrating the Importance of High Contrasts

significance to the observer decreases and the significance of the edge contrast increases. This effect would probably be even more pronounced with more complex shapes and nonuniform backgrounds where there may be many such small high-contrasted areas across the face of the target and within the back-ground itself. Thus, to obtain a single contrast measure representative of the target, it would seem logical to combine values of the edge and internal con-trasts, redundant and the relative sizes of its contrasted area. However, it is not clear how these different weights should be determined. For example, for targets shown in Figure 15, values of the two edge contrasts are much lower than the internal contrast measrued at any point along the intersection of the black and white areas of the target. If each of these values were weighted evenly,

one would obtain a contrast somewhere between the high internal contrast and the lower of the two edge contrasts. Although it is clear that the internal contrast is most important in this case and should receive a greater weight, there is no known methodology for determining this relative weight. In the following section, the contrasts C_{HB}, S_{SF}, and C_I, between the different pairs of contrasted areas of the target and surroundings are treated as independent stimuli and the theoretical glimpse probability for the whole target.

Estimation of Glimpse Probability for Simplified Target

In the previous section the target was conceptualized as a spherical solid presenting three contrasted areas, C_{HB}, C_{SF}, and C_I, to the observer. Little is known about how patterns consisting of different contrasted areas stimulate the visual system. About all that can be said is that each contrasted area should contribute to the overall detection stimulus in proportion to the intensity of its contrast and the size of the contrasted area relative to the size of the whole pattern. The relative importance of size (angular subtense) and intensity of contrast in determining detection probabilities for a single homogeneous target is reflected in the formula for glimpse probability, g, given in Chapter 2, equation 2.14.Thus, instead of using the magnitude of each contrast, C_{HB}, C_{SF}, and C_I, and the respective sizes of these contrasted areas to determine some average (effective)contrast to be used, it is more reasonable to treat these areas as three distinct targets with glimpse probabilities, g_{HB},

g_{SF}, and g_I. Treating these targets as if they were independent, i.e., assuming that the probability of detecting any one of them in a single glimpse is independent of the probability of detecting any of the remaining two, then

$$g = 1 - (1 - g_{HB})\,(1 - g_{SF})\,(1 - g_I), \tag{3.7}$$

where g is the probability of detecting at least one of the objects in a single glimpse.

to support this contention, Morris (1959), states:

> "the discernible elements of the patterned target may be considered as several independent targets simultaneously viewed, each with its own detection range"

From equation 2.14, in Chapter 2, the probabilities g_{HB}, g_{SF}, and g_I, are given by:

$$g_{HB} = \Phi\left[\frac{\left\{C_{HB}/KC_t(\Omega_H)\right\} - 1}{.434}\right], \tag{3.8}$$

$$g_{SF} = \Phi\left[\frac{\left\{C_{SF}/KC_t(\Omega_S)\right\} - 1}{.434}\right], \text{ and} \tag{3.9}$$

$$g_I = \Phi\left[\frac{\left\{C_I/KC_t(\Omega_I)\right\} - 1}{.434}\right], \tag{3.10}$$

where it is understood that C_{HB}, C_{SF}, and C_I, are apparent contrasts.[9] The threshold contrast, $C_t(\Omega)$, of a circular target whose diameter subtends an angle, Ω, at the observer's eye is shown sketched in Figure 11 of Chapter 2 for different values of adaption brightness (luminance of the surrounding area).[10] These data are not directly usable in equations 3.8, 3.9 and 3.10 since the pairs of areas corresponding to the contrasts, C_{HB}, C_{SF}, and C_I, will rarely be circular even for a smooth-surface spherical target. Thus, Ω_H, Ω_S, and Ω_I, must be interpreted as equivalent angles. Means of approximating these equivalent angles are given in the ensuing discussion.

A spherical target will appear circular to an observer with shadowed and highlighted areas as shown in Figure 16, depending on the angle which the light rays strike the target. Consider the diameter, d_{sun} of this circular area drawn parallel to the sun's rays. This diameter will be partially highlighted and partially shaded as illustrated in Figure 17. The fraction P_H of the diameter d_{sun} highlighted is given by:

$$P_H = \frac{(1 + \cos(90 - \alpha)\cos\delta)}{2}, \qquad (3.11)$$

---

[9] A field factor K=6.5 is used as recommended in Chapter 2 since all factors used to calculate the field factor are present.

[10] An accurate tabulation of these data is given in Bush (1946).

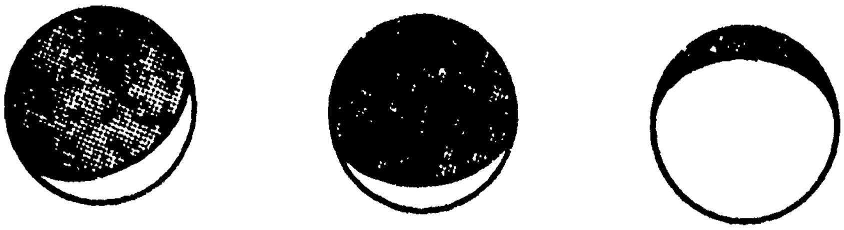

Fig. 16.--Examples of Shading on Simplified Representation of Target

where α is the sun zenith angle and δ is the azimuth angle of the observer's path of sight relative to the sun.[11] Methods for computing the highlighted surface area of spherical targets, such as shown in Figure 16, are very complex. It is assumed that the highlighted area can be useful approximated by the area of the highlighted segment shown cross-hatched in Figure 17; an expression for this area is given below:

$$A_H = \begin{cases} \dfrac{\pi d^2}{1440} - \dfrac{d^2 \sin\{180^\circ + 2\sin^{-1}(\cos\delta\cos(90-\alpha))\}}{8}, & (0 \le P_H \le 0.5) \\[2ex] \dfrac{\pi d^2}{4} - \dfrac{\pi d^2}{1440} + \dfrac{d^2 \sin\{180^\circ - 2\sin^{-1}(\cos(90-\alpha)\cos\delta)\}}{8}, & (0.5 \le P_H \le 1.0) \end{cases} \quad (3.12)$$

[11] The angles, α and δ, are discussed later in this chapter.

and,

$$A_{SF} = \begin{cases} \dfrac{\pi d^2}{4} - \dfrac{\pi d^2}{1440} + \dfrac{d^2 \sin\{180^\circ + 2\sin^{-1}(\cos\delta \cos(90-\alpha))\}}{8}, & (0 \le P_H \le 0.5) \\ \\ \dfrac{\pi d^2}{1440} - \dfrac{d^2 \sin\{180^\circ - 2\sin^{-1}(\cos(90-\alpha)\cos\delta)\}}{8}, & (0.5 \le P_H \le 1.0) \end{cases} \tag{3.13}$$

where $d = d_{sun}$ is given by,

$$d = \sqrt{\frac{2\,VU_a}{\pi}} \quad .$$

The angles, Ω_H and Ω_S, subtended by the diameters of circular objects having areas A_H and A_S, respectively, can be calculated using equation 3.6.

In the case of the internal contrast, C_I, it is assumed that the larger of the two areas, A_H and A_S, is the background against which the other area is silhouetted. Thus, the angular subtense Ω_I of the "object" having a contrast C_I is

$$\Omega_I = \min(\Omega_H, \Omega_S) \quad .$$

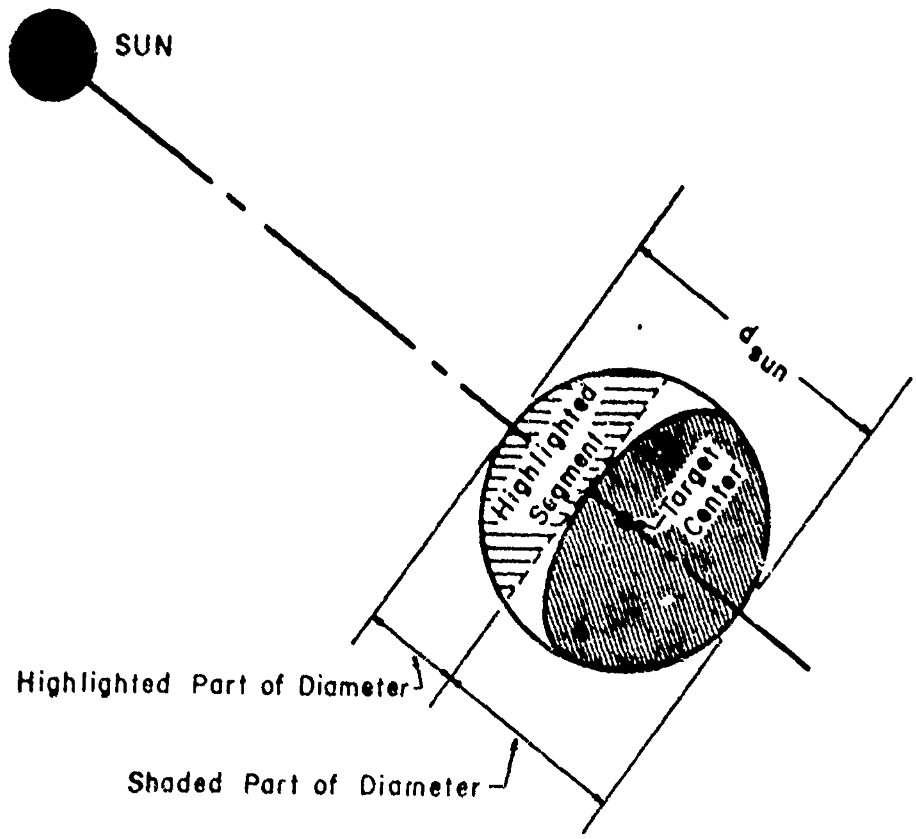

Fig. 17.--Highlighted and Shaded Parts of the Diameter in the Plane Normal to the Observer's Line of Sight Formed by the Intersection of the Sun's Rays with the Target's Center

The angular subtenses Ω_H, Ω_S, and Ω_I, then, are used to determine the single glimpse probabilities given in equations 3.9, 3.10, and 3.11.

The apparent contrasts C_H, C_S, and C_I, are dependent on the inherent luminances of the foreground and background features, and of the shaded and highlighted parts of the target. A means of predicting the luminances of the target's surfaces and its surroundings is discussed below.

Luminance Prediction

The inherent luminance, L, of a surface depends on its directional reflectance, ρ, and the illumination, I, striking that surface. The directional reflectance, ρ, of a surface is defined by Gordon (1964) as: ". . . the ratio of inherent luminance in the direction of the specified path of sight to the total illuminance on a fully exposed horizontal plane at ground level." That is,

$$L = \rho I \,, \tag{3.14}$$

where ρ is a function of the impinging light's incidence angle for direct illumination and the distribution of incidence angles for indirect illumination.

Brown (1952) has determined the total illumination, in footcandles, for an unobscured sun as a function of the sun zenith angle α. These data are reproduced in Figure 18. As shown in this figure, the illumination when the sun is at the horizon (sun zenith angle 90°) is approximately 70 footcandles,

while, when the sun is directly overhead (zenith angle 0^o), the illumination is approximately 10,000 footcandles.

The directional reflectance, ρ, of a surface is a function of the azimuth angle, δ, of the path of sight relative to the sun, the zenith angle, ϕ, of the path of sight, the wavelength of the impinging light rays, the surface roughness, the atmospheric conditions, the sun zenith angle, α, and the sun azimuth angle, β (Gordon, 1964).[12] The angles α and β, which describe the position of the sun in the sky are illustrated in Figure 19. The angles δ and ϕ which describe the position of the observer relative to the sun and target, respectively, are illustrated in Figure 19. In Figure 19 the target is assumed to be at ground level, while the observer can be considered either elevated ($\phi > 0$) or at ground level ($\phi = 0$).

Scripps Institute of Oceanography (Gordon, 1964; Boileau and Gordon, 1965; Gordon and Church, 1966) has measured the directional reflectance of several common background surfaces for various values of the angles α, ϕ, and δ. These measurements are in Tables B.1, B.2, and B.3 of Appendix B. The greatest amount of data are for an unobscured sun at a zenith angle of 40 to 45 degrees. The sources of these data were contacted and data for other sun angles and weather conditions other than a clear sky were found to be unavailable.

---

[12] This functional form is not known, so empirical measurements of these conditions had to be used.

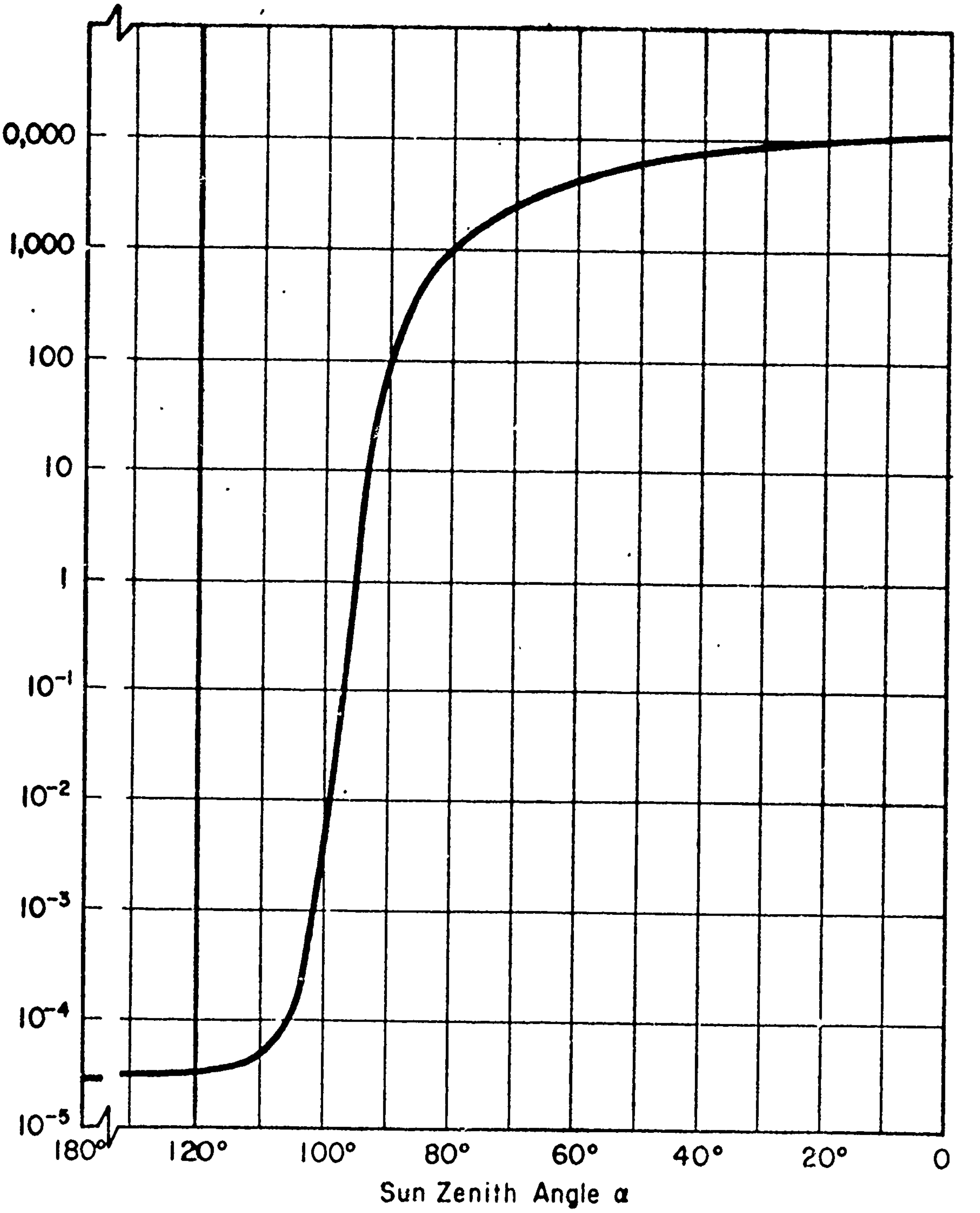

Fig. 18.--Natural Illumination Levels (Adapted from Brown, 1952)

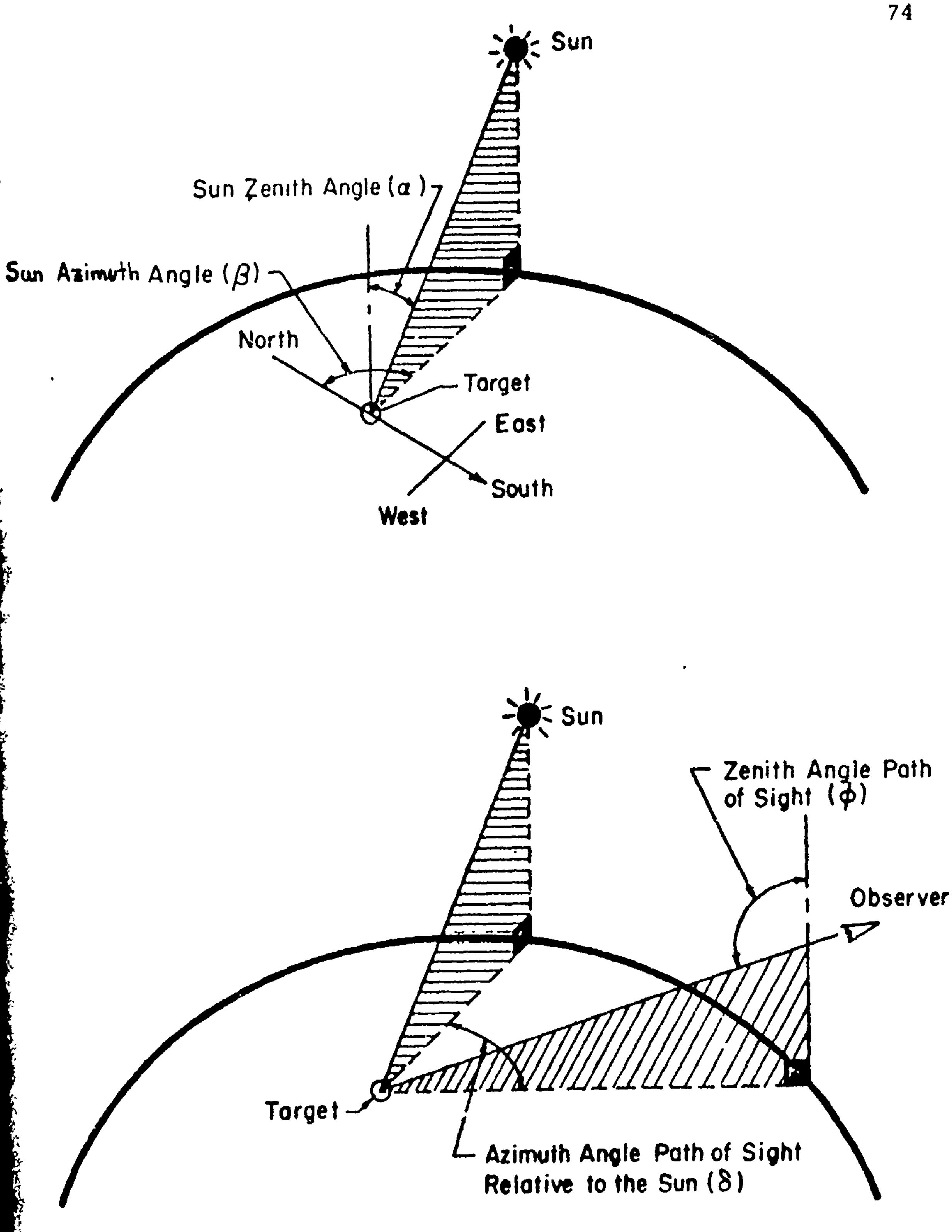

Fig. 19.--Sun and Observer Path of Sight Angles

The effect of the sun position and meteorological conditions on surface reflectance is discussed in Appendix B. The use of the data of Table B.3 of Appendix B for predicting the luminance of terrain features is discussed in the next section.

Luminance of Terrain Features

The luminances of terrain features directly behind and in front of the target, i.e., in its background and foreground, are required to determine the contrast of different areas on the target. First, the location of the target relative to the sun and the observer, and the directional reflectances of the background and foreground features along the observer's line of sight to the target must be determined. The steps necessary to determine the luminances of terrain features in the target's foreground and background, are outlined in the flow chart shown in Figure 20. The data required as input to the calculations appearing in this flow chart are:

1. the target's coordinates, (X_t, Y_t, Z_t),
2. the observer's coordinates, (X_o, Y_o, Z_o),
3. the sun azimuth angle, β,
4. the location of the different terrain features on the battlefield, such as meadows, grass, trees, and roads, and
5. typical horizon sky luminances, such as those given in Table 7, taken from Duntley (1946; 1948). A value for sky luminance would be determined before each DYNTACS run and used throughout the battle.

As indicated in Figure 20, the directional reflectance, ρ, of the background feature whose luminance is to be calculated from equation 3.14 can be

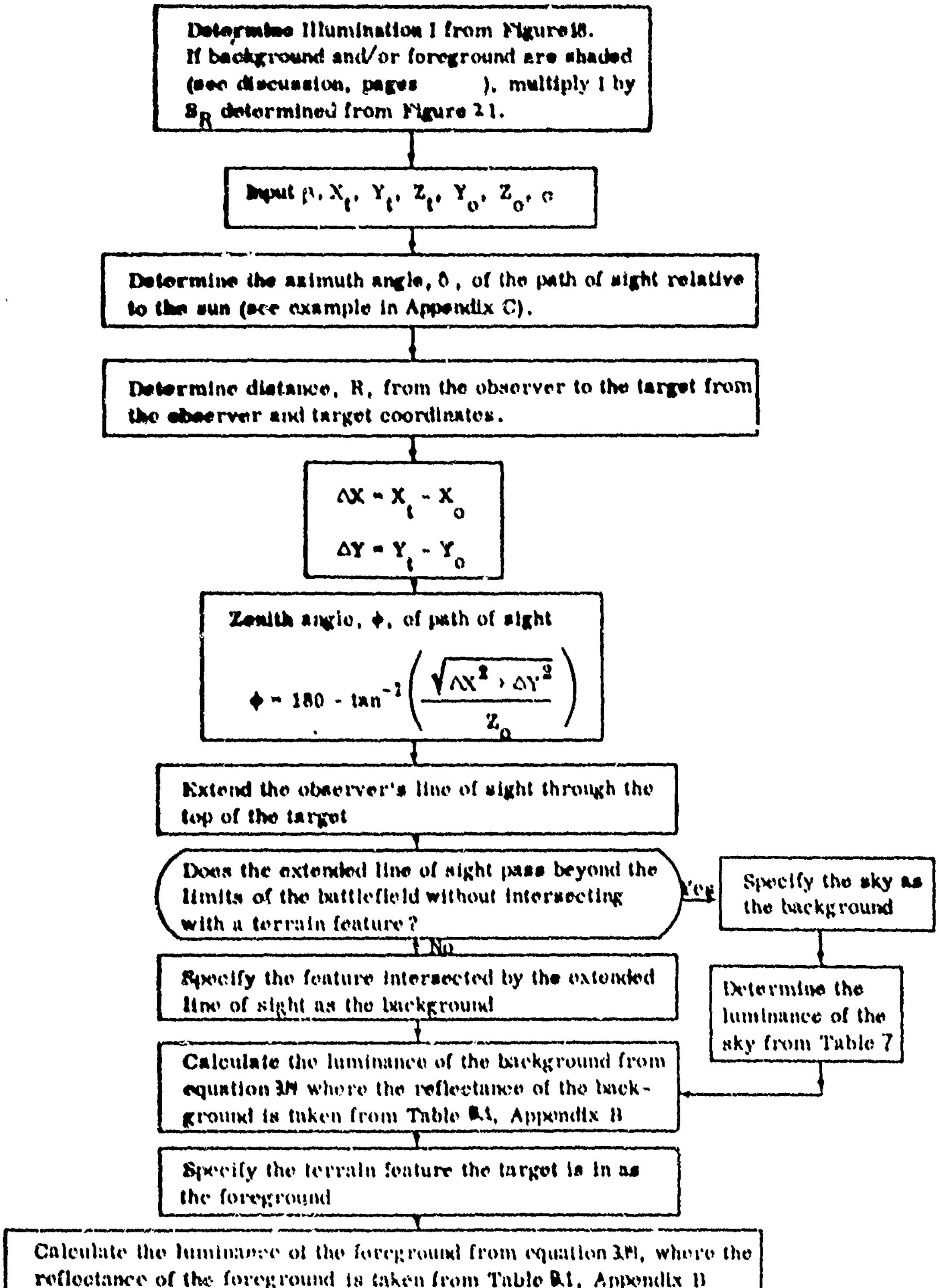

Fig. 20.--Flow Chart for Determination of Background and Foreground Luminance

TABLE 7

HORIZON SKY LUMINANCES
(not a function of location of the illuminating source)

Description	Luminance (ft-L)
Full daylight	1000
Overcast sky	100
Very dark day	10
Twilight	1
Deep twilight	10^{-1}
Full moon	10^{-2}
Quarter moon	10^{-3}
Starlight	10^{-4}
Overcast starlight	10^{-5}

determined from Table B.3of Appendix B given the azimuth angle, δ, of the path of sight relative to the sun and the zenith angle, ϕ, of the path of sight. Thus, the luminance, L, at a point on the surface of a terrain feature exposed to direct sunlight is determined from the sun's direct illumination level, I_D, by

$$L = \rho I_D \quad , \tag{3.15}$$

where I_D is given as a function of the sun zenith angle in Figure 18, and the reflectance, ρ, of the terrain feature can be determined from Table B.3of Appendix B. Since the data on the directional reflectance of terrain features

exposed to indirect illumination (in shadows) are not available, it must be assumed that the data of Appendix B apply to both directly and indirectly illuminated surfaces.[13]

Thus, the inherent luminance, L, at a point on a surface of a terrain feature exposed to indirect illumination is calculated from

$$L = \rho I_S \tag{3.16}$$

where ρ is read from Table B1 of Appendix B, and I_S is the indirect illumination from the sun. Equation 3.16 can be written as

$$L = S_R I_D \rho \tag{3.17}$$

where S_R is the ratio of indirect to direct illumination[14] from the sun. A graph, prepared from data given by Brown (1952), of the ratio S_R versus the sun zenith angle α is given in Figure 21.

Methodology for determining whether a target or its background (or both) are in shadows and the effect of such shadows on the single glimpse detection probability are discussed later in this chapter. The following section describes how target-to-background contrasts are determined given the illuminances of background and foreground features.

---

[13]This assumption was discussed with Miss J. Gordon of the Scripps Institute of Oceanography. She agreed with the authors suppositions.

[14]Direct Illumination includes both illumination from the illuminating source directly and the indirect(prevailing) illumination. Indirect Illumination is only the prevailing part of the illumination from the source.

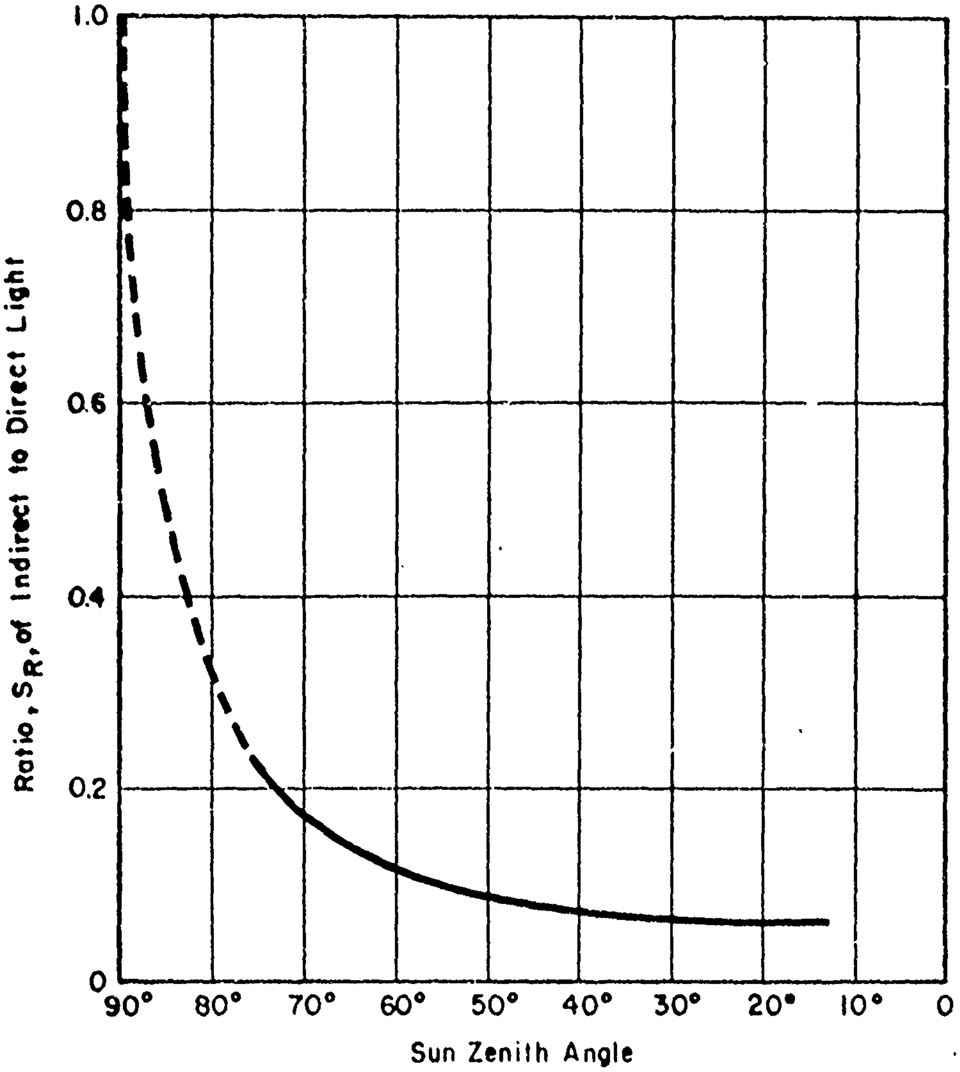

Fig. 21.--Ratio of Indirect to Direct Illumination Due to the Sun as a Function of the Sun Zenith Angle

Target-to-Background Contrast

Once the luminance of background and foreground terrain features are calculated, the inhe nt contrasts, C_{HB_0}, C_{SF_0}, and C_{I_0} can be determined from equation 3.3 providing the luminances L_H and L_S of the highlighted and shaded parts of the target, respectively, can be specified. Then the apparent contrasts, C_{HB}, C_{SF}, and C_I, can be determined from C_{HB_0}, C_{SF_0}, and C_{I_0} using equation

The inherent luminance, L_H, of a point on the highlighted part of the target is given by

$$L_H = I_D \rho_H , \tag{3.18}$$

where I_D is the illumination from the sun on the highlighted surface and ρ_H is the reflectance of the surface at that point. Similarly, the inherent luminance, L_S, at any point on the shaded part of the target is

$$L_S = S_R I_D \rho_S , \tag{3.19}$$

where ρ_S is the directional reflectance of the target when indirectly illuminated and S_R is given in Figure

The surfaces of combat vehicles are quite different than those of components of the terrain. Because of the special nature of the finish, highlights and shadows are created when illuminated by a source such as the sun. Duntley (1964) explains that:

> "Man-made surfaces invariably exhibit pronounced gloss characteristics, particularly when the solar zenith angle exceeds 60°."

Because of the complex nature of the targets surface this is certainly not an uncommon event. For this reason, unlike the surface of terrain features, the reflectance of surfaces highlighted and shaded are considered to have different reflectances.

Gordon (1964) measured the directional reflectance of variously oriented surfaces of an olive drab painted object for a sun zenith angle of approximately 40°. Most values ranged from 0.10 to 0.26 but readings as low as 0.01 and as high as 0.490 were recorded. Values of 0.10 and 0.26 were chosen to be representative of the reflectance of shaded and highlighted surfaces, respectively; that is, it is assumed that $\rho_S = 0.10$ and $\rho_H = 0.26$. For these values of reflectance, the luminances of the highlighted and shaded parts of the target are

$$L_H = .26\, L_D \tag{3.20}$$

and

$$L_S = .10\, L_D S_R \quad , \tag{3.21}$$

respectively. The luminances of the highlighted and shaded parts of the target's surface, as calculated above, are used to determine the inherent contrasts,

C_{HB_o}, C_{SF_o}, and C_{I_o}, of the target's surface with its surroundings, as outlined below.

According to equations 3.20 and 3.21, the inherent internal contrast, C_{I_o}, is given by

$$C_{I_o} = \frac{.26\, I_D - I_D S_R (.10)}{I_D S_R (.10)} \quad , \tag{3.22}$$

which reduces to

$$C_{I_o} = \left(\frac{2.6}{S_R}\right) - 1 \quad . \tag{3.23}$$

The inherent edge contrasts, C_{HB_o} and C_{SF_o}, are given by

$$C_{HB_o} = \frac{L_H - L_B}{L_B} \quad , \tag{3.24}$$

and

$$C_{SF_o} = \frac{L_S - L_F}{L_F} \quad , \tag{3.25}$$

where L_H and L_S, the luminances of the highlighted and shaded parts of the target, are given by equations 3.20 and 3.21, respectively, and means for determining the luminance's L_B and L_F of the background and foreground for

both direct and indirect illumination were discussed earlier in this chapter (see equations 3.15 and 3.17). It should be noted that when the target and its background (or foreground) are subject to the same illumination, i.e., either direct or indirect, the edge contrasts C_{HB_0} and C_{SF_0} reduce to the ratio of the difference in the reflectances of the target and the terrain feature to the reflectance of the terrain feature. That is, if ρ_B is the reflectance of the background and ρ_F is the reflectance of the foreground, we have

$$C_{HB_0} = \frac{\rho_H - \rho_B}{\rho_B}$$

and

$$C_{SF_0} = \frac{\rho_S - \rho_F}{\rho_F} ,$$

where ρ_H and ρ_S are the directional reflectances of the highlighted and shaded parts of the target, respectively. Thus, as a result of our assumption that the data of Table B.3 of Appendix B can be used for either directly or indirectly illuminated features, the reflectances ρ_B and ρ_F of these features as well as the contrasts C_{HB_0} and C_{SF_0} will be the same for direct and indirect illumination. However, shadows, which cause the target to be indirectly illuminated, still affect the single glimpse detection probabilities, g_{HB} and g_{SF}, as pointed out in the following section.

Effect of Shadows

As the sun zenith angle changes, shadows are created on the surfaces of the terrain features facing away from the sun as shown in Figure 22. These shadows may cover the target if it is close to the feature, or serve as the background for the target if it is not close to the feature.

To determine whether a target is within a shadow created by a terrain feature, such as a forest, a line is extended from the target to the sun. If this line intersects some part of a terrain feature, it is assumed that the target is in the shadow of that feature. In such cases, neither the target nor its background and foreground are directly illuminated by the sun. As pointed out in the previous section, the assumption that the reflectance values given in Table of Appendix B hold under indirect as well as direct illumination implies that a target in the shadow of a feature will have the same contrast as a target in the same location when it and its background are both illuminated directly by the sun (see equation 3.3). However, this assumption does not imply that the single-glimpse detection probability for a target located in a shaded area is the same as that for a target exposed to full sunlight. As can be seen from equations 3.8, 3.9 and 3.10 the single-glimpse detection probability for two targets of equal contrast will vary with the relative magnitudes of their threshold contrasts $C_t(\Omega)$. The threshold contrast, in turn, depends on the luminance of the background (see

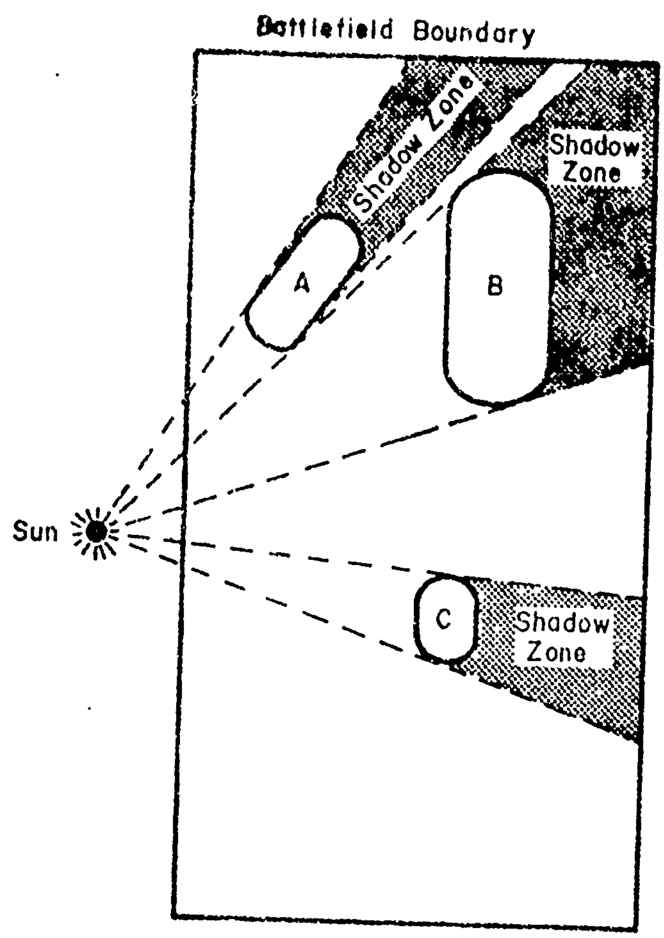

Fig. 22.--Location of Shadow Zones

Figure 12 of Chapter 3). For backgrounds exposed to direct illumination, this luminance is determined from equation 3.15 whereas for indirect illumination this luminance is given by equation 3.17.

Shadows also can affect the glimpse probability g_{HB} without actually covering the target by changing the luminance of the background against which the target is silhouetted. To determine if the target's background is shaded (in a computer simulation), a line of sight through the target is extended until it intersects some point on the terrain, and, then, a line is extended from that point to the sun. If this latter line intersects some point of a terrain feature within the bounds of the combat area, the target's background is considered to be shaded. Then, the luminance L_B used in equation 3.24 to calculate the contrast of a target silhouetted against a shaded surface of a terrain feature is calculated using equation 3.17.

Discussion

More realistic predictions of glimpse probabilities could be made by improving the description of the luminance properties of background and foreground features. For example, substantial improvements could be made if directional reflectance data could be obtained for:

1. a wider variety of environmental factors such as meteorological visibility and cloud cover,

2. sun zenith angles other than 45°,

3. a wider range of the angles θ and ϕ ,

4. various degrees of shading, and

5. ambient light levels associated with twilight or nighttime.

In addition, descriptions of target luminance patterns could be improved by the collection of reflectance data for various orientated surfaces of the different materials commonly used to make tank armor.

Luminance measurements at various points on tank vehicles were taken by Ballistic Research Laboratories (Downs, et al., 1965) under a variety of meteorological conditions. These raw data are in the form of continuous graphs of surface luminance at constant distance positions along the tank as shown in Figure 23. In this figure, luminance is measured at each trace along the x-axis. However, reduction of these data into a usable form could not be accomplished within the scope of this effort. Further study and analysis of the BRL data would result in more realistic estimates of the following quantities used in this chapter:

1. the luminance of variously highlighted and shaded surfaces under different meteorological conditions including different sun positions, and various levels of meteorological visibility, and

2. the fraction of a tank highlighted and shaded for various sun positions.

In addition, analysis of the BRL data could provide the information required to develop methods for estimating the effect of cloud cover on target contrast and detection.

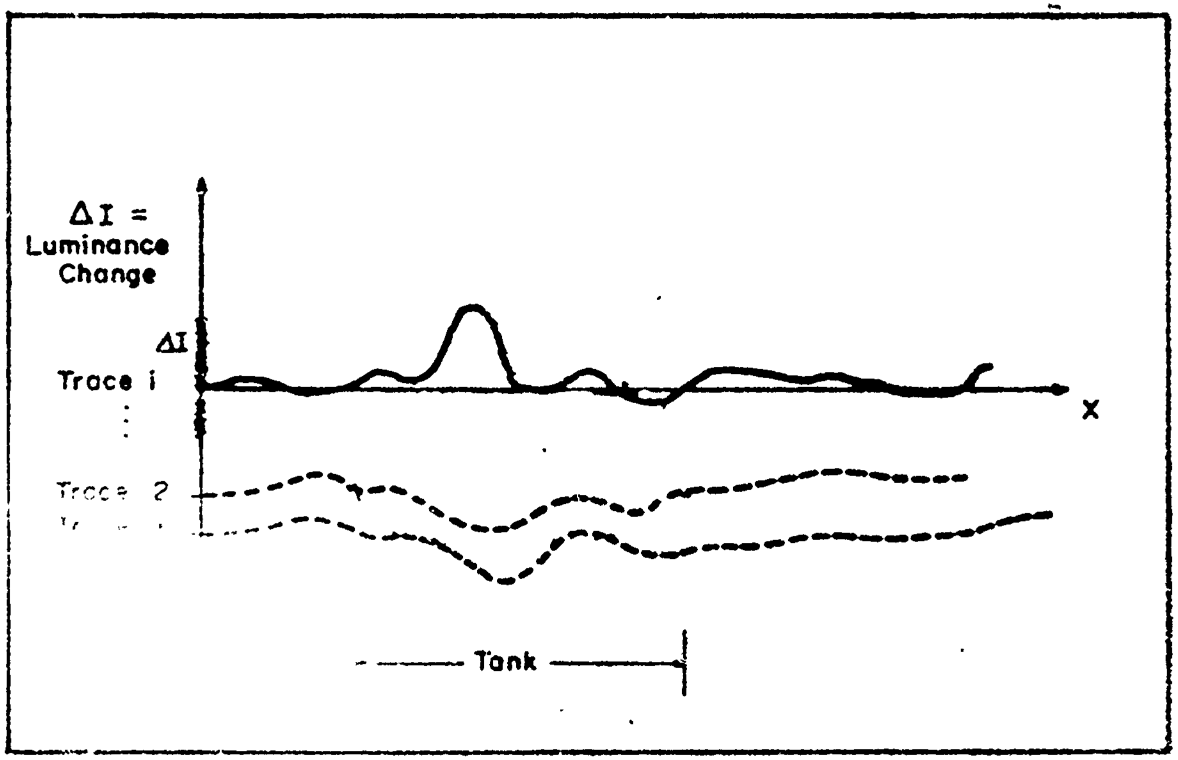

Fig. 23.--Example Showing the Form of the BRL Tank Luminance Data
(Downs, *et al.*, 1965)

Additional realism could be gained by introducing the probability and effect of cloud cover into the detection model. When clouds pass between the sun and the target, as in the case of a target located in the shadow of a terrain feature, the single glimpse detection probability is reduced because of a general reduction in the overall luminance of the scene. The luminance, L_B, of the background can be calculated, as indicated by equation 3.12 from

$$L_B = \rho_B I$$

where ρ_B would be taken from Table B.3 of Appendix B and the illumination, I, striking the ground when the sun is obscured by a cloud is given in Figure 24.

The probability P_S that a cloud-free line of sight exists between a target and the sun has been estimated by the Air Weather Service (1965), as a function of the sun zenith angle α, for different values of the mean total percent cloud cover. This probability is given in Figure 25. The probability, $1-P_S$, that the target and its immediate surroundings are shaded by a cloud, could, with some further study, be used to determine whether or not an object is shaded by a cloud during the simulated battle.

With minor modifications, the results of this chapter could be used to determine the contrast of the target with its surroundings at night. A target illuminated by moonlight has approximately the same contrast as a traget illuminated by direct sunlight since the directional reflectance remains fairly

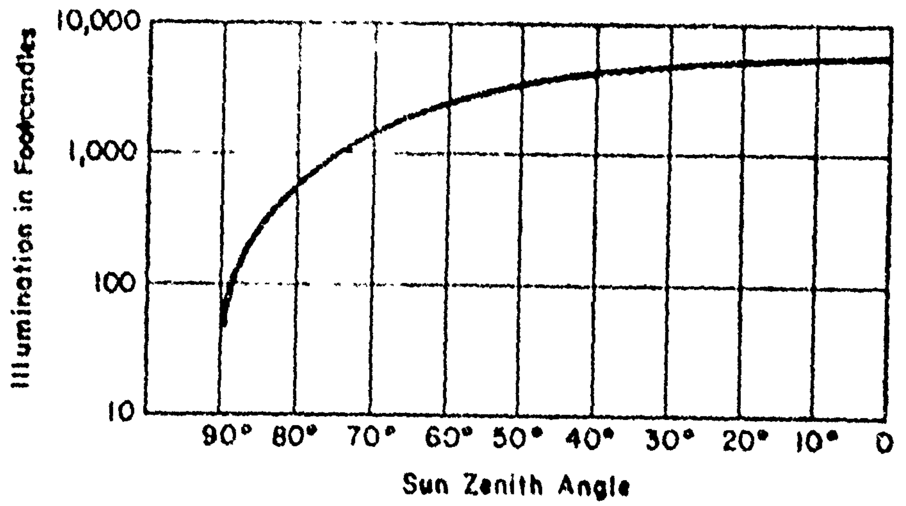

Fig. 24.--Illumination under Average Cloud Conditions(Brown, 1952)

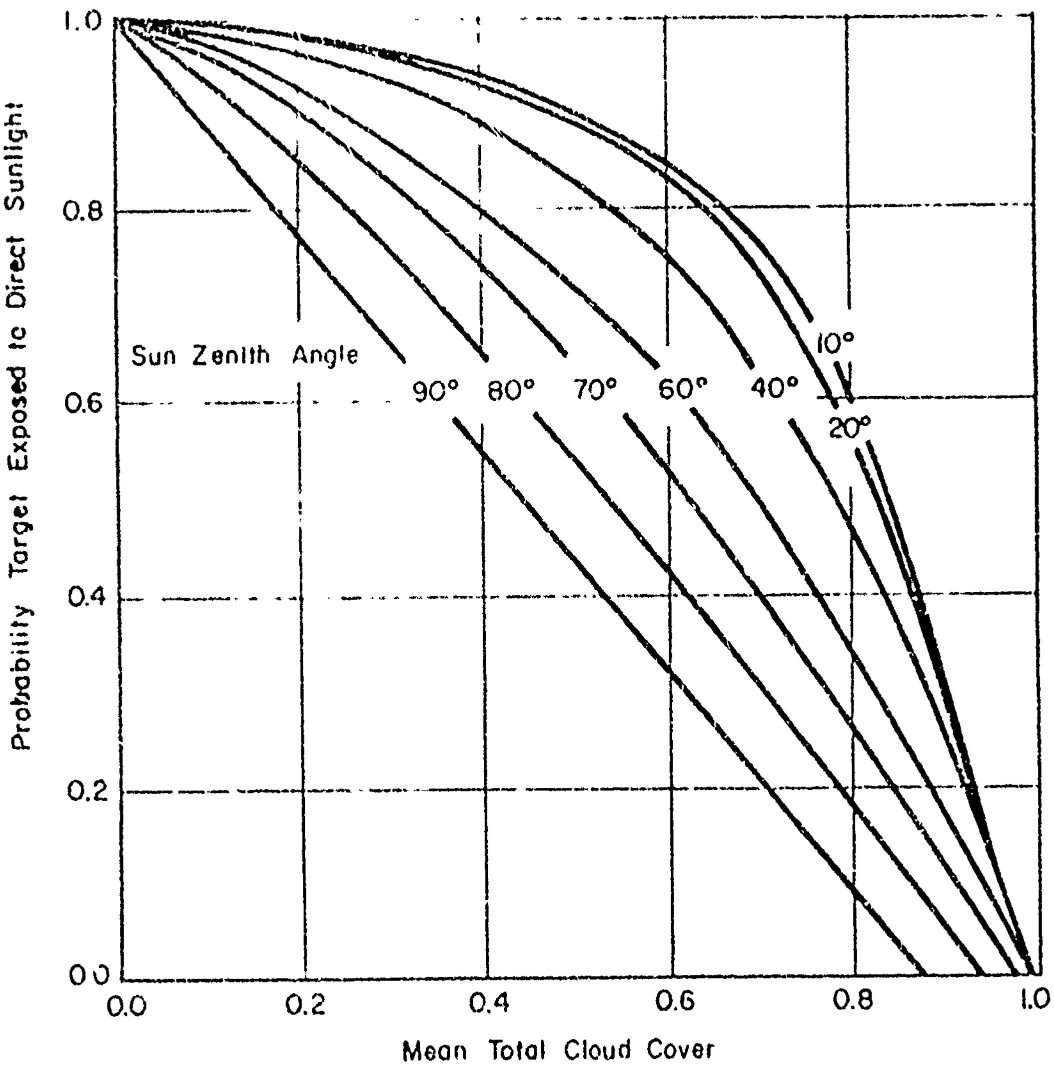

Fig. 25.--Probability of Target Exposure to Direct Sunlight as a Function of the Mean Cloud Cover and Sun Zenith Angle

constant (Gordon, 1964). However the prevailing illumination changes. The direct illumination under moonlight conditions, tabulated by Brown (1952) as a function of the moon zenith angle, is given in Figure 26. However, as in daylight shadows will be present within the object and on the surfaces of terrain features facing away from the moon. As with daytime conditions, the luminance of a shaded area can be expressed in terms of the ratio, S_R, of indirect to direct illumination (see equation 3.17). However, data are not available for this ratio for moonlight conditions. As an interim measure, it could be assumed that values of this ratio given for daylight (see Figure 21) hold for the reduced illumination levels at night.

Summary and Conclusions

In this chapter, the tank-target was represented as a sphere. A method was given for estimating the internal contrasts, C_I, between the highlighted and shaded parts of the spherical target and the two edge contrasts: C_{HB}, the contrast of the highlighted part with the background and C_{SF}, the contrast of the shaded part with the foreground. Relationships discussed between these contrast values and the single-glimpse detection probability for use in equation 2.12 of Chapter 2 are summarized in the flow chart in Figure 27. Although the representation of the target is very simplified, a more detailed representation of the target's shape would be of dubious value until the effect of different contrast patterns on

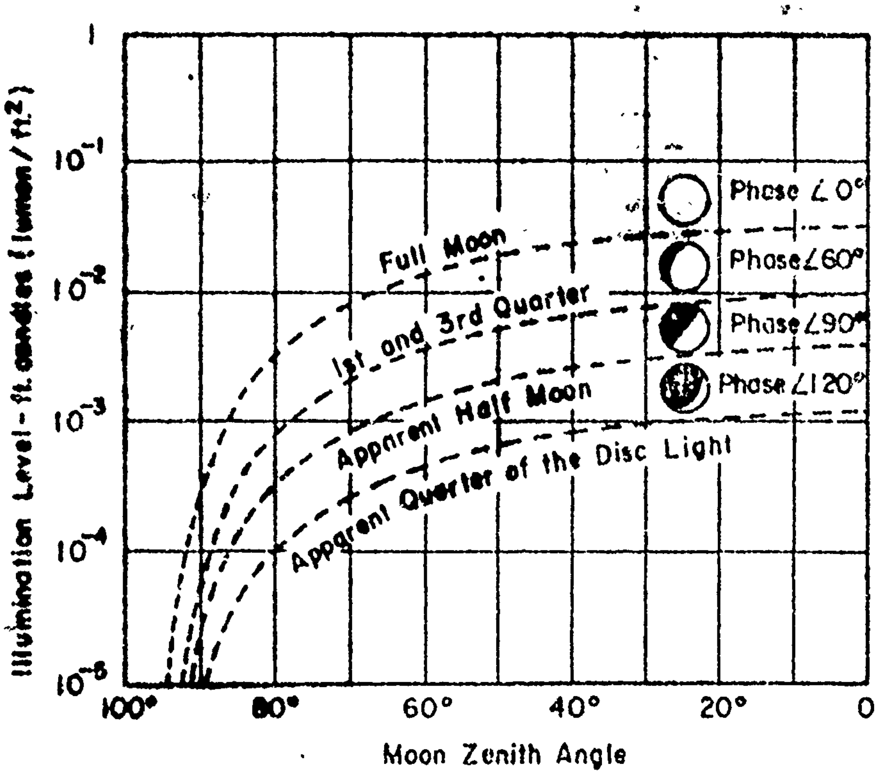

Fig. 26.--Illumination in Foot Candles for Various Phases of the Moon

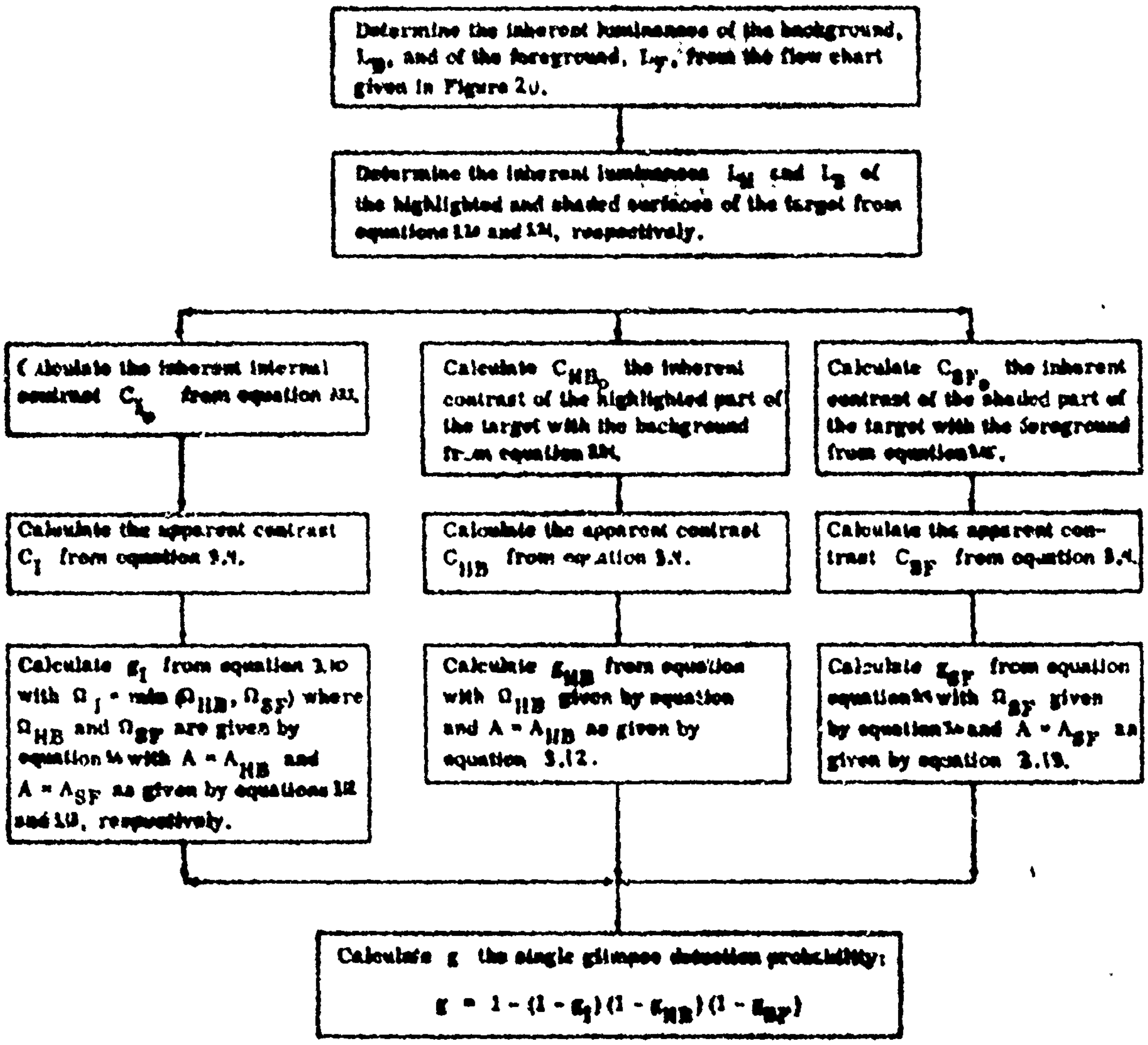

NOTE:

The threshold $C^*(\Omega)$ can be determined from Figure 8 of Chapter 2 or from tabulated data in [illegible] (1946) for the appropriate values of background luminance L_B.

Fig. 27.--Flow Chart for Determination of Target Equivalent Single Glimpse Detection Probability

detection can be accurately described. That is, even if a large number of point measures of contrast could be predicted, it is, at present, difficult to say which are most important to the observer in making a detection.

In the next chapter this model is used in a probability model which predicts observer performance when searching for the target in a complex display. An attempt to validate the model is also discussed at the end of the following chapter.

CHAPTER 4

PROBABILITY MODELS

In the preceding chapter, a model for predicting the probability, g, that a target is detected on a single-glimpse was developed. By dividing the target into two distinct areas, one highlighted and one shaded, three point measures of contrast were calculated:

C_{HB} = the apparent contrast of the highlighted part of the target with the background,

C_{SF} = the apparent contrast of the shaded part of the target with the foreground, and

C_I = the apparent internal contrast

Using equations 3.8, 3.9 and 3.10, the single-glimpse detection probabilities g_{HB}, g_{SF}, and g_I of areas having contrast C_{HB}, C_{SF}, and C_I, respectively were calculated. The single-glimpse detection probability, g, for the entire target was then related to these three measures of glimpse probability by the equation:

$$g = 1 - (1 - g_I)\ (1 - g_{HB})\ (1 - g_{SF}) \qquad (4.1)$$

An analytic procedure for predicting luminances of terrain features and target surfaces was also presented in Chapter 3. The calculations required for these luminance descriptions were geared toward efficient execution on an electronic computer while preserving the resolution requirements of the combat simulation. In this chapter, this predicted value of the single-glimpse detection probability (equation 4.1) is

used in a probability model which accounts for search of the scene by the observer.

As discussed in Chapter 1, Stollmack (1964) suggests that the probability, P (t), that detection occurs in time t or less is given by:

$$P(t) = 1 - e^{-\int_0^t \lambda(\Upsilon)\, d\Upsilon}, \tag{4.2}$$

where $\lambda(\Upsilon)$ is the conditional detection rate. Two forms of this conditional rate were suggested in Chapter 1.

The first, called the "glimpse model" incorporates the model predicting single-glimpse detection probability developed in Chapter 3. This model yields a continuous function for the glimpse probability of a target moving with respect to its surroundings. Since the target is moving, such factors as the relative sizes of the highlighted and shaded areas and the contrasts of these areas with the surroundings change. These changes result in a glimpse probability which is a continuous function of some set of environmental variables and time, $g(S,\Upsilon)$. Given this function $g(S,\Upsilon)$, the conditional detection rate, $\lambda(\Upsilon)$, can be written as,

$$\lambda(\Upsilon) = \mu\, p\, g(S,\Upsilon),$$

where p is a function correcting for forms in the scene which abstract the observer's attention (confusing forms) and μ is the glimpse rate.

The second form of $\lambda(\Upsilon)$ is a simplification of the first. In this model it is assumed that the conditional detection rate is a step function, changing instantaneously at discrete points in time along

the movement path of the target. This simplified model, hereafter called the "step" model assumes that the single-glimpse detection probability remains fairly constant between points in time where major changes occur. The reason for making this simplification is that parameters of this simplified distribution can be estimated by the method of maximum likelihood from detection-time data. (Such efforts for the continuous model would be extremely difficult because of the nature of the distributions involved.) These estimates can then be related to values of the conditional detection rate generated by the glimpse model to test the validity of the glimpse model. However, attempt at validation were not successful because the necessary data could not be obtained. These difficulties are also discussed in this chapter.

In the following section the glimpse model is discussed.

The Glimpse Model

The probability that a target is detected on a single glimpse has been suggested (in Chapter 3) to be a function of its internal contrast its contrast with the elements of the terrain against which it is silhouetted, and the size of the highlighted and shaded areas apparent to the observer. For a moving target, this glimpse probability is continually changing since the environmental variables affecting glimpse probability (discussed in Chapters 2 and 3) change with time. Lawson and Stollmack (1968) have shown that the instantaneous conditonal detection rate, $\lambda(\tau_i)$, at a time τ_i is of the form,

$$\lambda(\tau_i) = \kappa p \varsigma \qquad (4.3)$$

where μ is the glimpse rate, $p = \frac{1}{n}$, where n is the number of confusing forms in the scene (discussed in Chapter 2) and g is the instantaneous single-glimpse detection probability. Changes in the conditional detection rate are most likely explained by changes in the single-glimpse detection probability. Since the fixation rate, μ, remains essentially constant (White and Ford, 1960) and the number of confusing forms, n, is a function of the scene content not time. With this assumption and a single-glimpse detection probability changing with time, equation 4.3 becomes

$$\lambda(\Upsilon) = \mu p\, g(\Upsilon). \tag{4.4}$$

Using the method developed in Chapter 3, the single-glimpse detection probability for moving targets can be calculated everywhere along the targets movement trace. For any one scene, a function similar to that shown in Figure 28 might be expected. As a convention, the continuous model treating the conditional detection rate as a function of the single-glimpse probability model developed in Chapter 3, will be called the "Glimpse Model". Prediction of the glimpse rate, μ, and the equivalent number of confusing forms in the scene is discussed below.

Prediction of the Glimpse Rate and the Equivalent Number of Confusing Forms

As discussed in Chapter 2, considerable work has been devoted to measuring the rate at which fixations are made on a display. This rate is a function of various factors, including the scene content (Townsend, Enoch and Fry; 1958) and the display size (Enoch and Fry, 1958). White (1964) suggests that 3 fixations per second can be expected under most

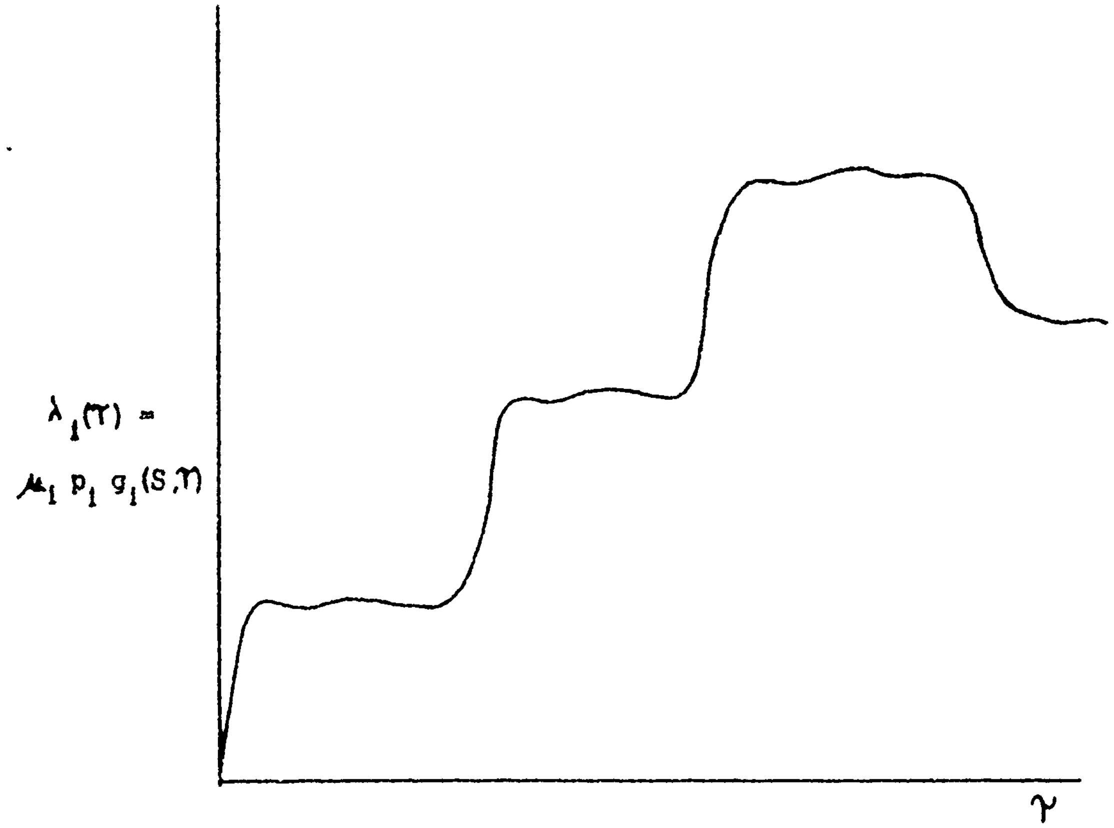

Fig. 28.--Conditional Detection Rate as a Function of Time for the I^{th} Scene

search situations. This value of fixation rate is widely accepted and has been used in numerous models of detection (Ryll, 1962). Boynton, Elsworth and Palmer (1958) investigated the relationship between an observer's detection performance and the number of forms in the scene resembling the target in size, shape, and contrast (see Chapter 2). A relationship between target detection probability, p, the number of confusing forms, n, and the exposure time, T, is indicated by Figure 7 of Chapter 2. The empirical fit given by Ryll (1962) for all target sizes and contrast investigated in the Boynton, __et al.__, study is:

$$p = \frac{1}{1 + \left[\dfrac{n}{29(T)^{.93}}\right]^{1.29}} \qquad (4.5)$$

If T, the exposure time is taken to be 1/3 second, the time for a single glimpse, equation 4.5 becomes

$$p = \frac{1}{\left[1 + \left(\dfrac{n}{10.44}\right)\right]^{1.29}} \qquad (4.6)$$

This expression can be solved explicitly for n in terms of p as follows:

$$n = 10.44 \left[\frac{1 - p}{p}\right]^{.775} \qquad (4.7)$$

Using this equation, the effective number of confusing forms for the terrain scene can be predicted if a value of p is known. A means of estimating $\hat{p}$, the value of p for each scene is discussed below.

If an observer makes fixations at a target scene at a constant rate μ, it has been shown that the probability, P(t), that a stationary target is detected in time t or less is

$$P(t) = 1 - e^{-\mu g p} \qquad (4.8)$$

where g is the single-glimpse detection probability determined from equation 4.1, and p is the detection probability used in equation 4.7 to predict the equivalent number of confusing forms. Given estimates, $\hat{\lambda}$, of the detection rate of a stationary target in a natural environment, $\hat{p}$, an estimate of p, is given by:

$\hat{p} = \hat{\lambda}/3g$, if the fixation rate, μ is assumed to be a constant 3 per second. Substituting this into equation 4.7 yields the expression

$$n = 10.44 \left(\frac{3g - \hat{\lambda}}{\hat{\lambda}} \right)^{(.775)} \qquad (4.9)$$

as an estimate of the number of confusing forms in each scene. Discussed below is a method of determining a statistical distribution of the number of confusing forms contained in a typical terrain scene.

Distribution of the Number of Confusing Forms

In the preceding section, a method of estimating the effective number of confusing forms in a terrain scene was suggested.

To make the glimpse model completely general, it is desirable to have a value of the effective number of confusing forms to enter into equation 4.4 for a specific terrain type. To obtain an estimate of n, it is necessary to measure detection times for several observers viewing a stationary target. From these detection times, an estimate, $\hat{\lambda}$, of the

λ would [illegible] ated. Substituting this value of $\hat{\lambda}$ into equation 4.9, an estim[illegible] would be calculated.

[illegible] experimental effort is impractical for each scene because of the large number of possible scenes a single experiment with several classifications of terrains would permit the determination of a statistical distribution of the number of confusing forms. Typical terrain classifications are:

1. Flat, no trees or schrubs, with tall grass.
2. Flat, small schrubs and grass.
3. Flat, trees and schrubs.
4. Flat, barren with trees in background.
5. Rolling, with schrubs and trees.
6. Rolling, with sparse vegetation.
7. Heavily vegetated (jungle).

Of course, the above list contains only a few of those terrains which might be considered. The choice of these classifications depends on the environment in which detections are to be expected to occur. Once a list of the terrain types in which detection might occur have been compiled, an experiment to determine a statistical distribution of the number of confusing forms is necessary. Suggestions for planning such an experiment are given below. Given several examples of one terrain type a few typical target locations in the scenes would be selected. As seen in equation 4.9 an estimate of the detection rate for scene is needed to calculate [illegible]. Several subjects are asked to find the targets in each scene using the method given by Brown (1956), an estimate, $\hat{\lambda}_{ij}$ of the detection rate for the i^{th} scene in terrain classification j is calculated.

Then g_{ij} is calculated using the method discussed in Chapter 3 for predicting the single-glimpse detection probability. Given $\hat{\lambda}_{ij}$ the effective number of confusing forms, $\hat{n}_{ij}$ for scene i in the j^{th} terrain type is calculated from:

$$\hat{n}_{ij} = 10.44 \left(\frac{3g_{ij} - \hat{\lambda}_{ij}}{\hat{\lambda}_{ij}} \right)^{(.775)} \tag{4.10}$$

Given N_j values of the effective number of confusing forms for terrain type j, the statistical distribution of n_{ij} could be estimated from a histogram of the data. Stollmack and Lawson (1968) have shown that for 9 scenes from the tank ranges at Fort Knox, the effective number of confusing forms is approximately distributed according to a Poisson distribution with a mean of 9.83. The scenes in this group come from several different terrain classifications but contain a good sample of what might be classified as a "Fort Knox" terrain. Since there were only 9 scenes it was not feasible to classify their content and divide them into categories, because any further breakdown would reduce the size of the sample upon which the distribution of n is based. To apply the model, during a simulation run the distribution of the effective number of confusing forms is determined by Monte-Carlo methods for each terrain type in which detections are made.

Time and funds prohibit the completion of the analysis outlined above since an extensive amount of terrain analysis and data collection and reduction are required. Performance of the analytic procedure outlined in this section is recommended if the glimpse model is to be applied to a general [illegible] (one containing several terrain classifications).

Given a constant fixation rate of 3 glimpses per second and an estimate of the equivalent number of confusing forms in a scene, the probability, P(t), that a target is detected in t seconds or less (equation 4.4) according to the glimpse model becomes:

$$P(t) = 1 - e^{-\int_0^t 3g(\Upsilon)/n \, d\Upsilon} \quad . \qquad (4.11)$$

This form of the probability P(t) results from a conditional detection rate which is a continuous function of time, such as that shown in Figure 28. In the next section, the form of this conditional detection rate is reduced to a step function with instantaneous changes at known discrete points in time during the movement of the target.

The Step Model

The Glimpse model developed in the preceding section yields a continuous function for the conditional detection rate, $\lambda(\Upsilon)$, as shown in Figure 28. In this figure, it is suggested that subtle changes at finite times in target-background-observer conditions cause changes in the detection rate at several points in time. Since detection times from the movies taken by Brown (1966) are to be used to estimate the effect of changes in these conditions, a statistically significant number of data points must be available to estimate $\lambda(\Upsilon)$ for each rate change. In this section, a simplification in the form of the function $\lambda(\Upsilon)$ is suggested so that statistical estimates of the detection rates during the target's exposure time can be calculated. This simplified form of $\lambda(\Upsilon)$ called the "step model" is discussed below.

Examination of films of moving targets taken by Brown indicates that changes in the appearance of the target occur several times during

its movement across the scene. If these changes are instantaneous and remain at some essentially constant level during a certain time interval, a simplication can be made in the form of $\lambda(\Upsilon)$ as predicted by the Glimpse model. If the single-glimpse detection probability iduring this time interval is a constant g, the conditional detection rate $\lambda(\Upsilon)$ is a constant given by equation 4.3 as

$$\lambda(\Upsilon) = \mu g\, p \tag{4.12}$$

where μ and p, defined previously,are constant for each scene. The conditional detection rate, $\lambda_i(\Upsilon)$, for the i^{th} such time interval is given by,

$$\lambda_i(\Upsilon) = \mu\, p\, g_i\,, \tag{4.13}$$

where g_i, the single-glimpse detection probability in the interval is calculated from equation 4.1. If the times $T_i (i = 0, \ldots, N)$ that the glimpse probability changes occur are subjectively measured from examination of the films the functional form of the new $\lambda(\Upsilon)$ might appear as shown in Figure 29. (In this figure the form as suggested by the Glimpse model is superimposed.) In this figure the target becomes intervisible to the observer at time T_0 and the conditional detection rate is constant λ_0. At known points in time, $T_i (i = 1, \ldots, 3)$ the rate assumes some constant level $\lambda_i (i = 1, \ldots, 3)$ and remains at that level until time T_{i+1}, when it instantaneously changes to a level λ_{i+1}. In Figure 28, it is noticed that the simplified form of $\lambda(\Upsilon)$ closely approximates the continuous from suggested by the Glimpse model only if the changes in $\lambda(\Upsilon)$ are essentially instantaneous. This simplification is

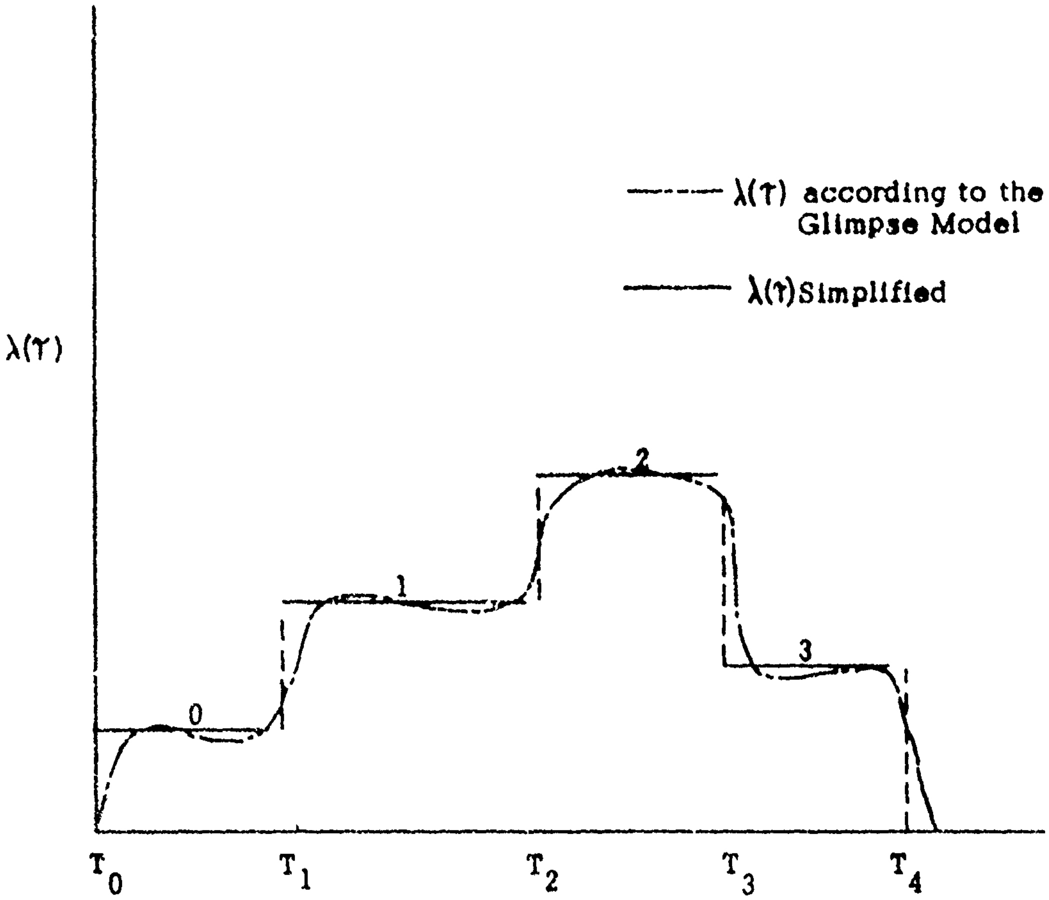

Fig. 29.—Simplified Form of $\lambda(\tau)$ Superimposed on the Form as Suggested by the Glimpse Model

fairly consistant with the conditions actually observed on the films taken by Brown (1966). The condition of the target does change almost instantaneously at several points along its movement path. These changes are caused by several factors:

1. The target may become silhouetted against another element of the background, thus, changing its target-to-background contrast,

2. The exposure angle (angular subtence) of the target may change as the amount of the target concealed by some terrain feature such as a low bush or high grass changes,

3. The orientation of the vehicle may change due to a rise or fall of the target with respect to position of the observer and the illuminating source. This change in orientation alters the appearance of the target by changing the relative magnitudes of the percent of the target highlighted and shaded,

4. A change in the crossing velocity of the target relative to the observer, and

5. A change in direction of advance.

According to the simplified model, when any one of these or other events changing the detection rate occur, the rate changes immediately by a constant amount and remains at its new levwl for a finite period of time. Of course, the change in detection rate may not be instantaneous but increase or decrease to some constant level at a constant rate as a function of time. This case and the problems it introduces are discussed at the end of this chapter. In the following section, the distribution of detection times for a target-motion scene with N changes in the glimpse rate is developed.

<u>Distribution of Detection Times</u>

Stollmack (1963) has developed an expression for the distribution of detection times of a stationary target viewed by a moving observer.

In this model changes in the conditional detection rate occur at discrete points in time just as in the Simplified model discussed in the preceding section. Therefore, the only difference between the model derived by Stollmack and the Simplified model is that rate changes are caused by target motion rather than observer motion. Regardless of the cause of the change, the distribution of detection times is the same if the conditional detection rates are the same. The distribution of detection times for the Simplified model is discussed below. This development is a direct extension of the work contained in Stollmack (1965).

In the general Step model, the conditional detection rate $\lambda(\Upsilon)$ is a step function changing at N determinable points in time as shown in Figure 30. In this figure, the target emerges from a terrain feature at time T_0 and becomes completely hidden from the observer at time T_N. At discrete points T_i $(i = 0, \ldots, N-1)$ within the movement trace of the target, the conditional detection rate assumes some constant level $\lambda_i (i=0, \ldots, N-1)$, and remains at that level until time T_{i+1}. Given that no detection has occurred up to the time T_i, the conditional cumulative probability, $P_i(t-T_i)$, that detection will occur at time t or before in the interval $[T_i, T_{i+1})$ is equal to

$$P_i(t - T_i) = 1 - e^{-\lambda_i(t - T_i)} \tag{4.14}$$

for $i = 0, \ldots, N-1$, and $T_i \leq t < T_{i+1}$. Furthermore, the unconditional cumulative probability, $P(t)$ that detection will occur at or before time t, where $T_i \leq t < T_{i+1}$, can be written as:

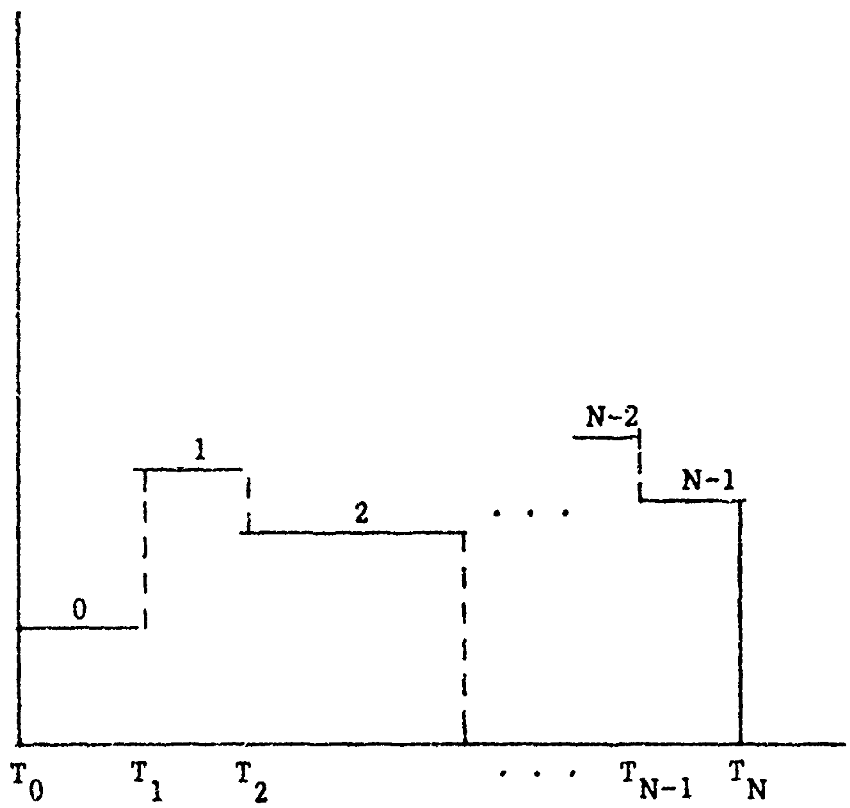

Fig. 30.--General Case of Changing Constant Detection Rate

$$
\begin{aligned}
P(t) = {} & P(\text{detection occurs before time } T_i) + \\
& P(\text{no detection before time } T_i) \cdot P(\text{detection} \\
& \text{at time } t \mid \text{no detection before time } T_i), \\
& (T_i \le t < T_{i+1})
\end{aligned} \qquad (4.15)
$$

Denoting the probability the detection does occur at or before time T_i as the cumulative probability of detection, $P(T_i)$, and the probability that no detection occurs at or before T_i, $Q(T_i)$, as:

$Q(T_i) = \{1 - P(T_i)\}$, equation 4.15 becomes,

$$
P(t) = \begin{cases} P(T_i) + \{1 - P(T_i)\} \quad P_i(t - T_i), \\ \quad T_i \le t < T_{i+1}, \\ \quad i = 1, \ldots, N-1 \\ P(T_N) \quad , \quad t \ge T_N \end{cases} \qquad (4.16)
$$

if it is assumed detection occurs with probability one at or before time T_N.

Equation 4.16 can be written as:

$$
P(t) = \begin{array}{ll} P(T_0) + \{1 - P(T_0)\} \; P_0 (t - T_0) , & T_0 \le t < T_1 \\ P(T_1) + \{1 - P(T_1)\} \; P_1 (t - T_1) , & T_1 \le t < T_2 \\ \quad \vdots & \\ P(T_{N-1}) + \{1 - P(T_{N-1})\} \; P_{N-1}(t - T_{N-1}) , & T_{N-1} \le t < T_N \\ P(T_N) , & t \ge T_N . \end{array} \qquad (4.17)
$$

In equation 4.17, the probability, $P(t)$ that detection occurs at or before time t, where T_0 t T_1, is written

$$
P(t) = P(T_0) + \{1 - P(T_0)\} \quad P_0(t - T_0) \qquad (4.18)
$$

If the target is initially completely hidden, the cumulative probability, $P(T_0)$, of detection at or before time T_0 is equal to zero. Setting T_0, the initial appearance time equal to zero, equation 4.18 becomes:

$$P(t) = P(0) + \{1-P(0)\} \quad P_0(t-0)$$

which reduces to

$$P(t) = P_0(t)$$

from equation 4.14, P(t) becomes

$$P(t) = 1 - e^{-\lambda_0(t-0)}$$

which reduces to

$$P(t) = 1 - e^{-\lambda_0 t} \quad , \; 0 \leq t < T_1 \tag{4.19}$$

the cumulative probability of detection at time t or before $0 \leq t < T_1$. Furthermore, the cumulative probability, P(t) of detection during the second time interval $[T_1, T_2)$, taken from equation 4.17 is given by:

$$P(t) = P(T_1) + \{1-P(T_1)\} \; P_1(t-T_1), \; T_1 \leq t < T_2 \tag{4.20}$$

In equation 4.20, $P(T_1)$ is the cumulative probability that detection occurs at or before time T_1. This probability is given by equation 4.19 as,

$$P(T_1) = 1 - e^{-\lambda_0 T_1} \tag{4.21}$$

The probability, $P_1(t - T_1)$, that detection occurs in the time interval (T_1, T_2) given by equation 4.14 is:

$$P_1(t - T_1) = 1 - e^{-\lambda_1(t - T_1)} \quad , \; T_1 \leq t < T_2 \tag{4.22}$$

Substituting 4.21 and 4.22 into 4.20, the cumulative probability of detection, P(t), at or before time $0 \leq t < T_2$ is given by;

$$P(t) = (1 - e^{-\lambda_0 T_1}) + (e^{-\lambda_0 T_1})(1 - e^{-\lambda_1 (t - T_1)}) \quad (4.23)$$

or

$$P(t) = 1 - e^{-\lambda_0 T_1 - \lambda_1 (t - T_1)} \quad (4.24)$$

In a similar manner, the cumulative probability of detection at or before T_3 is given by:

$$P(t) = (1 - e^{-\lambda_0 T_1 - \lambda_1 (T_2 - T_1)}) + (e^{-\lambda_0 T_1 - \lambda_1 (T_2 - T_1)})(1 - e^{-\lambda_2 (t - T_2)})$$

which reduces to

$$P(t) = 1 - e^{-\lambda_0 T_1 - \lambda_1 (T_2 - T_1) - \lambda_2 (t - T_2)} \quad (4.25)$$

Repeating this procedure, the general form of P(t) (equation 4.14) in the i^{th} time interval is given by:

$$P(t) = 1 - e^{-\lambda_0 T_1 - \lambda_1 (T_2 - T_1) - \ldots - \lambda_{i-1} (T_i - T_{i-1}) - \lambda_i (t - T_i)} \quad (4.26)$$

where $(T_i \leq t < T_{i+1})$, and $i = 0, \ldots, N-1$

Furthermore, by definition, at time T_N or beyond,

$$P(t) = 1 - e^{-\lambda_0 T_1 - \lambda_1 (T_2 - T_1) - \ldots - \lambda_N T_N} = 1, \; t \geq T_N.$$

From the cumulative distribution of detection times, given in equation 4.26, the probability density function, p(t) of detection times is given by:

$$
p(t)=\begin{cases}
\lambda_0 e^{-\lambda_0 t}, & 0 \le t < T_1 \\
e^{-\lambda_0 T_1}\lambda_1 e^{-\lambda_1(t-T_1)}, & T_1 \le t < T_2 \\
e^{-\lambda_0 T_1 - \lambda_1(T_2-T_1)}\lambda_2 e^{-\lambda_2(t-T_2)}, & T_2 \le t < T_3 \\
\vdots & \\
e^{-\lambda_0 T_1 - \lambda_1(T_2-T_1) - \ldots - \lambda_{i-1}(T_i-T_{i-1})}\lambda_i e^{-\lambda_i(t-T_i)}, & T_i \le t < T_{i+1} \\
e^{-\lambda_0 T_1 - \lambda_1(T_2-T_1) - \ldots - \lambda_{N-2}(T_{N-1}-T_{N-2})}\lambda_{N-1} e^{-\lambda_{N-1}(t-T_{N-1})}, & T_{N-1} \le t < T_N \\
0, & t \ge T_N
\end{cases}
\quad (4.27)
$$

In the next section, estimation of the parameters of this distribution from detection-time data is discussed. These estimates are used for comparison with predictions obtained from the Glimpse model discussed at the beginning of this chapter.

Estimation of $\lambda_i (i = 0, \ldots, N-1)$ fror Detection-Time Data

Estimates of the conditional detection rate for each target presentation can be computed using the method of maximum likelihood (Hogg and Craig, 1960). Partitioning the n subjects put on test(having a chance to detect the target) during the targets movement across the scene into N sets, we obtain:

$$
\begin{array}{lll}
r_0 & \text{detections in} & [T_0, T_1) \\
r_1 & \text{detections in} & [T_1, T_2) \\
r_2 & \text{detections in} & [T_2, T_3) \\
 & \vdots & \\
r_i & \text{detections in} & [T_i, T_{i+1}) \\
 & \vdots & \\
r_{N-1} & \text{in} & [T_{N-1}, T_N) \\
n - \sum_{k=0}^{N-1} r_k & \text{detections in} & [T_N, \infty) \ .
\end{array}
\tag{4.28}
$$

An unbiased maximum likelihood estimator for $\hat{\theta}_i = \frac{1}{\lambda_i}$, derived in Appendix D, is given by:

$$
\frac{1}{\lambda_i} = \hat{\theta}_i = \frac{\sum_{\ell=1}^{r_i} (t_\ell^{(i)} - T_{i-1}) + (n - \sum_{m=0}^{i} r_m)(T_i - T_{i-1})}{r_i} \tag{4.29}
$$

where

θ_i = an estimate of the value of $\frac{1}{\lambda_i}$ in $[T_i, T_{i+1})$,

r_i = the number of detections in the time interval $[T_i, T_{i+1}) (i = 0, \ldots, N-1)$,

n = the number of observers tested,

T_i $(i = 0, \ldots, N)$ are previously defined, and

$t_i^{(i)}$ $(l = 1, \ldots, r_i)$ are the detection times in the interval $[T_i, T_{i+1})$.

The value of the conditional detection rate given in equation 4.33 should be equivalent to that predicted by the Glimpse model for the i^{th} time interval. Equation 4.13 and 4.29,

$$\frac{\sum_{\ell=1}^{r_i} (t_\ell^{(i)} - T_{i-1}) + (n - \sum_{m=0}^{i} r_m)(T_i - T_{i-1})}{r_i} = \frac{1}{\mu p g_i} \quad (4.30)$$

In this equation, μ and p, defined earlier, are constant for each scene (independent of the value of i). Equation 4.30 provides a method for checking the validity of the Glimpse model. If the method for computing the single-glimpse detection probability is correct, the right and left sides of equation 4.30 should be equivalent. To calculate the glimpse probability, g_i, given in equation 4.30, it is necessary to measure certain quantities such as contrast and size from the films taken by Brown (1966). The detection times used to calculate estimates of $\hat{\lambda}_i$ were obtained from observers viewing these films. A procedure for validating the Glimpse model by comparing the right and left sides of equation 4.30 is discussed in the following section.

Model Validation

In this chapter, two probability models have been developed, the first called the Glimpse model, gives the conditional detection rate, $\lambda(\tau)$, as a continuous function of several environments variables and time. The second, called the Step model, approximates $\lambda(\tau)$ as a step function. In the Step model, the detection rate changes instantaneously at discrete determinable times during the movement trace of the target. Given these times, estimates of the reciprocal of the conditional detection rate, $\hat{\theta}_i$,

for the i^{th} interval of movement are calculable from equation 4.29. Equating $\frac{1}{\theta_i}$ and the predicted value of $\frac{1}{\lambda(\tau)}$ in the i^{th} time interval,

$$\frac{1}{\theta_i} = \mu p g_i$$

Validation of the model will entail comparison of the right and left sides of this equation.

The films taken by Brown (1966) were thought to contain sufficient information to perform this validation. By examining the films, any changes in the value of contrast or any of the other variables used to calculate the single-glimpse detection probability were noted. These changes could be considered as the times that the rate changes in the Simplified model ($T_1, T_2, \ldots, T_N$). To calculate the single-glimpse probability using the methods of Chapter 3, the following quantities would have to be measured at several points along the movement trace of the target on the films:

1. The apparent contrast of the highlighted target area with the foreground,

2. The apparent contrast of the shaded target area with the background,

3. The apparent contrast of the highlighted target area with the shaded target area,

4. The horizontal and vertical angular subtense of the target, and

5. The relative amounts of the target area which are highlighted and shaded.

In addition to these measures at several points along the movement trace, the same quantities must be determined for the slides from which the detection-time data are used to calculate the effective number of

confusing forms given by equation 4. Given all of the above data, the conditional detection rate in the th time interval is determined from:

$$\hat{\lambda}_i = \mu g_i \; n$$

where n_i is given by equation 4.9, μ is a constant 3 per second, and g_i is given in Chapter 3 as:

$$g_i = 1 - (1 - g_I)\,(1-g_{HB})(1-g_{SF})$$

and g_I, g_{HB}, and g_{SF} are calculated from equations 3.8, 3.9, and 3.10 respectively.

Attempts at Collecting Data for Validation

Unfortunately, attempts to collect the data necessary to validate the model were unsuccessful. Upon careful examination of the films taken by Brown (1966) several difficulties were encountered which prevented collection of useful data. These difficulties were caused primarily by the quality of the movies taken. They include:

1. The film resolution was not adequate to permit separation of the target into distinct areas of highlighting and shading.

2. The film, when examined at normal operating speed (24 frames per second) was quite clear and details seemed to be distinguishable. However, examination of individual frames revealed a great deal of smearing. This is due to a slight motion in the film as it moved past the shutter when the original films were taken

A Prichard photometer with a six-minute aperture was used to measure the luminance of various points around and within the target to obtain estimates of the target-scene contrast. Because of the problems with resolution discussed above, inconsistant and often contradictory values of contrast were obtained. In addition, it was extremely difficult to

measure the angular size of the target during its movement. This problem is also related to the resolution problem discussed earlier, since no clearly defined border between the target and its background was present when viewed on an increased scale.

Summary and Conclusions

Two models predicting probability that detection occurs in a time t or less have been developed in this chapter. An attempt was made to study the correspondence between the two models by comparing the right and left sides of equation 4.34 . However, to calculate the single-glimpse detection probability, it was necessary to obtain measurements of contrast and target exposure size from motion picture films. The quality and resolution of these films were not sufficient to permit the collection of the required data in the event such an experiment is conducted in the future, it would be necessary to take the photographs on a higher quality camera to alleviate the smearing problem which was encountered. Furthermore, the film taken by Brown was 16 millimeters in width, making the size of the target image extremely small. It would seem appropriate to use either 32 or 64 millimeter film for the further studies. In addition to the better equipment and film, care should also be taken to focus the image at all points on the scene if possible. The films taken by Brown were out of focus at several points in many of the scenes.

In place of the improved film, measurements of the variables necessary to calculate the single-glimpse detection probabilities could be measured in the field. However, it is felt that the improved equipment and film will alleviate the data-collection problems more

economical while also creating a permanent record of the experiments conditions.

As mentioned earlier in the chapter, the change in the conditional detection rate may not be instantaneous as assumed in the Step model. If the conditional detection rate, λ_i, is proportional to time in the i^{th} time interval, where

$$\lambda_i = \alpha_{0i} + \alpha_{1i}\ t,$$

the solution procedure used to develop maximum likelihood estimators for α_{0i} and α_{1i} could not be performed by standard algebraic methods. The only alternative would be to use a numerical analysis technique to obtain solutions for α_{0i} and α_{1i}. Because time and funds were limited, this analysis was not pursued further.

In the next chapter, the two models are summarized and recomendations for future research are suggested.

CHAPTER 5

SUMMARY AND CONCLUSIONS

The research problem posed in Chapter 1 was to develop a model of visual detection for a combat computer simulation which predicts detection time performance of an observer searching for a moving target in a complex terrain scene. As indicated in Chapter 2, very little experimental work has been performed on the detection of complex objects in natural terrain displays. In this literature review, results of several experiments over the past few decades were discussed in some detail. The results of these experiments give a clue to the variables affecting detection of targets in a complex display as opposed to those contained in a laboratory-type display of uniform luminance and content. The problem of detection in a homogeneous display has been treated in some detail by other authors (Lawson, 1969), but no significant contributions concerning complex displays are apparent.

A model based on the information derived from results of the experiments discussed in Chapter 2 and the intuition of the author is presented in Chapter 3, which predicts the single-glimpse detection probability of a target in a natural environment. This model treats the target as three independent objects, each having its own detection probability. The probability of detecting the entire object on a single glimpse is a function of the probabilities that these three objects are detected. The calculations necessary to determine the single-glimpse detection probability are easily executable on an electronic computer, making the model applicable to a computer-played combat simulation.

Given the single-glimpse detection probability, $g(\tau)$, the probability that the target is detected in a display containing n forms similar in appearance to the target was shown to be

$$P(t) = 1 - e^{-\int_0^t \frac{\mu g(\tau)}{n} d\tau}$$

where μ is the fixation rate. Since the form of the function $g(\tau)$ was not estimable from detection-time data, a simplifying assumption was made. By assuming $g(\tau)$ to be a step function which changes at determinable times during the motion of the target, an approximation to the functional form of $g(\tau)$ was made. This simplified functional form permitted the estimation of parameters of the step function. An attempt was made to relate the estimates of the conditional detection rate from the simplified model to those predicted by the glimpse model. However, attempts proved futile because necessary data could not be extracted from films of moving targets in a natural terrain scene. Suggestions for alleviating this problem in future experiments of this nature were presented.

The model which predicts single-glimpse detection probability relies heavily on a simplification in the shape of the target. A complex multi-luminance target is seen by the observer. However, no basic contrast threshold data are available for such targets. Since the only available data are for circular targets of uniform luminance, it was necessary to simplify the target shape somewhat by converting all rectangular solids into spheres having the same cross-sectional area. It is obvious that the obtaining of contrast-threshold data for complex objects

viewed against non-homogeneous backgrounds is highly desirable, since values of contrast threshold for circular targets are very optimistic when compared with the contrast thresholds of the complex traget-scenes.

In addition to this basic psychophysical data on contrast thresholds, the concept of the term "confusing forms" needs further examination. In Chapter 4, it was assumed that distinct objects in the display attract the attention of the observer. However, this may not be the case, since the observer may not select distinct objects to investigate, but instead may use the total content of the scene to perform an orderly search. No search data confirming the latter supposition has been found in the literature. An experiment to investigate this hypothesis therefore seems advisable.

The model predicting single-glimpse detection probability presented in Chapter 3, is completely general. However, its most valid application is for a clear bright sunlit day. As the illumination or visibility decreases, some of the assumptions used to construct the model become untenable, so further investigation of the model's validity in these cases is advisable before a direct extension is made. These direct extensions have been discussed at the end of Chapter 3.

Increased interest has been expressed by the military in the detection of militarily significant objects at night by either unaided or aided (optical devices) vision. To extend the glimpse model to low illuminations, further study of the following factors would be necessary:

1. The concept of confusing forms. It seems logical to to assume that there are considerably more forms in the display which compete for attention because detection is so difficult at all but the shortest ranges if vision unaided.
2. The fixation rate, which most likely changes with illumination level and possibly other factors.

APPENDIX A

VISIBILITY DATA FOR THE SEMBACH, GERMANY, WEATHER STATION

Figure A.1 indicates the change in meteorological visibility with the month of the year. Figures A.2 and A.3 illustrate the variation in meteorological visibility with the time of day in the months of April and July, respectively. These figures were adapted from data supplied by the Air Weather Service (MATS, 1965) for the Sembach, Germany, Weather Station. Similar data are available for other weather stations. World wide visibility data has been compiled by H. P. Dudel (1966, 1967) of the U.S. Army Missile Command. These data are in the form of cumulative distribution functions similar to those shown in Figures A.2 and A.3.

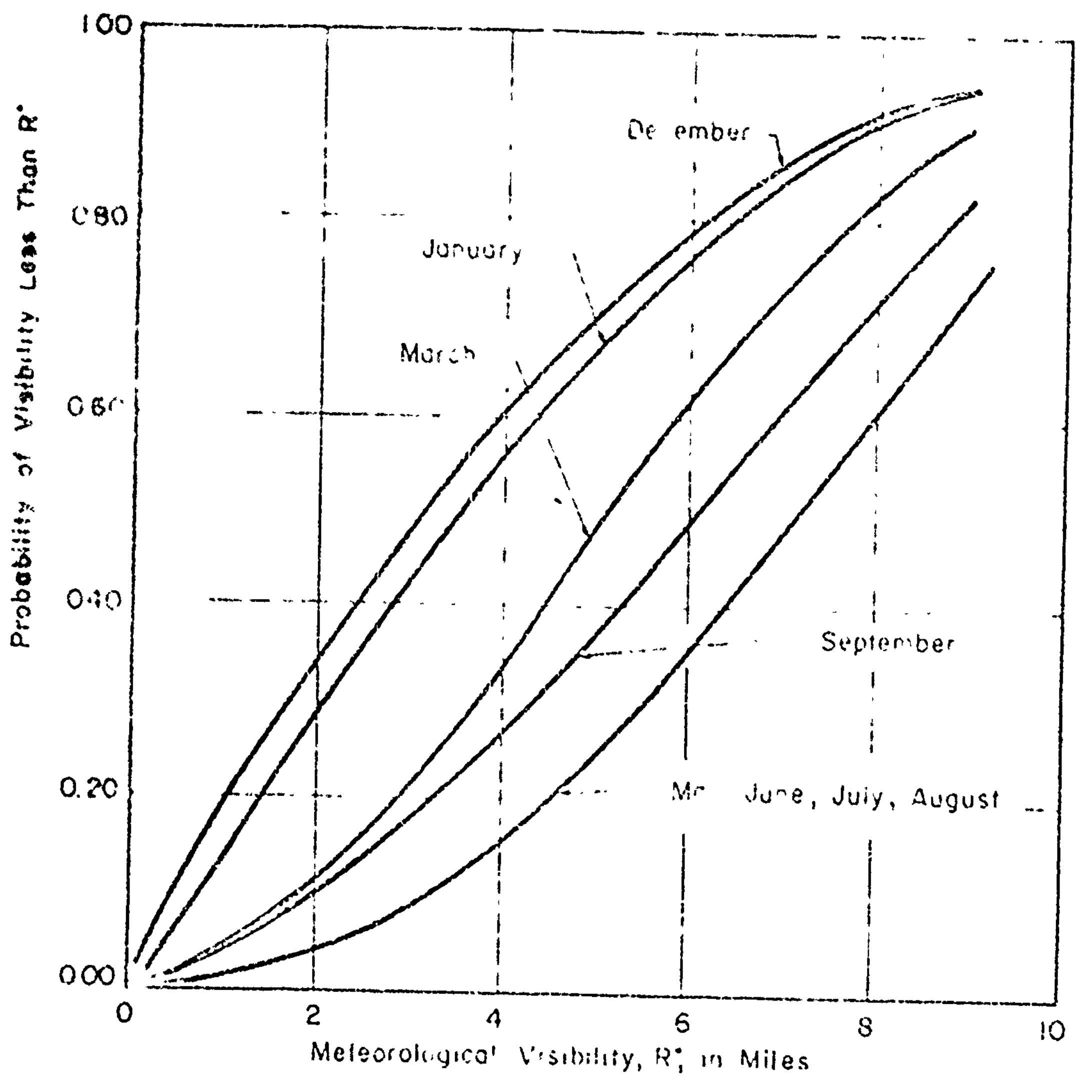

Fig. A. 1. --Monthly Meteorological Visibility at Seebach Airport

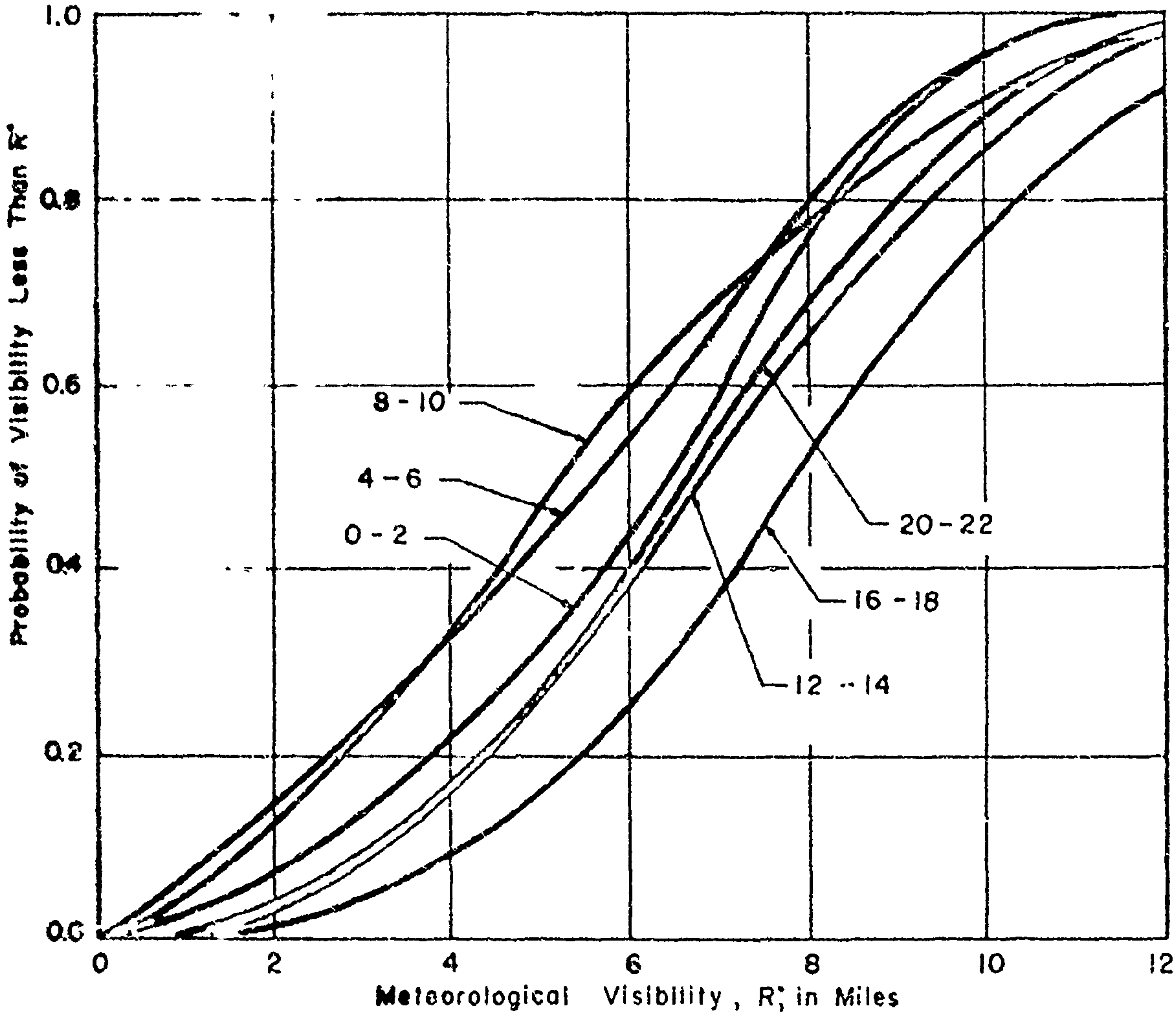

Fig. A. 2. --Hourly Meteorological Visibility at Sembach Airport during April Averaged for 0-2, 4-6, 8-10, 12-14, 16-18, and 20-22 L.S.T. Hours

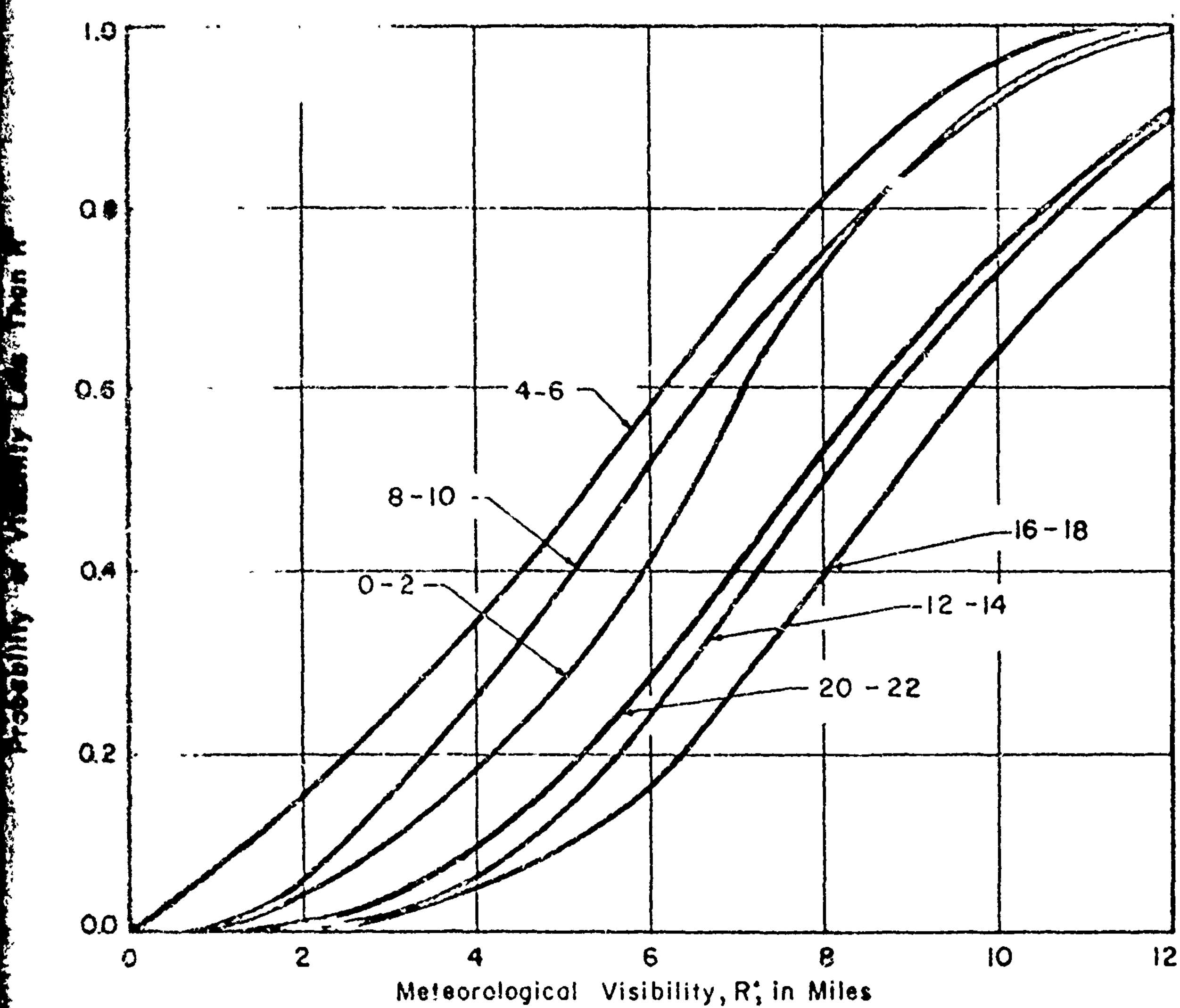

Fig. A-3.--Hourly Meteorological Visibility at Sembach Airport during July Averaged for 0-2, 4-6, 8-10, 12-14, 16-18, and 20-22 L.S.T. Hours

APPENDIX B

DIRECTIONAL REFLECTANCE DATA FOR REPRESENTATIVE TERRAIN FEATURE TYPES

Tables containing reflectance data for several terrain-features are given in this appendix. The data of Table B.1 were taken under an unobscured moderately high sun ($\alpha = 40^{\circ}$). Values are given for different azimuth angles θ of the path of sight relative to the sun and zenith angles ϕ of the path of sight. Similar, but much less extensive data are given in Table B.2 taken under an overcast sky. Table B.3 gives directional reflectances for dirt road when the sun is close to the horizon.

The change in the reflectance with obscuration of the sun and changes in the position of the sun in the sky can be seen from the data of Tables B.4 and B.5, respectively. The data of Table B.4 for a ploughed, moist, sand-loam soil, indicate that directional reflectance decreases as the illumination becomes more diffuse (that is, as the sun is obscured by a cloud). The data of Table B.5 for a freshly ploughed dirt road, indicate that directional reflectance decreases as the sun zenith angle α decreases.

TABLE B.1

DIRECTIONAL LUMINOUS REFLECTANCE OF TERRAIN BACKGROUNDS UNDER A MODERATELY HIGH SUN

Description	Sun Zenith Angle α	Azimuth angle θ of the path of sight relative to the sun	Zenith angle φ of path of sight							
			180	165	150	135	120	105	100	95
1. Pine trees--small, uniformly spaced.	41.5	0	0.0333	0.0241	0.0214	0.0214	0.0261	0.0379	0.0463	0.0559
		45		0.0322	0.0202	0.0194	0.0210	0.0303	0.0367	0.0549
		90		0.0316	0.0311	0.0317	0.0317	0.0337	0.0367	0.0463
		135		0.0335	0.0382	0.0392	0.0387	0.0438	0.0463	0.0572
		180		0.0402	0.0444	0.0578	0.0640	0.0711	0.0758	0.0825
2. Grass--thick, rather long, pale green, dormant, dryish; little ground showing.	41.5	0	0.088	0.081	0.076	0.077	0.088	0.094	0.096	0.094
		180		0.098	0.119	0.146	0.150	0.153	0.163	0.160
3. Asphalt--oily, with dust film blown onto oil.	42.0	0	0.061	0.057	0.056	0.060	0.063	0.090	0.104	0.127
		180		0.067	0.080	0.101	0.090	0.086	0.086	0.088
4. Grass--lush green, closely mowed thick lawn.	40.4	0	0.100	0.093	0.098	0.108	0.120	0.149	0.166	
	39.6	90		0.103	0.110	0.121	0.139	0.159	0.168	
	39.6	135		0.107	0.125	0.148	0.166	0.178	0.178	
	39.9	180		0.109	0.109	0.119	0.122	0.126	0.125	
5. Macadam--washed off and scrubbed.	48.5	0	0.113	0.115	0.119	0.128	0.148	0.194	0.228	
	60.1	90		0.110	0.108	0.118	0.112	0.139	0.147	
	46.0	180		0.126	0.141	0.156	0.166	0.172	0.176	

TABLE B.1.--Continued

Description	Sun Zenith Angle α	Azimuth angle δ of the path of sight relative to the sun	Zenith angle φ of path of sight							
			180	165	150	135	120	105	90	75
6. Dirt--hard packed, yellowish.	53.3	0	0.243	0.230	0.229	0.239	0.252	0.300	0.330	
	56.5	90		0.243	0.258	0.260	0.276	0.300	0.304	
	51.1	180		0.272	0.313	0.370	0.422	0.432	0.434	
7. Mixed green forest--deciduous (oak) and evergreen (pine).	39.0	0	0.0360	0.0325	0.0301	0.0305	0.0205	0.0342		
	37.0	180		0.0416	0.0493	0.0495	0.0820	0.263		
8. Pine forest.	33.5	0	0.0385	0.0395	0.0308	0.0245	0.0246	0.0200		
9. Grass--dry meadow, dense, mid-summer.	45	0	0.0855	0.0897	0.0960	0.0252	0.108	0.125		
	45	90		0.0778	0.0596	0.101	0.111	0.139		
	45	180		0.116	0.131	0.143	0.153	0.170		
	45	270		0.107	0.121	0.134	0.137	0.132		
10. Podzol--ploughed, moist.	50	0	0.0600	0.0586	0.0648		0.0553			
	50	90		0.0562	0.0853	0.0715	0.0614	0.0761		
	50	270		0.149	0.180	0.168	0.188	0.185		
11. Pasture meadow at end of summer.	45	0	0.0622							
	45	90				0.0882				
	45	180				0.0968				
12. Meadow (with clover and timothy)--dense growth, with flowers, mid-summer.	45	90				0.136	0.154			0.143

TABLE B.1. --Continued

Description	Sun Zenith Angle α	Azimuth angle δ of the path of sight relative to the sun	Zenith angle ϕ of path of sight							
			180	165	150	135	120	105	100	96
13. Meadow--with crow foot, dense grass with abundant flowers.	45	90				0.108	0.106			0.133
14. Dry meadow--sparse low grass.	45	90	0.0845			0.0879		0.126		
15. Dry meadow--more dense low grass.	45	0	0.0786							
	45	90				0.109				
	45	180				0.144				
16. Wheat--before harvesting.	50	0				0.0896	0.274			0.371
	50	180				0.111	0.292			0.386
17. Wheat--in the flowering period.	50	0				0.0792	0.122			0.268
	50	90					0.0863			0.306
18. Wheat--after mowing.	50	90					0.133			0.152
19. Soil--podsol, ploughed, dry.	45	0				0.105				
	45	90				0.189				
	45	180				0.179				
20. Soil--sandy loam, ploughed, moist.	45	0				0.203				
	45	90				0.112				
	45	180				0.212				
	45	270				0.180				

TABLE B.1.—Continued

Description	Sun Zenith Angle α	Azimuth angle δ of the path of sight relative to the sun	Zenith angle φ of path of sight: 180	165	150	135	120	105	100	93
21. Soil—sandy loam, ploughed, dry.	45	0	0.153			0.159				
	45	90				0.159				
22. Soil—black earth, rich, ploughed, wet.		0	0.0204			0.0574				
		180				0.0614				
23. Soil—black earth, rich, ploughed, dry.	45	0	0.0291			0.0339				
	45	90				0.0403				
	45	180				0.0466				
24. Dirt—flat desert road freshly bulldozed to remove encroaching sage.	42	90	0.226	0.228	0.229	0.234	0.247	0.261	0.271	0.270
25. Oiled dirt—flat desert road, oiled, with a light covering of dust.	42	90	0.100	0.102	0.102	0.104	0.109	0.113	0.121	0.124
26. Fir—late summer (mature forest); aircraft altitude 300 meters.	45	0	0.0319							
27. Edges of river bank—covered with sparse grass, almost dry, beginning of autumn.	45	0	0.146							
28. Alpine meadow—on mountain tops, covered with sparse grass, dried, beginning of autumn.	45	0	0.0605							

TABLE B.1 Continued

	Description	Sun Zenith Angle α	Azimuth angle β of the path of sight relative to the sun	Zenith angle ψ of path of sight							
				180	165	150	135	120	105	100	95
29.	Alpine meadow--on mountain tops, covered with sparse grass, mowed, dried, beginning of autumn.	45	0	0.110							
30.	Pasture meadow--beginning of autumn	45	0	0.0896							
31.	Lush meadow--lush dense grass, beginning of autumn.	45	0	0.0707							
32.	Dry meadow--sparse dry grass on hills beginning of autumn.	45	0	0.0790							
33.	Meadow--dense, low grass, beginning of autumn, aircraft altitude 300 meters.	45	0	0.0802							
34.	Shallows of river (in high water)--covered with grass.	45	0	0.112							
35.	Mountain side--low sparse grass, beginning of autumn.	45	0	0.133							
36.	Grass--near road, dusty.	45	0	0.0723							
37.	Hillside--short grass.	45	0	0.116							
38.	Soil--boggy; in boggy areas, very damp.	45	0	0.0588							

TABLE B. (Continued)

	Description	Sun Zenith Angle α	Azimuth angle δ of the path of sight relative to the sun	Zenith angle ε of path of sight							
				180	185	150	135	120	105	100	95
39.	Soil--grey podsol, ploughed, dry.	45	0	0.0529							
40.	Soil--black earth, leached, ploughed, slightly moist.	45	0	0.0874							
41.	Soil--black earth, rich, ploughed, wet.	45	0	0.0204							
42.	Soil--black earth, rich, ploughed, dry.	45	0	0.0291							
43.	Hill slope--bare, dry.	45	0	0.138							
44.	Turf--bare, dry.	45	0	0.0381							
45.	Earth road--heavily trampled, black earth, dry.	45	0	0.0832							
46.	Earth road--trampled, sand, loam.	45	0	0.0876							
47.	Earth road--grey podsol.	45	0	0.102							
48.	Edge of river bank--bare, dry.	45	0	0.149							
49.	Wind-eroded place--dry.	45	0	0.243							
50.	Shallows--sand with pebbles, moist.	45	0	0.111							

TABLE E. — Continued

Description	Sun Zenith Angle α	Azimuth angle δ of the path of sight relative to the sun	Zenith angle ϕ of path of sight 180	165	150	135	120	105	100	95
51. Earth road--black earth, leached.	45	0	0.139							
52. Earth road--little used, chestnut-brown earth.	45	0	0.184							
53. Earth road--trampled, podsol, dry.	45	0	0.198							
54. Earth road--covered with layer of loess, dry.	45	0	0.169							
55. Road--end of winter, yellowish after rain, wet.	45	0	0.756							
56. Road--paved cobblestone, dry.	45	0	0.202							
57. Road--paved cobblestone, dry.	45	0	0.318							
58. Meadow (with clover and timothy)--mowed.	45	90				0.0978				
59. Sedge meadow--dense grass in mid-summer.	45	90				0.136				
60. Meadow with daisies--period of abundant flowers.	45	90				0.130				
61. Grass--young, green.	45	90				0.149				

TABLE E.1. —Continued

	Description	Sun Zenith Angle α	Azimuth angle δ of the path of sight relative to the sun	Zenith angle ϕ of path of sight: 180	165	150	135	120	105	100	95
62.	Grass--last year's (dry), spring.	45	90				0.115				
[illegible]	Grass--summer green.	45	90				0.0796				
64.	Clay--dry, individual sample.	45	90				0.666				
[illegible]	Earth road--muddy and wet.	45	90				0.0548				
[illegible]	Road--paved cobblestone, dry.	45	90				0.155				
67.	Road--paved cobblestone, [illegible]	45	90				0.0598				
[illegible]	Stones--gathered in a pi[illegible]	45	90				0.192				

TABLE B. 2

DIRECTIONAL LUMINOUS REFLECTANCE OF TERRAIN BACKGROUNDS UNDER OVERCAST SKY

Description	Sun Zenith Angle α	Azimuth angle θ of the path of sight relative to the sun	Zenith angle φ of path of sight							
			180	165	150	135	120	105	100	95
1. Weeds--dense growth, drying and brownish (beginning of autumn).	--	90	0.0384		0.0952	0.0476				
2. Pasture meadow--at end of summer.	--	90	0.113		0.163		0.290			
3. Meadow (with clover and timothy)--mowed, wet after rain	--	90				0.101	0.137			0.228
4. Virgin Steppe--low grass, burnt by sun, beginning of autumn			0.0819		0.0668		0.100			
5. Soil--sandy loam, ploughed, moist		90	0.0562	0.0562	0.0630	0.0934	0.116			
6. Earth road--trampled, sand loam					0.142					

TABLE B. 3

DIRECTIONAL REFLECTANCE OF A DIRT ROAD ILLUMINATED BY A LOW SUN

Description	Sun Zenith Angle α	Azimuth angle δ of the path of sight relative to the sun	Zenith angle ϕ of path of sight							
			180	165	150	135	120	105	100	95
1. Low sun	77.8	90	.230	.243	.264	.275	.314	.330	.426	.458

TABLE B.4

CHANGE IN REFLECTANCE FOR OBSECURED SUN

Sun	α	δ	Directional reflectance for zenith angle of path of sight = 135°
Unobscured	45	90	.112
Obscured	45	90	.092

TABLE B.5

CHANGE IN REFLECTANCE WITH POSITION OF SUN IN SKY

	α	δ	Directional reflectance for zenith angle of path of sight = 180°	150°	120°	95°
1. Low sun	77.8	90	.230	.264	.314	.458
2. High sun	42.0	90	.226	.229	.247	.270

APPENDIX C

EXAMPLE OF THE DETERMINATION OF AZIMUTH ANGLE OF THE PATH OF SIGHT RELATIVE TO SUN

Given the sun azimuth angle β and the observer azimuth angle γ, the azimuth angle δ of the path of sight relative to the sun can be calculated from

$$\delta = \gamma - \beta$$

where the angles γ, β, and δ are illustrated in Figure C. 1. An example illustrating the calculation of δ is given in Figure C. 1.

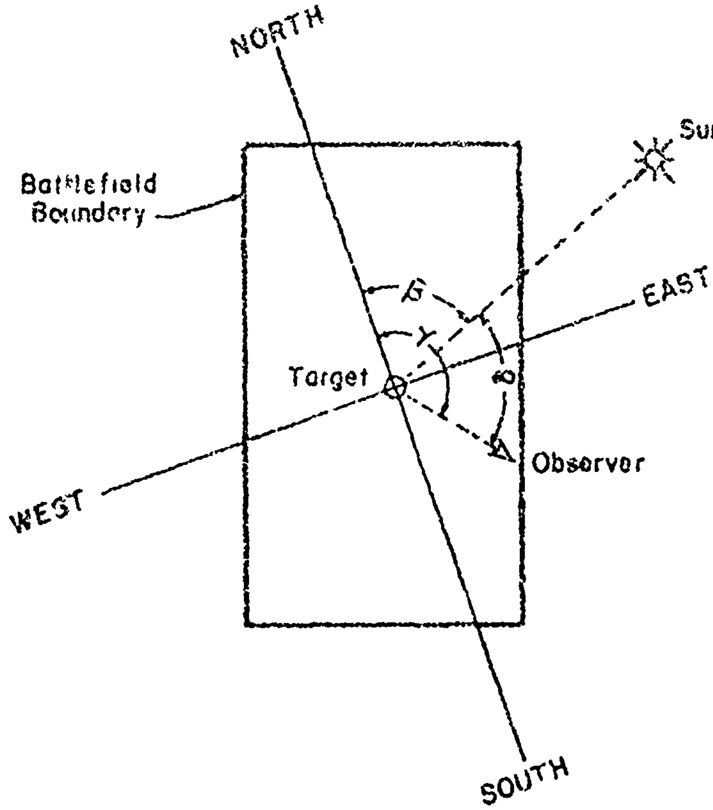

Fig. C. 1. --Example Illustrating the Calculation of the Azimuth Angle of the Path of Sight

APPENDIX D

DERIVATION OF MAXIMUM-LIKELIHOOD ESTIMATOR OF θ_i AND PROOF THAT IT IS UNBIASED

The distribution derived in Chapter 4 is a negative exponential with an N-stage step function as the conditional detection rate and known location parameters. If a total of n independent subjects have an opportunity to detect the target, an analogy can be drawn between the detection phenomena and reliability applications. In reliability terminology, the equivalent condition would be n mechanical systems whose failure rates are an equivalent function. Because of the above correspondence, this model of Chapter 4 can be used in reliability problems of this nature.

In general, the n total items put on test (subjects who have an opportunity to detect) can be partitioned into N + 1 groups as follows:

r_0 observers detect the target in $\left[T_0, T_1\right)$

r_1 observers detect the target in $\left[T_1, T_2\right)$

$\vdots$

$$r_i \text{ observers detect the target in } \left[T_i, T_{i+1}\right) \tag{D.1}$$

$\vdots$

r_{N-1} observers detect the target in $[T_{N-1}, T_N]$

$r \quad n - \sum_{m=0}^{N-1} r_m$ observers detect the target in $[T_N, \infty)$

The probability density function of detection times, given in Chapter 4 is,

$$
p(t) = \begin{cases}
\lambda_0 e^{-\lambda_0 t}, & 0 \le t < T_1 \\
e^{-\lambda_0 T_1} \lambda_1 e^{-\lambda_1 (t - T_1)}, & T_1 \le t < T_2 \\
e^{-\lambda_0 T_1 - \lambda_1 (T_2 - T_1)} \lambda_2 e^{-\lambda_2 (t - T_2)}, & T_2 \le t < T_3 \\
\vdots & \\
e^{-\lambda_0 T_1 - \lambda_1 (T_2 - T_1) - \cdots - \lambda_{i-1}(T_i - T_{i-1})} \lambda_i e^{-\lambda_i (t - T_i)}, & T_i \le t < T_{i+1} \\
\vdots & \\
e^{-\lambda_0 T_1 - \lambda_1 (T_2 - T_1) - \cdots - \lambda_{N-2}(T_{N-1} - T_{N-2})} \lambda_{N-1} e^{-\lambda_{N-1} (t - T_{N-1})}, & \\
 & T_{N-1} \le t < T_N \\
0 & , T_N \le t
\end{cases}
$$

substituting $\lambda_i = \frac{1}{\theta_i}$ into this probability density function, p (t) becomes[1]

[1]The maximum likelihood estimator of λ_i turns out to be biased, therefore the reciprocal of λ_i is taken since it is unbiased (Clark, 1968).

$$
p(t) = \begin{cases}
\frac{1}{\theta_0} e^{-\left(\frac{t}{\theta_0}\right)}, & 0 < t \leq T_1 \\
e^{-\frac{T_1}{\theta_0}} \left\{ \frac{1}{\theta_1} e^{-\left(\frac{t-T_1}{\theta_1}\right)} \right\}, & T_1 \leq t < T_2 \\
e^{-\frac{T_1}{\theta_0} - \frac{(T_2-T_1)}{\theta_1}} \left\{ \frac{1}{\theta_2} e^{-\frac{(t-T_2)}{\theta_2}} \right\}, & T_2 \leq t < T_3 \\
e^{-\frac{T_1}{\theta_0} - \frac{(T_2-T_1)}{\theta_1} - \cdots - \frac{(T_{N-1}-T_{N-2})}{\theta_{N-2}}} \left\{ \frac{1}{\theta_{N-1}} e^{-\left(\frac{t-T_{N-1}}{\theta_{N-1}}\right)} \right\}, & T_{N-1} \leq t < T_N \\
0, & T_N \leq t
\end{cases}
$$

The probability of the partitioning given in equation D.1 is

$$
P(n; r_0, r_1, \ldots, r_{N-1}) = K\, p_0^{r_0} \cdot p_1^{r_1} \cdot \ldots \cdot p_{N-1}^{r_{N-1}} \cdot (1 - p_0^{r_0} \cdot p_1^{r_1} \cdot \ldots \cdot p_{N-1}^{r_{N-1}})^{\bar{r}}
$$

where $\bar{r} = n - \sum_{m=0}^{N-1} r_m$, and

$$
K = \frac{n!}{r_0!\, r_1! \cdot \ldots \cdot r_{N-1}!\, \bar{r}!}
$$

and

$$
p_0 = 1 - e^{-\frac{T_1}{\theta_0}}
$$

$$
p_1 = \left[e^{-\frac{T_1}{\theta_0}}\right]\left[1 - e^{-\frac{(T_2 - T_1)}{\theta_1}}\right]
$$

$$
p_2 = \left[e^{-\frac{T_1}{\theta_0} - \frac{(T_2 - T_1)}{\theta_1}}\right]\left[1 - e^{-\frac{(T_3 - T_2)}{\theta_2}}\right]
$$

$$
\vdots
$$

$$P_i = \left[e^{-\frac{T_1}{\theta_0} - \frac{(T_2 - T_1)}{\theta_1} - \cdots - \frac{(T_i - T_{i-1})}{\theta_{i-1}}}\right]\left[1 - e^{-\frac{(T_{i+1} - T_i)}{\theta_i}}\right]$$

$$\vdots$$

$$P_{N-1} = \left[e^{-\frac{T_1}{\theta_0} - \frac{(T_2 - T_1)}{\theta_1} - \cdots - \frac{(T_{N-1} - T_{N-2})}{\theta_{N-1}}}\right]\left[1 - e^{-\frac{(T_N - T_{N-1})}{\theta_{N-1}}}\right]$$

Given these values of $P_0, \ldots, P_{N-1}$, the probability of the partitioning given in equation (D.1) becomes

$$P(r_0, \ldots, r_{N-1}, \bar{r} \mid n) = \left(1 - e^{-\frac{T_1}{\theta_0}}\right)^{r_0} \cdot \left(\left[e^{-\frac{T_1}{\theta_0}}\right]\left[1 - e^{-\frac{(T_2 - T_1)}{\theta_1}}\right]\right)^{r_1} \cdot$$

$$\left(\left[e^{-\frac{T_1}{\theta_0} - \frac{(T_3 - T_1)}{\theta_1}}\right]\left[1 - e^{-\frac{(T_3 - T_2)}{\theta_2}}\right]\right)^{r_2} \cdot$$

$$\cdots \left(\left[e^{-\frac{T_1}{\theta_0} - \frac{(T_2 - T_1)}{\theta_1} - \frac{(T_{N-1} - T_{N-2})}{\theta_{N-2}}}\right]\left[1 - e^{-\frac{(T_N - T_{N-1})}{\theta_{N-1}}}\right]\right)^{r_{N-1}} \cdot$$

$$\left[(1 - P_0 - P_1 - \cdots - P_{N-1})^{\bar{r}}\right]$$

and $\bar{r} = n - \sum_{m=0}^{N-1} r_m$

Assuming independence of the individual detection times, the conditional density of obtaining the ordered observations $t_1^{(0)}, \dots, t_{r_0}^{(0)}$, given r_0 and $t_j^{(0)} \le T_1$ is

$$P\left(t_1^{(0)}, \dots, t_{r_0}^{(1)} \;\middle|\; t_j^{(0)} \le T_1, r_0\right) = \frac{\prod_{j=1}^{r_0} \left(\frac{1}{\theta_0} e^{-\frac{t_j^{(0)}}{\theta_0}}\right)}{\left(1 - e^{-\frac{T_1}{\theta_0}}\right)^{r_0}}$$

Similarly for the second time interval, the conditional density of obtaining the ordered observations $t_1^{(1)}, \dots, t_{r_1}^{(1)}$ given r_1 and $T_1 \le t_j^{(1)} \le T_2$ is given by:

$$P\left(t_1^{(1)}, \dots, t_{r1}^{(1)} \;\middle|\; T_1 \le t_j^{(1)} \le T_2, r_i\right) = \frac{\prod_{j=1}^{r_1} \left(\frac{1}{\theta_1} e^{-\frac{(t_j^{(1)} - T_1)}{\theta_1} - \frac{T_1}{\theta_0}}\right)}{\left(e^{-\frac{T_1}{\theta_0}} \quad 1 - e^{-\frac{(T_2 - T_1)}{\theta_1}}\right)^{r_1}}$$

For the third time interval,

$$P\left(t_1^{(3)}, \dots, t_{r2}^{(2)} \;\middle|\; T_2 \le t_j^{(2)} \le T_3, r_2\right) =$$

$$\frac{\prod_{j=1}^{r_2} \left(\frac{1}{\theta_2} e^{-\frac{(t_j^{(2)} - T_2)}{\theta_2} - \frac{T_1}{\theta_0} - \frac{(T_2 - T_1)}{\theta_1}}\right)}{\left(\left[e^{-\frac{T_1}{\theta_0} - \frac{(T_2 - T_1)}{\theta_1}}\right]\left[1 - e^{\frac{-(T_3 - T_2)}{\theta_2}}\right]\right)^{r_2}}$$

and so on; for $i = 3, \dots, N - 1$.

It then follows that the likelihood, L, for the sample is

$$L = \frac{n!}{r_0! \cdots r_{N-1}!\, \bar{r}!} \prod_{j=1}^{r_0} \left(\frac{1}{\theta_0} \exp\left[-\frac{t_j}{\theta_0} \right] \right) \prod_{j=1}^{r_1} \left(\frac{1}{\theta_1} \exp\left[- \frac{(t_j^{(1)} - T_1)}{\theta_1} - \frac{T_1}{\theta_0} \right] \right)$$

$$\prod_{j=1}^{r_2} \left(\frac{1}{\theta_2} \exp\left[- \frac{(t_j^{(2)} - T_2)}{\theta_2} - \frac{T_1}{\theta_0} - \frac{(T_2 - T_1)}{\theta_1} \right] \right) \cdots$$

$$\cdot \prod_{j=1}^{r_i} \left(\frac{1}{\theta_i} \exp\left[- \frac{(t_j^{(i)} - T_i)}{\theta_i} - \frac{T_1}{\theta_0} - \cdots - \frac{(T_i - T_{i-1})}{\theta_{i-1}} \right] \right) \cdots$$

$$\prod_{j=1}^{r_{N-1}} \left(\frac{1}{\theta_{N-1}} \exp\left[- \frac{(t_j^{(N-1)} - T_{N-1})}{\theta_{N-1}} - \frac{T_1}{\theta_0} - \cdots - \frac{(T_{N-1} - T_{N-2})}{\theta_{N-2}} \right] \right)$$

Taking the natural logarithim of both sides and differentiating with respect to θ_i (i = 1,...,N-1) , we obtain

$$\frac{\partial \ln L}{\partial \theta_0} = \frac{-r_0}{\theta_0} + \frac{1}{\theta_0^2} \sum_{j=1}^{r_0} t_j^{(0)} + \frac{(n - r_1)\, T_1}{\theta_0^2} = 0$$

which yields

$$\theta_0 = \frac{\sum_{j=1}^{r_0} t_j^{(0)} + (n - r_1)\, T_1}{r_0}$$

$$\frac{\partial \ln L}{\partial \theta_1} = -\frac{r_1}{\theta_1} + \frac{1}{\theta_1^2} \sum_{j=1}^{r_0} (t_j^{(1)} - T_1) + \frac{(n - r_1 - r_2)(T_2 - T_1)}{\theta_1^2} = 0$$

$$\theta_1 = \frac{\sum_{j=1}^{r_1} (t_j^{(1)} - T_1) + (n - r_1 - r_2)(T_2 - T_1)}{r_1}$$

$$\frac{\partial \ln L}{\partial \theta_2} = 0$$

which yields,

$$\theta_2 = \frac{\sum_{j=1}^{r_2} (t_j^{(2)} - T_2) + (n - r_1 - r_2 - r_3)(T_3 - T_2)}{r_2}$$

$\cdot$
$\cdot$
$\cdot$

$$\frac{\partial \ln L}{\partial \theta_i} = 0$$

which yields,

$$\theta_i = \frac{\sum_{j=1}^{r_i} (t_j^{(i)} - T_i) + (n - \sum_{k=0}^{i} r_k)(T_{i+1} - T_i)}{r_i} \qquad \text{(D.2)}$$

A physical interpretation of the leading term,

$$\frac{(n - \sum_{k=0}^{i} r_k)(T_{i+1} - T_i)}{r_i}$$

in the preceding equation is that observers which have not detected by time T_{i+1}, $(n - \sum r_k)$ of them, may never detect, so the sum of their cumulative search times

$$(n - \sum_{k=0}^{i} r_k)(T_{i+1} - T_i)$$

up to the end of the i^{th} time interval must be averaged over all of the observers which detect in the interval (T_i, T_{i+1}) to raise the average. Equation D.2 is an estimate of the reciprocal of the conditional detection rate, λ_i, in the time interval (T_i, T_{i+1}). A proof that this estimate is unbiased is given below.

An unbiased estimator, $\hat{\theta}$, has the property that the expected value of $\hat{\theta}$ is equal to the true value of the parameter θ (Hogg and Craig, 1960), i.e.,

$$E(\hat{\theta}) = \theta$$

Given k ordered observations $x_1, \ldots, x_k$ of s items placed on test, Johnson and Leone (1966) show that the distribution $p(y_k)$ of

$$y_k = \sum_{i=1}^{k-1} x_i + (s - k + 1)\, x_k \qquad \text{(D.3)}$$

is:

$$p(y_k) = \left(\frac{\lambda^k}{\Gamma(k)}\right) y_k^{k-1} e^{-\lambda y_k} \tag{D.4}$$

which is $(2\lambda)^{-1}$ times a χ^2 with 2k degrees of freedom. In the case of the maximum-likelihood estimator given by equation D.2, $n - \sum_{m=0}^{i} r_m$ observers are available for detection in the interval $\left[T_i, T_{i+1}\right]$, and only r_i of them do detect. If there are a large number of detection times in each interval $t_{r_i}^{(i)}$, the final detection time in $\left[T_i, T_{i+1}\right)$ approaches T_{i+1}, and equation D.2, the estimate of θ_i, becomes

$$\hat{\theta}_i = \frac{\sum_{m=1}^{r_i-1} (t_m^{(i)} - T_i) + \left\{(n - \sum_{j=1}^{i-1} r_j) - r_i + 1\right\} (t_{r_i}^{(i)} - T_i)}{r_i} \tag{D.5}$$

which is of the same form as equation D.3 with $x_i = (t_m^{(i)} - T_i)$, $s = (n - \sum_{j=1}^{i-1} r_j)$, $k = r_i$, and $x_k = (t_{r_i}^{(i)} - T_i)$. Johnson and Leone (1966) also state that the conditional distribution of a quantity $(x_i - X)$ given $x_i > X$, is the same as the unconditional distribution of x_i. Using this fact, the expected value of $\hat{\theta}$, (Equation D.5) is gamma distributed, and

$$E(\hat{\theta}) = \frac{\theta_i \; r_i}{r_i} = \theta_i$$

which proves the unbiasedness.

BIBLIOGRAPHY

Air Weather Service (MATS), Estimating Mean Cloud and Climatological Probability of Cloud-Free Line of Sight, Technical Report 186, November, 1965.

Air Weather Service (MATS), Visibility at the Sembach Airport, 1965.

Alpern, M., The Eye, Volume 3, New York : Academic Press, 1962.

Blackwell, H. R., "Contrast Thresholds of the Human Eye," Journal of the Optical Society of America, Volume 36, Number 11, November, 1946.

Blackwell, H.R., The Effects of Certain Psychological Variables upon Target Detectability, Engineering Research Institute University of Michigan, Ann Arbor, Michigan, Report No. 2455-12-F, June, 1958.

Blackwell, H.R., "Neural Theories of Simple Visual Discriminations," Journal of the Optical Society of America, Volume 53, Number 1, January, 1963.

Blackwell, H.R., "The Evaluation of Interior Lighting on the Basis of Visual Criteria," Applied Optics, Volume 6, Number 9, September, 1967.

Blackwell, H.R., and Austin, G. A., "Spacial Summation in the Central Fovea," Journal of the Optical Society of America, Volume 42, November, 1952.

Blackwell, H.R., and Bixel, G. A., Final Report the Visibility of Non-Uniform Target-Background Complexes, The Ohio State University, Columbus, Ohio, Report Number RADC-TDR-63-184.

Blackwell, H.R., and Law, O. T., University of Michigan, Ann Arbor, Michigan, Report Number 2144-344-T, 1959.

Blackwell, H.R., and McCready, D. W., Foveal Contrast Threshold for Various Durations of Single Pulses, Engineering Research Institute, University of Michigan, Ann Arbor, Michigan, Report Number 2455-12-F, June, 1958.

Blackwell, H.R., and Smite, S. W., University of Michigan, Ann Arbor, Michigan, Report Number 2144-344-T, 1959.

Boileau, A. R., and Gordon, J. I., Atmospheric Properties and Reflectances of Objects and Background for a Low Sun, Scripps Institute of Oceanography, June, 1965, Report 65-10.

Boynton, R. M., and Bush, W. R., Laboratory Studies Pertaining to Visual Air Reconnaissance, University of Rochester, Rochester, New York, Report Number 55-304, September, 1955.

Boynton, R. M., and Bush, W. R., Laboratory Studies Pertaining to Visual Air Reconnaissance, The University of Rochester, Rochester, New York, Technical Report Number 55-304, Part 2, April, 1957.

Brown, D. R. E., Natural Illumination Charts, Report No. 374-1, Bureau Of Ships, Department of Navy, September, 1952.

Brown, P. J., Application of the Negative Exponential Model to Detection Time Distributions For Military Targets in Natural Terrain Backgrounds, Unpublished Masters Thesis, The Ohio State University, 1966.

Bush, V., et al., Visibility Studies and Some Applications in the Field of Camouflage, National Defense Research Committee, Washington, D. C, 1946, AD 22102.

Deese, J., Complexity of Contour in the Recognition of Visual Form, Wright Air Development Center, Wright-Patterson Air Force Base, Ohio, Report Number WADC 56-60, 1956.

Downs, A. R., Ager, L.W., LaGrange, A. E., Luminance Measurements on Tanks, U.S. Army Ballistic Research Labs, Aberdeen, Maryland, MR 1659, May, 1965 (Confidential).

Dudel, H. P., A Compilation of Tables of Meteorological Visibility Statistics, U.S. Army Missile Command, Redstone Arsenal Alabama, Report Number RR-TR-66-10, July, 1966.

Dudel, H. P., Some Climatic Information on Surface Visibility, U.S. Army Missile Command, Redstone Arsenal, Alabama, Report Number RR-TR-67-5, April 1967.

Duntley, S. Q., "Summary," Applied Optics, 3, No. 5, May, 1964, p. 551.

Duntley, S. Q., "The Visibility of Distant Objects," Journal of the Optical Society of America, 38, No. 3, March, 1948.

Duntley, S. Q., Visibility Studies and Some Applications in the Field of Camouflage, Summary Tech. Report Div. 16, NDRC, Vol. 2, 1946, p. 65.

Ford, A., White, C. T., and Lichtenstein, M., "Analysis of Eye Movements during Free Search," Journal of the Optical Society of America, Volume 49, Number 3, March 1959.

Fox, W. R., Visual Discrimination as a Function of Stimulus Size, Shape, and Edge Gradient. Unpublished doctorate dissertation, Boston University, 1956.

Franklin, M. E., Research on Visual Target Detection, Part I: Development of an Air-to-Ground Detection/Identification Model, Human Sciences Research, Inc., McLean, Virginia, 1965.

Gordon, D. A., Visual Detection and Identification, Military Applications, The University of Michigan, Ann Arbor, Michigan, Report Number 2144-Z-1114, September, 1958.

Gordon, J. I., "Optical Properties of Objects and Backgrounds," Visibility, Scripps Institute of Oceanography, 1964.

Gordon, J. I., and Church, P.V., "Overcast Sky Luminances and Directional Luminous Reflectances of Objects and Backgrounds Under Overcast Skies," Applied Optics, 5, No.6, June, 1966, p. 919.

Hogg, R. V., and Craig, A. T., Introduction to Mathematical Statistics The Macmillan Company, New York, 1965.

Kause, R. H., Interpretation of Complex Images; Literature Survey, Goodyear Aerospace Corporation, Akron, Ohio, February, 1965.

Kincaid, W. M., Blackwell, H.R., and Kristofferson, A. B., "Neural Formulation of the Effects of Target Size and Shape Upon Visual Detection," Journal of the Optical Society of America, Volume 50, Number 2, February, 1960.

Kristofferson, A. B., "Visual Detection as Influenced by Target Form" (in) Wulfeck, I.W., and Taylor, J.H., (eds) Form Discrimination --as Related to Military Problems, National Academy Science, National Research Council Publication, 561, 1957.

Kristofferson, A. B., and Blackwell, H. R., "Effects of Target Size and Shape on Visual Detection: Continuous Foveal Targets at Moderate Background Luminance," Journal of the Optical Society of America, Vol. 47, 1957, p. 114.

Lamar, E. S., Hecht, S., Shlaer, S., and Hendley, C. E., "Size, Shape, and Contrast in Detection of Targets by Daylight Vision I., Data and Analytical Description," Journal of the Optical Society of America, 37, July 1947, pp. 531-545.

Lawson, R. M., The Distribution of the Time Required by Ground-Based Observers to Detect Aerial Targets, Unpublished Masters Thesis, The Ohio State University, 1969.

Middleton, W. E. K., Vision Through the Atmosphere, University of Toronto Press, 1968.

Morris, A., Pattern Target Analysis, Part I: A Theory, Part II: A Psychophysical Experiment, Scripps Institute of Oceanography, San Diego, California, S10 Ref. 59-62, November, 1959.

Nachman, M., The Influence of Size and Shape on the Visual Threshold of the Detectability of Targets, Boston University Optical Research Laboratory Technical Note 109, December, 1953.

Rhodes, F., Predicting the Difficulty of Locating Targets from Judgments of Image Characteristics, Air Force Systems Command, Wright-Patterson Air Force Base, Ohio, Report Number AMRL-RDR-64-19, March, 1964.

Richardson, W. H., A Study of the Factors Affecting the Sighting of Surface Vessels from Aircraft, Scripps Institute of Oceanogaphy, San Diego, California, Reference Number S10-62-13, June, 1962.

Ryll, E., Project Trace-Aerial Observer Effectiveness and Nap-of-the-Earth, Cornell Aeronautical Labs, February, 1962, AD468570.

Smith, S. W., Time Required for Target Detection in Complex Abstract Visual Display, The University of Michigan , Ann Arbor, Michigan, Report Number 2900-235-R, April, 1961.

Smith, S. W., and Semmelroth, C., An Experimental Study Relating Search Peripheral Visual Discriminability of Objects, University of Michigan, Ann Arbor, Michigan, Report Number 2900-95-M, 1961.

Steedman, W. C., and Baker, C. A., Target Size and Visual Recognition, Aerospace Medical Laboratory, Wright-Patterson Air Force Base, Ohio, Report Number 60-93, February, 1960.

Stollmack, S., Analytical Procedures for Determining the Time Required to Detect a Stationary Target, Unpublished Masters Thesis, The Ohio State University, 1965.

Stollmack, S., and Lawson, R. M., "Contrast Dependent Detection Model," Chapter 3 (in) A. B. Bishop and S. Stollmack (eds) The Tank Weapon System, RF-573, AR-68-1, Systems Research Group, The Ohio State University, December, 1968.

Taylor, J. H., "Use of Visual Performance Data in Visibility Prediction," Applied Optics, Volume 3, Number 5, May, 1964.

Taylor, J. H., Visual Contrast Thresholds for Large Targets, Part I: The Case of Low Adapting Luminances, Scripps Institute of Oceanography, San Diego, California, S10 Reference 60-25, June, 1960a.

Taylor, J. H., Visual Contrast Thresholds for Large Targets, Part II: The Case of High Adapting Luminances, Scripps Institute of Oceanography, San Diego, California, S10 Reference 60-31, June, 1960b.

Taylor, J. H., Contrast Thresholds as a Function of Retinal Position and Target Size for the Light-Adapted Eye. Scripps Institute of Oceanography, San Diego, California, S10 Reference 61-10, March, 1961.

Townsend, C., Fry, G. A., and Enoch, J. M., The Effect of Image Degradation on Visual Search: Aerial Haze, The Ohio State University Research Foundation, Columbus, Ohio, Report No. (696)-13-269, January, 1958.

White, C. T., "Ocular Behavior in Visual Search," Applied Optics, Volume 3, Number 5, May, 1964.

Wulfeck, J.W., and Taylor, J.H., (eds) Form Discrimination as Related to Military Problems, National Academy of Sciences, Washington, D. C., Publication 561, April 1957.

Wulfeck, J. W., et al., Vision in Military Aviation, Wright Air Development Center, Wright-Patterson Air Force Base, Ohio, Report Number 58-399, November, 1958.

Zusne, L., and Michels, K. M., "Geometricity of Visual Form," Perceptual and Motor Skills, Vol. 14, 1962, pp. 147-154.

Zusne, L., and Michels, K. M., "More on the Geometricity of Visual Form," Perceptual and Motor Skills, Vol. 15, 1962, pp. 55-58.

DISCLAIMER NOTICE